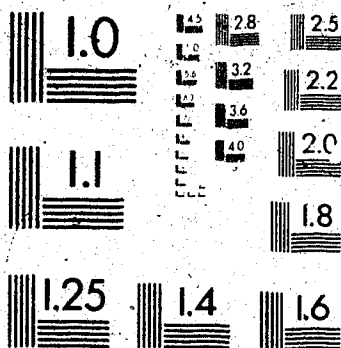


# 1



WITH THE NEW MICROFILM SYSTEM

**MICROFILM**

FOR THE STORAGE OF INFORMATION



National Library  
of Canada

Bibliothèque nationale  
du Canada

Canadian Theses Service

Service des thèses canadiennes

Ottawa, Canada  
K1A 0N4

## NOTICE

The quality of this microform is heavily dependent upon the quality of the original thesis submitted for microfilming. Every effort has been made to ensure the highest quality of reproduction possible.

If pages are missing, contact the university which granted the degree.

Some pages may have indistinct print especially if the original pages were typed with a poor typewriter ribbon or if the university sent us an inferior photocopy.

Previously copyrighted materials (journal articles, published tests, etc.) are not filmed.

Reproduction in full or in part of this microform is governed by the Canadian Copyright Act, R.S.C. 1970, c. C-30.

## AVIS

La qualité de cette microforme dépend grandement de la qualité de la thèse soumise au microfilmage. Nous avons tout fait pour assurer une qualité supérieure de reproduction.

S'il manque des pages, veuillez communiquer avec l'université qui a conféré le grade.

La qualité d'impression de certaines pages peut laisser à désirer, surtout si les pages originales ont été dactylographiées à l'aide d'un ruban usé ou si l'université nous a fait parvenir une photocopie de qualité inférieure.

Les documents qui font déjà l'objet d'un droit d'auteur (articles de revue, tests publiés, etc.) ne sont pas microfilmés.

La reproduction, même partielle, de cette microforme est soumise à la Loi canadienne sur le droit d'auteur, SRC 1970, c. C-30.

THE UNIVERSITY OF ALBERTA

MICROSEISMICITY IN COLD LAKE, ALBERTA AREA

by

C

SOTIRIS KAPOTAS

A THESIS

SUBMITTED TO THE FACULTY OF GRADUATE STUDIES AND RESEARCH

IN PARTIAL FULFILMENT OF THE REQUIREMENTS FOR THE DEGREE

OF MASTER OF SCIENCE

IN

GEOPHYSICS

DEPARTMENT OF PHYSICS

EDMONTON, ALBERTA

FALL 1987

Permission has been granted to the National Library of Canada to microfilm this thesis and to lend or sell copies of the film.

The author (copyright owner) has reserved other publication rights, and neither the thesis nor extensive extracts from it may be printed or otherwise reproduced without his/her written permission.

L'autorisation a été accordée à la Bibliothèque nationale du Canada de microfilmer cette thèse et de prêter ou de vendre des exemplaires du film.

L'auteur (titulaire du droit d'auteur) se réserve les autres droits de publication; ni la thèse ni de longs extraits de celle-ci ne doivent être imprimés ou autrement reproduits sans son autorisation écrite.

ISBN 0-315-40951-7

THE UNIVERSITY OF ALBERTA

RELEASE FORM

NAME OF AUTHOR SOTIRIS KAPOTAS  
TITLE OF THESIS MICROSEISMICITY IN COLD LAKE,  
ALBERTA AREA  
DEGREE FOR WHICH THESIS WAS PRESENTED MASTER OF SCIENCE  
YEAR THIS DEGREE GRANTED FALL 1987

Permission is hereby granted to THE UNIVERSITY OF ALBERTA LIBRARY to reproduce single copies of this thesis and to lend or sell such copies for private, scholarly or scientific research purposes only.

The author reserves other publication rights, and neither the thesis nor extensive extracts from it may be printed or otherwise reproduced without the author's written permission.

(SIGNED)

PERMANENT ADDRESS:

K. DIMITRIOU 12  
KALAVRYTA, ACHAIAS  
HELLAS - GREECE

DATED July 22.....1987

THE UNIVERSITY OF ALBERTA  
FACULTY OF GRADUATE STUDIES AND RESEARCH

The undersigned certify that they have read, and recommend to the Faculty of Graduate Studies and Research, for acceptance, a thesis entitled MICROSEISMICITY IN COLD LAKE, ALBERTA AREA submitted by SOTIRIS KAPOTAS in partial fulfilment of the requirements for the degree of MASTER OF SCIENCE in GEOPHYSICS.

....E. R. Kasanin....

Supervisor

....Do. Chylo....

....R. A. Brown....

....J. S. Rye....

Date...June 2, 1987.....

## DEDICATION

στη Σοφία

"...για λόγους που γνωρίζει καλά,  
και ξέρει γιατί..."

## ABSTRACT

A six-station digitally recording seismic network with 10 sensors within a radius of 11 km has been operated by Alberta Environment for 5 years near Cold Lake, Alberta, in order to establish the nature of micro-tremors reported in the area. These stations are in an area where heavy oil is being extracted using an in situ process of steam injection.

The tremors range from 20 to more than 100 per year and are classified as microseisms. The area is also close to a Canadian Forces Weapons Range and the array was designed to discriminate between sonic arrivals from supersonic flights, bombing practices on the range, and tremors originating in the solid earth. The local earth tremors are mostly less than magnitude 2 and appear to follow a topographic linearity through the heavy oil project area and the geomorphological characteristics of the bedrock topography.

Analysis of the results indicates that the microearthquakes fall into three regions, one related with the geomorphology of the area the other at focal depths associated with steam injection and oil production formation levels and the final related to waste water disposal SE of the array. Focal mechanism analysis gave us directions of compression in the area, which are concordant with the dip of the local formation. Also in this study an automatic procedure for obtaining first arrival times will be introduced for analysing data.



## ACKNOWLEDGEMENTS

Professor E. R. Kanasewich deserves *ad ultimum fides* *et noscere academia* for the euphoria of discussions and supervision of this work, to him I am deeply grateful. I wish to acknowledge the inspiration and motivation provided to me by Professor D.I. Gough, for the science of geophysics. To the academic staff of the physics department, and especially Professor E. Nyland, giving me the insight knowledge to achieve this goal, I express my sincere appreciation.

I am grateful to Dr. D. Bingham and his staff, C. Holt-Odura and W. Laidlaw on the Earth Sciences Division of the Alberta Environment for assisting in the basic operations of the seismic array. I wish to acknowledge the invaluable assistance provided by Mr. Charles McCloughan in completing most of the graphical representations of this work. To my colleagues that during the development of this work provided helpful discussions and information, I am thankful. I wish to thank Dr. S. Bharatha and Mr. M. Gronseth from Esso Resources Canada Limited for providing usefull information for most part of this research.

Major financial assistance for this research was obtained from Esso Resources Canada Limited and Alberta Environment. Additional support was provided by the Natural Sciences and Engineering Research Council, and in the form of teaching assistanceship by the University of Alberta.

## Table of Contents

| Chapter  | Page |
|--|------|
| LIST OF TABLES .....                                 | ix   |
| LIST OF FIGURES .....                                | x    |
| 1. INTRODUCTION .....                                | 1    |
| 1.1 MICROSEISMICITY - A REVIEW .....                 | 1    |
| 1.1.1 Permanent Networks .....                       | 4    |
| 1.1.2 Temporary Networks .....                       | 4    |
| 1.2 GENERAL APPLICATIONS OF MICROSEISMICITY .....    | 5    |
| 1.2.1 Aftershock Studies .....                       | 5    |
| 1.2.2 Induced Seismicity Studies .....               | 5    |
| 1.2.3 Geothermal Exploration .....                   | 7    |
| 1.2.4 Crustal and Mantle Studies .....               | 7    |
| 1.3 SPECIFICATION OF THE STUDY .....                 | 9    |
| 1.4 INSTRUMENTATION AND OPERATIONS .....             | 13   |
| 1.5 GEOLOGY AND HYDROGEOLOGY OF THE STUDY AREA ..... | 22   |
| 1.5.1 Lower Cretaceous .....                         | 32   |
| 1.5.2 Upper Cretaceous .....                         | 37   |
| 1.5.3 Tectonic History .....                         | 38   |
| 1.5.4 Bedrock Topography and Buried Valleys .....    | 39   |
| 1.6 HEAVY OIL RECOVERY .....                         | 44   |
| 1.6.1 Cyclic Steam Stimulation .....                 | 46   |
| 1.6.2 Heavy Oil Recovery in Cold Lake .....          | 49   |
| 2. PROCESSING PROCEDURES .....                       | 55   |
| 2.1 DATA PROCESSING .....                            | 55   |
| 2.2 EVENT DETECTION - CATEGORIZATION .....           | 59   |
| 2.3 EVENT PROCESSING .....                           | 66   |
| 2.3.1 Direct Plotting .....                          | 66   |

|       |  |     |
|-------|--|-----|
| 2.3.2 | Spectral Analysis and Filtering .....            | 67  |
| 2.3.3 | Tapering .....                                   | 76  |
| 2.3.4 | Automatic processing .....                       | 78  |
| 2.4   | DATA ANALYSIS .....                              | 78  |
| 2.4.1 | Hypocenter determination .....                   | 82  |
| 2.4.2 | Magnitude Determination .....                    | 86  |
| 2.4.3 | Focal mechanisms - Fault plane solutions ..      | 90  |
| 3.    | AUTOMATIC SEISMIC ANALYSIS .....                 | 101 |
| 3.1   | INTRODUCTION .....                               | 101 |
| 3.2   | AUTOPICK .....                                   | 104 |
| 3.3   | APPLICATIONS OF AUTOPICK .....                   | 118 |
| 4.    | INTERPRETATION AND DISCUSSION .....              | 127 |
| 4.1   | INTRODUCTION .....                               | 127 |
| 4.2   | INDUCED SEISMICITY AND HYDROGEOLOGY .....        | 132 |
| 4.3   | INDUCED SEISMICITY AND HEAVY OIL RECOVERY .....  | 138 |
| 4.4   | INDUCED SEISMICITY AND WASTE WATER DISPOSAL .... | 149 |
| 4.5   | CONCLUSIONS .....                                | 153 |
|       | Bibliography .....                               | 156 |

## LIST OF TABLES

| Table | Description  | Page |
|-------|--|------|
| 1     | Earthquake Classification by Magnitude.....  | 2    |
| 2     | General system specifications Cold Lake<br>Seismic Recording System. Installed October, 1981..   | 14   |
| 3     | Channel List of the Cold Lake seismic stations....   | 15   |
| 4     | Cold Lake Array station locations. The<br>listings are in three different coordinates.....   | 16   |
| 5     | Geological Horizons used for the analysis of<br>microseismicity in Cold Lake area.....   | 35   |
| 6     | Bedrock Valley Dimensions .....  | 41   |
| 7     | Crustal model for Cold Lake as determined by<br>two test explosions and verification with HYPO71..   | 81   |
| 8     | Description of the parameters used for<br>epicentral determination using HYPO71.....   | 87   |
| 9     | Trial results of hypocenter determination<br>produced from HYPO71.....   | 88   |
| 10    | Local Magnitude estimates for "A" type<br>events recorded by the Cold Lake seismic array....   | 91   |
| 11    | Results obtained from AUTOPICK routine used<br>to estimate first arrivals and first motions<br>automatically. Good estimates (top), less<br>reliable (bottom)..... | 121  |
| 12    | Comparison between visually obtained results<br>and the ones obtained from AUTOPICK.<br>Reliable (top), less accurate (bottom).....                                | 122  |
| 13    | Hypocenter determinations for "A" type events....  | 131  |

## LIST OF FIGURES

| Figure | Page  |
|--------|---|
| 1      | Cold Lake Induced Seismicity Monitoring Array.....12  |
| 2      | Remote Field Station Configuration and S-500<br>Seismometer Description. Modified from Druid<br>Electronics Design. ....18  |
| 3      | Amplitude Response of Amplifiers. ....19  |
| 4      | Base Station ELE configuration and<br>operation. Modified from Druid Electronics Design.21  |
| 5      | Daily digital recording performance on the<br>Cold Lake Seismic Array for 1985.....23   |
| 6      | Block diagram of the instrumentation at the<br>field sites, the base station near Cold Lake<br>and the Cold Lake Seismic Data Centre at the<br>University of Alberta, Edmonton.....24 |
| 7      | 3D representation of Cold Lake area Topography....26  |
| 8      | 3D - Thickness of drift cover, Cold Lake area.....27  |
| 9      | 3D - Top of smoothed bedrock in the Cold<br>Lake area.....28  |
| 10     | 3D representation - elevations of Base of<br>Fish Scales.....29   |
| 11     | 3D representation of the elevation of top of<br>Colony.....30   |
| 12     | 3D representation - elevations of top of McMurray.31  |
| 13     | 3D representation - elevations of Paleozoic.....32  |
| 14     | 3D representation - elevations of Precambrian.....33  |
| 15     | Bedrock Valleys and the Drainage system of<br>the Northern Great Planes. ....43   |
| 16     | Cyclic Steam Stimulation Performance.....48   |
| 17     | Cold Lake Leming Pilot Pad & Well Locations.<br>Modified from Esso Resources Canada Ltd. 1985.....50  |
| 18     | Average Steam Injection rate for Leming   |

|    |  |    |
|----|--|----|
|    | Pilot Plant during 1983.....   | 52 |
| 19 | Average Steam Injection Volume for Leming<br>Pilot Plant during 1983.....  | 53 |
| 20 | Average Oil Production Volume for Leming<br>Pilot Plant during 1983.....   | 54 |
| 21 | Histogram showing the number of events<br>transferred from a Field Tape to a Scratch Tape....  | 56 |
| 22 | An event recorded by the Cold Lake Seismic<br>Array and plotted versus WWVB time..Also<br>file and block numbers as well as the date<br>are shown.....                     | 60 |
| 23 | Type "A" event recorded by the Cold Lake<br>Seismic Array. Note the strong Surface Wave<br>present and short duration of oscillation.....                                  | 61 |
| 24 | Type "B" event recorded by the Cold Lake<br>Seismic Array. Possible explosion to the NW<br>of the array.....   | 63 |
| 25 | Type "C" event recorded by the Cold Lake<br>Seismic Array. It is a sonic arrival from<br>aircraft flying.....  | 64 |
| 26 | Type "D" event recorded by the Cold Lake<br>Seismic Array. This is an earthquake of<br>magnitude 6.0 from Greece on 17 January 1983.....                                   | 65 |
| 27 | Direct plot of an "A" type event as it is<br>saved at the magnetic tape. The<br>characteristics of such an event are clearly<br>present.....                               | 68 |
| 28 | Amplitude Spectrum of 10 sec noise signal<br>before a P- arrival from station MLE. It is<br>clear that only a small amount of energy is<br>present at low frequencies..... | 70 |
| 29 | Amplitude Spectrum of a P- arrival from<br>station MLE. It is clear that the energy is<br>concentrated between 1.0 to 8.0 Hz.....  | 71 |
| 30 | Band Pass filtered "A" type event between<br>1.0 and 8.0 Hz. A significant improvement in<br>signal quality is evident.....  | 73 |
| 31 | Band Pass filtered "A" type event between<br>0.4 and 5.0 Hz. The signal appearance is<br>quite satisfactory for analysis.....  | 74 |

|    |  |     |
|----|--|-----|
| 32 | Band Pass filtered "A" type event between 0.4 and 5.0 Hz. The hand picked P- wave arrivals are indicated with arrows.....  | 75  |
| 33 | A plot of a tapered "A" type event. High amplitudes linearly decrease with time by a factor indicated to the right of the signal.....  | 77  |
| 34 | Seismograms of B 3 and B 4 February 15 (UT). Event B3 is 11 kg. of explosives detonated in a single hole at a depth of 20m.. Event B4 is a 34 kg. total charge at depth of 20m. ....   | 79  |
| 35 | Local Magnitude of "A" type events for a period starting in January 1982 to December 1986..  | 92  |
| 36 | Focal Mechanisms of an earthquake: first motion study. A small sphere is drawn around the focus of the earthquake resulting to a movement along the segment a-b. This results in compression and dilatation in opposite quadrants..... | 94  |
| 37 | Single couple (Top) and double couple fault mechanisms, with their radiation pattern of first motions for P- waves (b) and S- waves (c)....  | 95  |
| 38 | Fault orientation in relation to principal stress and strain axis. A. Normal fault, B. Thrust fault and C. Strike-slip fault. (Modified from Park, 1983). ....   | 96  |
| 39 | Focal mechanism solution for an event at depth 150m. There is ambiguity which is the fault and auxiliary plane. As seen we have a dip of 40° NE with a strike 7° NW. ....  | 99  |
| 40 | Focal mechanism solution for an event at depth 470m. It has a dip of 80° NW with a strike 32° NE. ....   | 100 |
| 41 | The logic steps ( blocks ) that the AUTOPICK routine follows in order to perform automatic analysis.....   | 106 |
| 42 | MLE station raw field data before any analysis from the AUTOPICK has been done.....  | 107 |
| 43 | Band-pass filtered data from station MLE ready to be processed by the automatic seismic recognition routine.....   | 108 |
| 44 | Modified amplitude signal of an "A" type event using the AUTOPICK routine. Most of   |     |

|    |  |     |
|----|--|-----|
|    | the DC component has been removed.....   | 109 |
| 45 | Flow chart of the AUTOPICK routine steps. These steps are done before the operation goes through the criteria routine.....   | 112 |
| 46 | Short term average of the modified time series used to detect first arrivals. The sharp change at the arrival point is evident.....  | 113 |
| 47 | Long term average of the modified time series. This function is used as a threshold criterion. It also verifies the presence of noise.....   | 114 |
| 48 | Logical steps followed by the Criteria routine. If these conditions are met an event is declared and stored.....   | 115 |
| 49 | Graphical representation of the operation used to choose the first zero crossing with respect to triggered time position.....  | 117 |
| 50 | Autopick results for an "A" type event that occurred on January 22, 1984. The arrows indicate the automatically obtained first break..   | 119 |
| 51 | Autopick results for an "A" type event that occurred on December 25, 1982. The arrows indicate the automatically obtained first break..  | 120 |
| 52 | Autopick results for an "A" type event that occurred on December 28, 1982. Noise contamination effected the stability of the routine. The results cannot be considered accurate..... | 124 |
| 53 | Autopick results for an "A" type event that occurred on January 24, 1984. No satisfactory results were obtained as can be seen by the arrows.....                                    | 125 |
| 54 | Daily occurrence of "A" type events for the period of January 1982 to December 1986.....   | 128 |
| 55 | Location of "A" type events recorded at the Cold Lake Seismic Array. ....  | 130 |
| 56 | Location of shallow "A" type events with respect to bedrock topography.....  | 134 |
| 57 | Water table level from well 1947E Burque Lake. The period is from 1980 to the end of 1986. No major variation are present.   |     |



|    |  |     |
|----|--|-----|
|    | Modified from Alberta Environment information....  | 135 |
| 58 | Earthquake epicenters for the Western Canada area. Data compiled by E.R. Kanasevich and C.M. McCloughan from GSC and USCG listings.....              | 137 |
| 59 | Focal mechanism solution for shallow events. ....  | 139 |
| 60 | Location of "A" type events at depths of 300m to 1000m.....  | 142 |
| 61 | Average steam injection rate for Leming Pilot Plant. The period covered is January 1982 to December 1986.....  | 143 |
| 62 | Frequency of "A" type events during the total period of study. Each histogram indicates the number of events recorded per month.....                 | 144 |
| 63 | Crosscorrelation between average steam injection rate and "A" type event occurrence per month. A 2 and 4.5 month lag shows the best correlation..... | 145 |
| 64 | Focal mechanism solution for events at depths 300 to 470m. ....  | 147 |
| 65 | Waste fluid disposal well locations and "A" type event epicenters at depth of 620m.....  | 150 |
| 66 | Composite focal mechanism solution for de 00:04:51 A5/5, A2/6, A45/5. ....   | 151 |

## 1. INTRODUCTION

### 1.1 MICROSEISMICITY - A REVIEW

The term seismicity refers to the earthquake activity in the field of seismology. Earthquakes of magnitude less than 3.0 are considered to be microearthquakes. Table 1 shows the earthquake magnitude spectrum and the different categories present, based on magnitude variations.

Microearthquake studies were initiated after the definition of magnitude scale by Richter in 1935. The magnitude scale is a logarithmic, narrow band (20sec.), measure of amplitude, corrected for the distance of the event.

In order to extend seismological studies to the microearthquake range, it is necessary to have a group of closely spaced and highly sensitive seismographic stations. One calls this array a microearthquake network. Usually it is operated by either telemetering seismic signals to a central recording site or by recording at individual stations.

The basic purpose of a microearthquake network is to study the nature and state of local short period tectonic processes. According to Lee et al. (1981), some applications include: monitoring seismicity for earthquake prediction purposes, mapping of active faults for hazard evaluation, exploring for geothermal resources, investigating the structure of the crust and upper mantle, studying aftershock

| Magnitude (M) | Classification        |
|---------------|-----------------------|
| $M > 7$       | Major earthquake      |
| $5 < M < 7$   | Moderate earthquake   |
| $3 < M < 5$   | Small earthquake      |
| $-1 < M < 3$  | Microearthquake       |
| $M < -1$      | Ultra-microearthquake |

Table 1.... Earthquake Classification by Magnitude.

activity, and detecting induced seismicity. In the latter category one has effects due to nuclear explosions, mining activity, filling reservoirs, fluid injection, and other artificial crustal disturbances.

Technological advances in instrumentation in the 1960s made possible the operation of seismic arrays. Many networks were developed for detection of nuclear explosions and also to discriminate these artificially made vibrations from natural teleseismic earth tremors. The largest network, no longer in operation, was the Large Aperture Seismic Array (LASA) in Montana. Four smaller arrays, that are, still in operation, were located in Eskdalemuir, Scotland; Yellowknife, Canada; Gauribidanur, India and Warramunga, Australia (Lee et al, 1981). The University of Alberta has operated several temporary networks called VASA (Variable Aperture Seismic Array). In 1966 the United States Geological Survey began the installation of a microearthquake network along the San Andreas fault system in central California. This network telemeters seismic signals from field stations to a center at Menlo Park, California. The number of stations in this array was 250 by early 1980.

These types of networks have evolved into regional and topical seismic networks for various research purposes. "Permanent" earthquake networks are those consisting of stations whose signals are telemetered into a central site reducing labor in collection and processing of seismic data

and improving the precision of timing. "Temporary" microearthquake networks are portable and developed for short duration operations.

#### 1.1.1 Permanent Networks

This type of network is used for basic research. For a given region in the world major earthquakes usually occur at intervals of years or tens of years. This requires long-term studies in order to collect the necessary data. On the other hand, in order to study microseisms, one needs high-sensitivity seismometers located within the earthquake source region. If these microseisms have shallow focal depth, less than 10km, station spacing of 10km is required in order to determine focal depths, reliably. Therefore, microearthquake networks must have densely located stations and the capability of processing large amounts of data. According to Lee et al. (1981), there are approximately 100 permanent networks in operation around the world, that follow the above characteristics for accurate detection and correct analysis. Generally, they range from a few stations to a few hundred stations.

#### 1.1.2 Temporary Networks

Temporary networks are usually arrays of portable seismographs used for reconnaissance surveys. Such portable seismographs consist of a seismometer, a method of measuring absolute time and a recorder with built in amplifier and

power supply. Such networks are used in many countries in order to study tectonic processes for a short period of time. This type of network is widely used for aftershock studies.

## 1.2 GENERAL APPLICATIONS OF MICROSEISMICITY

### 1.2.1 Aftershock Studies

One of the basic reasons for the emplacement of temporary microearthquake networks is perhaps to record aftershock activity. Because a large number of aftershocks follow a large earthquake, a plethora of data can be collected in a short time, if the array is located within 48 hours after a major event. The need for detailed studies after an earthquake is very important and requires as much data as possible. Temporary networks are deployed after a large earthquake and are in operation until aftershocks subside to a low level. In some cases if an earthquake occurs within an existing network extra portable seismographs can be used to give more accurate locations and focal mechanism solutions.

### 1.2.2 Induced Seismicity Studies

Human activity such as, testing of nuclear weapons, mining, filling reservoirs, and injecting fluid underground, may sometimes induce earthquakes. Many studies have been done related to these types of activity. During the 1960s, a

period of high nuclear testing, noticeable earthquake activity accompanied nuclear explosions. Many seismic arrays were deployed around the world to study this problem. Boucher et al. (1969), Ryall and Savage (1969) and Hamilton and Healy (1969); are among those that studied nuclear explosion induced earthquakes.

Stress concentrations are created during mining and rockbursts indicating strain release associated with mining operations. Microearthquake networks very close to the source have been used to study such tremors. Cook (1976), Hardy and Leighton (1977, 1980), give a good summary of such studies.

Moderate size earthquakes have been triggered in many cases by filling of reservoirs, Gough and Gough (1970, 1976) give a good analysis of the Lake Kariba (Rhodesia) dam associated earthquakes. In some cases seismicity in the areas has increased, showed no change or even decreased. Gupta and Rastogi (1976), Simpson (1976) give good reviews on this subject. A few microearthquake networks in such cases have been deployed before, during and after reservoir filling, in order to understand this problem in detail.

Another area of induced seismicity is fluid injection and extraction. The best known case was near Denver, Colorado where detailed studies of such seismicity were carried out by Healy et al. (1968). Other cases are reported by Teng et al. (1973), Ohtake (1974), Fletcher and Sykes (1977). In these cases seismicity was shown to be related to

fluid injection, and used in determining focal mechanisms and direction of stresses.

### 1.2.3 Geothermal Exploration

Microearthquakes have been observed in many geothermal areas, Ward (1972), Combs and Headly (1977), Majer and McEvilly (1979). Based on the correlation between microseismicity and geothermal activity, microearthquake networks can be a positive approach to geothermal exploration. By detailed mapping of microseisms, active faults may be located along which steam and hot water are brought to the earth's surface as noted by Lee et al. (1981). In other cases, Iyer (1975, 1979), Iyer and Stewart (1977), array processing techniques were used to study seismic noise anomalies in order to indentify potential geothermal sources. In these cases, P-arrival delay times across the microearthquake network were used in searching for anomalous regions in the crust and upper mantle.

### 1.2.4 Crustal and Mantle Studies

Velocity structure of the crust and mantle has been determined in some cases using arrival times and hypocenter data from microearthquake networks. Such data are obtained from local, regional and teleseismic earthquakes and explosions recorded at regional distances. Many studies use microearthquakes and explosions as sources to construct time-distance plots. These are interpreted by the usual



refraction method.

Mizoue (1971) studied the crustal structure of the Kii Peninsula using data from deep crustal reflections and from direct and refracted waves. Hadley and Kanamori (1977) using microseismic data, and data from artificial sources and teleseisms studied the seismic velocity structure of the Transverse Ranges in southern California. Seismic properties of the San Andreas fault zone have been determined (Kind, 1972; Healy and Peake, 1975).

Other techniques such as the time-term method have been applied to microseismic networks (Hamilton, 1970; Wesson et al., 1973b). Direct measurement of apparent velocities of P-waves have been made and from these, crustal structure under the network has been established (Kanamori, 1967; Burdic and Powell, 1980).

Computer advances in recent years have improved modeling techniques. Methods such as modeling velocity variation with depth (Aki and Lee, 1975), nonlinear least squares techniques using P - and S - readings (Mitchell and Hashim, 1977) to calculate apparent velocities. Inversion of arrival times to obtain three dimensional velocity structure (Aki et al., 1976), have been applied to microearthquake network data.

### 1.3 SPECIFICATION OF THE STUDY

A number of earth tremors were reported by residents of the Cold Lake area of east-central Alberta, Canada, in 1977 and 1978. This gave rise to a six month research study beginning in December 1978 by Dr E. R. Kanasewich of the University of Alberta using an array of three vertical motion seismometers. The array was installed on the Duckett farm near Ethel Lake (54.53 N, 110.331 W) and recorded data continuously from December 2, 1978 to June 19, 1979. The initial purpose of this study was to establish the level of seismic activity and to determine the azimuth and phase velocity of any local earth tremors.

Over 698 local impulsive events were observed during the initial recording period. Of these 172 were identified as due to sonic booms and 21 due to atmospheric waves generated by bombs set off on the military range, north of the Cold Lake area. The nature and location of the remaining local events was not established, except that they were generated locally within the crust. In addition 112 teleseismic events were also observed. During the recording period, at least one event was felt by local residents and recorded simultaneously by the array. Several others were reported, but not observed on array records. No structural damage was reported that could be associated with the seismicity. None of the events was of such an intensity as to have been recorded outside the Cold Lake area.

In view of the rather large number of unexplained local events and the objective documentation of felt tremors, Alberta Environment decided to assume responsibility for continuous seismic monitoring in the region. The issue had also been raised publicly at the Energy Resources Conservation Board (ERCB) hearings into the Esso Resources Canada Limited (ERCL) application for expansion of the existing pre-production pilot plants to full production status and at the Cold Lake Beaver River Water Demand Study public meeting held by the Planning Division of Alberta Environment (Kanasewich et al., 1982). In the fall of 1979, the Earth Sciences Division (ESD) and the Research Management Division (RMD) of Alberta Environment agreed to the proposal and initiated the first phase for a state of the art digital seismic monitoring array near Cold Lake.

ESD assumed project management responsibilities during design and construction of the array and agreed to sustain its maintenance throughout its active service life. RMD financed the construction of the array and assumed responsibility for the research program required for interpretation of data derived from the array. ESD also accepted responsibility for dissemination of data through its existing groundwater information service. The data was to be analyzed in the Seismology Laboratory at the University of Alberta under the direction of Professor E. R. Kanasewich.

A telemetered seismic array of 10 sensors at 6 sites was established by Alberta Environment in October and November, 1981. The recording system underwent extensive changes and testing during the initial period from November 13, 1981 to January 18, 1982. It was officially opened by Alberta Environment on October 1, 1982 but all 10 sensors were not in operation until December 21, 1982. Figure 1 shows the study area and the locations of the seismic stations.

It is the aim of this study to undertake an overall analysis of the locally originating microtremors. A uniform method of filtering, display, and timing the initial compressional and shear waves has been established. Epicentral and hypocentral locations, and focal mechanism solutions were carried out in order to correlate these events with potential sources. Sufficient background information has been obtained related to hydrogeology and the heavy oil recovery projects in the area. A study is to be made on the hypothesis that some events could be due to localized stress in the geomorphological feature with possible triggering mechanism due to disturbances of hydrology and pore pressure. Other events could be related directly to the steam injection or oil production at the level of the Clearwater Formation from the Heavy Oil Recovery Plants. The above hypothesis could lead to the separation of the local microearthquakes into two or more sub-categories.

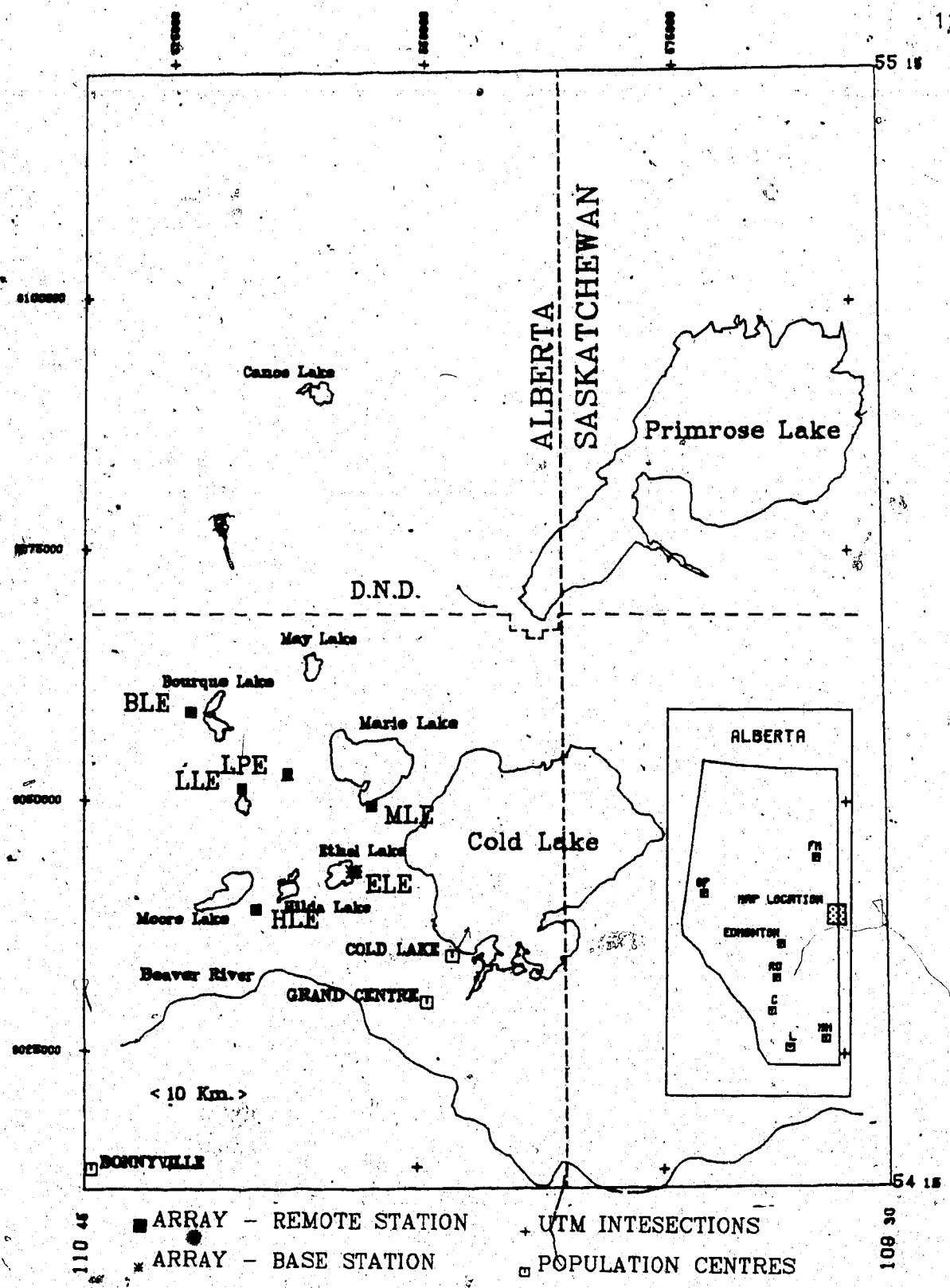


Figure 1... Cold Lake Induced Seismicity Monitoring Array.

#### 1.4 INSTRUMENTATION AND OPERATIONS

The instrumentation of the array was in accordance with specifications requested by Dr. E. R. Kanasewich. The detailed specifications were drawn up by Druid Electronics in March, 1980. Williams Electronics was responsible for the installation of the FM-UHF radio telemetry links while Druid Electronics installed the analog and digital recording system at the base station and the digital playback system in room 647, Physics Building, University of Alberta. The characteristics of the digital seismic monitoring array are shown in Table 2 and Table 3.

The sensors are Geotek -500 short-period seismometers with a sensitivity of 450 V/(m/sec). These are sealed in "bombs" at depths of 36 to 107 meters. The wells were drilled through the glacial drift into bedrock, cased and a cement plug was set at the bottom. Considerable difficulty was encountered in obtaining good coupling between the seismometers and the cement pad or bedrock. The holes were redrilled in September, 1982, and more satisfactory coupling was obtained. The seismometers are enclosed in a specially machined case to withstand the water pressure. The base station has five sensors including three vertical seismometers forming a tripartite array. One of the vertical sensors and two horizontal sensors form a unit and are seated at a depth of 1 meter (Kanasewich, 1983). The locations of these stations is shown in Figure 1 and listed in Table 4.

1. Recording System

- Recording Capacity - 48 Hr. (4 drives)
- Channel Capacity - 10 seismic - 1 High Frequency, 9 Low Frequency 1 Time Code
- Sampling Rate - 1 sample/6 ms High Frequency Seismic  
1 sample/18 ms Low Frequency Seismic  
1 sample/90 ms Time Code (LWVS)
- Recording Medium - 9 Track 1600 BPI ANSI standard IBM compatible magnetic tape
- Block Length - 4992 bytes
- Format - 68 bytes preamble  
4924 bytes data delta compressed 8 bits compressed/16 bits expanded
- Digitizing Accuracy - 12 bit bipolar A/D
- Bandwidth - Fast Seismic Channel 82Hz  
Slow Seismic Channel 27Hz  
Time Code Channel 5Hz
- Time Synchronization - Derived from quartz WWVB synchronized clock  
Relative accuracy : 5 ms  
Absolute accuracy : 10 ms from UTC

2. Local Display System

- 6 24 hour single channel drum recorders

3. Telemetry

5 channels are telemetered over FM UHF radio links. Seismic data is first converted to AF-FM within voice band then transmitted over the radio links. This AF-FM is discriminated at the base station.

## Links

- Direct Radio Links site 2 - 1  
3 - 1  
4 - 1
- Relay Links site 5 - 4 - 1  
6 - 4 - 1

FM UHF Frequencies 453.4125 MHz, 453-6625 MHz, 453.9125 MHz

FM UHF Audio Band Width 5KHz

AF FM Carrier Frequencies 680 Hz, 1020 Hz, 2040 Hz, 2380 Hz

AF FM Deviation  $\pm 125$ Hz

AF FM Signal Band Width 25Hz

AF FM Dynamic range 60dB

4. Seismometers and Amplification

Sensitivity 450 V/m/s  $\pm 5\%$

Gain Available 60 to 120dB in 6dB steps

Band 0.1-25 Hz Low Frequency Seismic Channel  
0.1-100 Hz High Frequency Seismic Channel

5. Array Structure

5 remote channels (one vertical seismometer each) Telemetered to base station - all seismometers in cased holes and positioned at bottom of drift.

5 local channels at base station

- 2 vertical seismometers in cased holes positioned at bottom of drift
- 1 vertical seismometer at 1 metre depth
- 1 North seismometer at 1 metre depth
- 1 East seismometer at 1 metre depth

Note: 1 of the local vertical downhole seismometers used for high frequency channel.

Table 2.... General system specifications Cold Lake Seismic Recording System. Installed October, 1981.

| Channel | Sampling Rate | Site | Description                                 | Designation | RF FM    | AFFM | Helicorder |
|---------|---------------|------|---|-------------|----------|------|------------|
| 1       | 6 ms          | 1    | East field Duckett Farm Ethel Lake Downhole | ELEH        | N/A      | N/A  | No         |
| 2       | 18 ms         | 1    | Shallow vertical Duckett Farm Ethel Lake    | ELEZ        | N/A      | N/A  | No         |
| 3       | 18 ms         | 1    | Shallow North Duckett Farm Ethel Lake       | ELEN        | N/A      | N/A  | No         |
| 4       | 18 ms         | 1    | Shallow East Duckett Farm Ethel Lake        | ELEE        | N/A      | N/A  | No         |
| 5       | 18 ms         | 1    | South pines Duckett Farm Ethel Lake         | ELE         | N/A      | N/A  | 1          |
| 6       | 18 ms         | 6    | Disposal well near Leming Plant             | LPE         | 453.9125 | 2380 | 6          |
| 7       | 18 ms         | 5    | Bourque Lake                                | BLE         | 453.4125 | 2040 | 5          |
| 8       | 18 ms         | 4    | Leming Lake Gas well                        | LLE         | 453.6625 | 1700 | 4          |
| 9       | 18 ms         | 3    | Bibeau's cottage Marie Lake                 | MLE         | 453.9125 | 1020 | 3          |
| 10      | 18 ms         | 2    | Roux's Farm                                 | HLE         | 453.4125 | 680  | 2          |
| 11      | 90 ms         | N/A  | WWVB code                                   | N/A         | N/A      | N/A  | No         |

Table 3..... Channel List of the Cold Lake seismic stations



## COLD LAKE ARRAY - STATION LOCATIONS

TABLE 4A

| <u>STATION</u><br><u>Code</u> | <u>SITE</u>   | <u>LATITUDE</u><br><u>N</u> | <u>LONGITUDE</u><br><u>W</u> | <u>SURFACE-ELEV</u><br><u>Meters</u> |
|-------------------------------|---------------|-----------------------------|------------------------------|--------------------------------------|
| BLE                           | BOURQUE LAKE  | 54.6776                     | 110.5823                     | 648.4                                |
| LLE                           | LEMING LAKE   | 54.6074                     | 110.5014                     | 599.9                                |
| LPE                           | LEMING PLANT  | 54.6208                     | 110.4302                     | 601.7                                |
| HLE                           | HILDA LAKE    | 54.5014                     | 110.4798                     | 557.8                                |
| MLE                           | MARIE LAKE    | 54.5938                     | 110.3007                     | 578.2                                |
| ELE                           | ETHYL LAKE    | 54.5321                     | 110.3299                     | 545.2                                |
| ELEH                          | ETHYL LAKE    | 54.5344                     | 110.3243                     | 545.8                                |
| ELEZ                          | ETHYL LAKE    | 54.5344                     | 110.3243                     | 545                                  |
| ELEN                          | ETHYL LAKE    | 54.5344                     | 110.3243                     | 545                                  |
| ELEW                          | ETHYL LAKE    | 54.5344                     | 110.3243                     | 545                                  |
|                               | Array centre: | 54.5892                     | 110.4364                     |                                      |

TABLE 4B

## UNIVERSAL TRANSVERSE MERCATOR GRID [UTM]

| <u>STATION</u><br><u>Code</u> | <u>SITE</u><br><u>No.</u> | <u>CHANNEL</u><br><u>No.</u> | <u>NORTHING</u><br><u>Meters</u> | <u>EASTING</u><br><u>Meters</u> | <u>ELEV</u><br><u>SENSOR</u> |
|-------------------------------|---------------------------|------------------------------|----------------------------------|---------------------------------|------------------------------|
| BLE                           | 5                         | 7                            | 6 058 777.0                      | 526 936.1                       | 541.7                        |
| LLE                           | 4                         | 8                            | 6 051 004.9                      | 532 207.9                       | 563.9                        |
| LPE                           | 6                         | 6                            | 6 052 527.5                      | 536 796.2                       | 549.9                        |
| HLE                           | 2                         | 10                           | 6 039 219.9                      | 533 688.0                       | 481.6                        |
| MLE                           | 3                         | 9                            | 6 049 605.3                      | 545 183.9                       | 489.2                        |
| ELE                           | 1                         | 5                            | 6 042 711.9                      | 543 363.3                       | 481.2                        |
| ELEH                          | 1A                        | 1                            | 6 042 979.9                      | 543 723.2                       | 544                          |
| ELEZ                          | 1B                        | 2                            | 6 042 937.1                      | 543 271.1                       | 544                          |
|                               | Array centre:             |                              | 6 048 774.4                      | 536 362.6                       |                              |

TABLE 4C

## THREE DEGREE TRANSVERSE MERCATOR GRID [3TM]

| <u>STATION</u><br><u>Code</u> | <u>COMPONENT</u> | <u>DEPTH</u><br><u>Meters</u> | <u>NORTHING</u><br><u>Meters</u> | <u>EASTING</u><br><u>Meters</u> |
|-------------------------------|------------------|-------------------------------|----------------------------------|---------------------------------|
| BLE                           | Vertical         | 106.7                         | 6 060 595.4                      | 26 944.1                        |
| LLE                           | Vertical         | 36.0                          | 6 052 820.9                      | 32 217.6                        |
| LPE                           | Vertical         | 51.8                          | 6 054 344.0                      | 36 807.3                        |
| HLE                           | Vertical         | 76.2                          | 6 041 032.4                      | 33 698.1                        |
| MLE                           | Vertical         | 89.0                          | 6 051 420.9                      | 45 197.4                        |
| ELE                           | Vertical         | 64.0                          | 6 044 525.5                      | 43 376.3                        |
| ELEH                          | Vertical         | 64.0                          | 6 044 793.6                      | 43 736.3                        |
| ELEZ                          | Vertical         | 1.                            | 6 044 750.6                      | 43 284.2                        |
| ELEN                          | Horizontal       | 1.                            | 6 044 750.9                      | 43 284.2                        |
| ELEW                          | Horizontal       | 1.                            | 6 044 750.9                      | 43 284.2                        |

Table 4.... Cold Lake Array station locations. The listings are in three different coordinates.

Each remote site has its own housing and antenna a short distance away from the well site. A block diagram of a remote station is shown in Figure 2. The huts are unheated and powered by either AC mains or propane direct conversion electrical power source. The radio-telemetry uses UHF-FM transmitters on frequencies of 453.4125, 453.6625, and 453.9125 MHz. Station LLE has a radio repeater to retransmit data from stations BLE and LPE (Figure 2). The signals are relayed to the base station with Western Radio 30 watt transmitters. The base station is on the Duckett Farm at Ethel Lake (ELE). The seismic signals are amplified by Geotech 42.50 seismic amplifiers with a pass-band of 0.2 to 25 Hz and are multiplexed with an audio carrier by a Geotech 46.22 system. The carrier frequencies are 2380, 2040, 1700, 1020, and 680 Hz. The AM-FM signal band width is 25 Hz, and the dynamic range is 60 dB (Figure 3).

The base station has 3 UHF receivers and 5 discriminators for demodulation. The analog data recorded for the 5 remote sites and one channel at the base station is stored in analog form on Helicorder recorders. A sixteen channel sample and hold device is used to obtain quasi-simultaneous (11 channels at 40,000 per second) samples of all channels before conversion from analog to digital form as 12 bit bipolar words in excess binary (2048) format. Nine of the channels are sampled every 18 milliseconds (55.56 Hz). The sensor from station ELEH is sampled every 6 milliseconds at a sampling rate of 166.7 Hz.

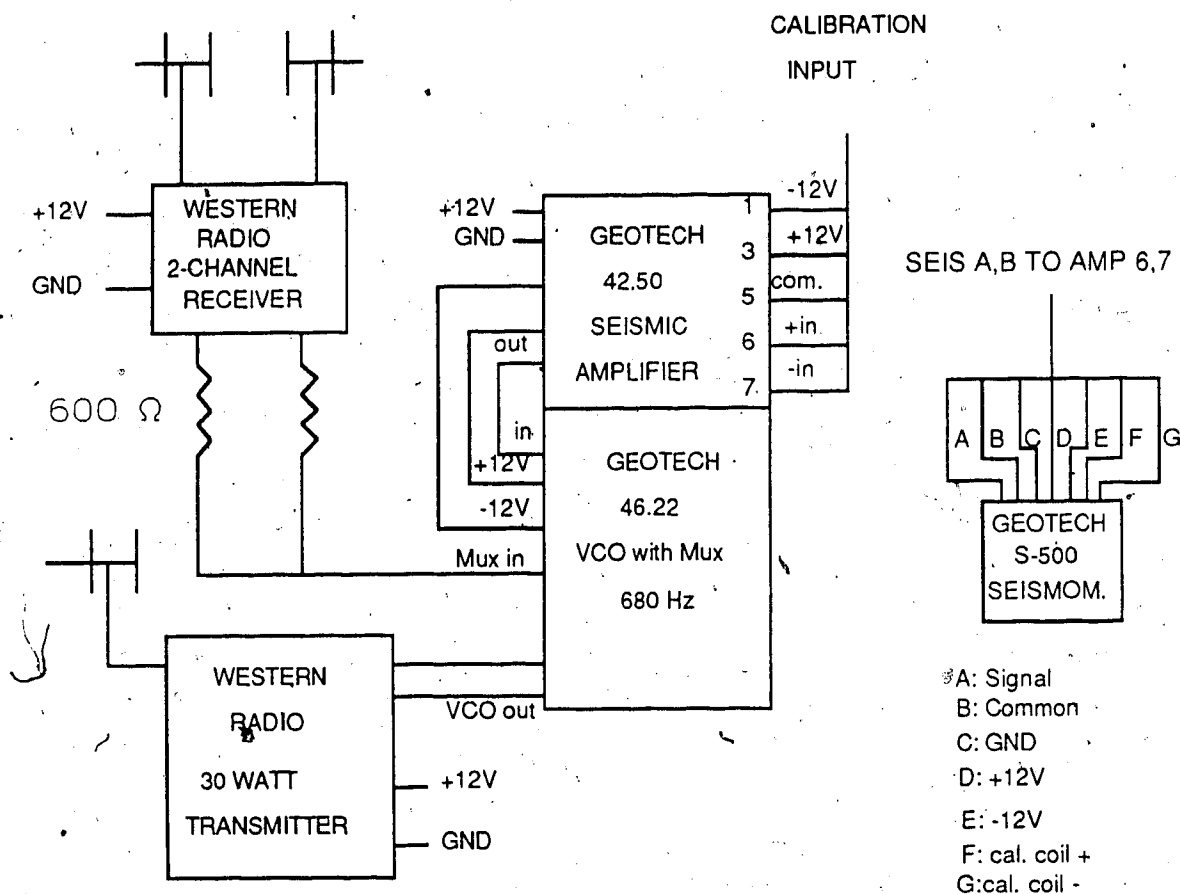


Figure 2.... Remote Field Station Configuration and S-500 Seismometer Discription. Modified from Druid Electronics Design.

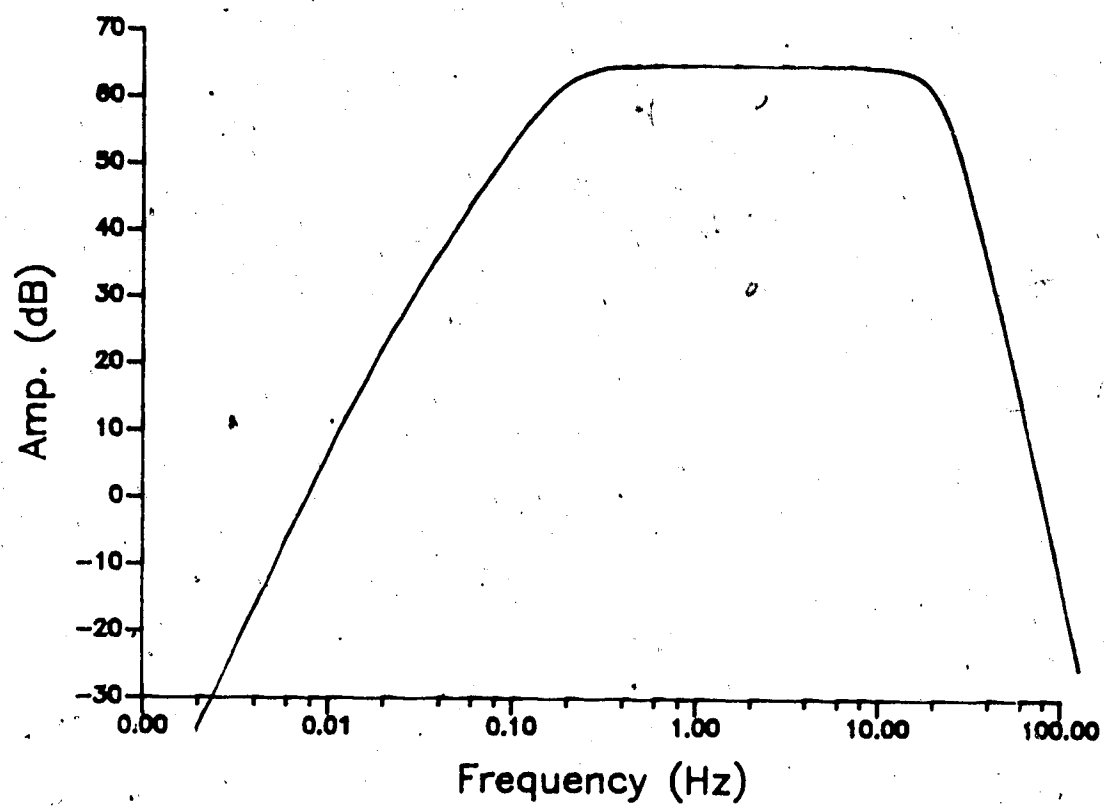


Figure 3..... Amplitude Response of Amplifier.

to retain information on high frequency components from local events. Figure 4 shows the operation of the base station.

The data is formatted by a RCA 1802 and a TI 990/101 microcomputer before being stored on tape by one of two 9-track, 1600 bpi Kennedy 9000 magnetic tape transports. Whenever possible the digital data is stored as one byte on the basis of the first difference between two adjacent words (delta compression). First differences on compressed words range from -120 to +119. Each block has a maximum of 4992 bytes of data, rarely attained. A preamble of 68 bytes containing the block number, an 8 byte time code correct to 1 ms obtained from a WWVB receiver, the first digital word as two bytes (in 16 bits) for each channel at the block start time. The time code includes the day of the year, hour, minute, second and milliseconds. The Kinematics N.B.S. receiver clock controls a quartz clock which maintains timing accuracy if the WWVB signal fails. The data is stored as 8 bit words in compressed format or a 16 bit word. An uncompressed word is identified by the presence of a hex F (1111) in the first nibble. Depending on the degree of compression, 1 block of data will normally contain 5-7 seconds of real time information.

Typically the first tape of the day will contain 15 hours of data and a maximum of 7800 blocks. The second tape will run for 9 hours and contain 4700 blocks. Two tapes are collected daily at the base station and sent by Loomis

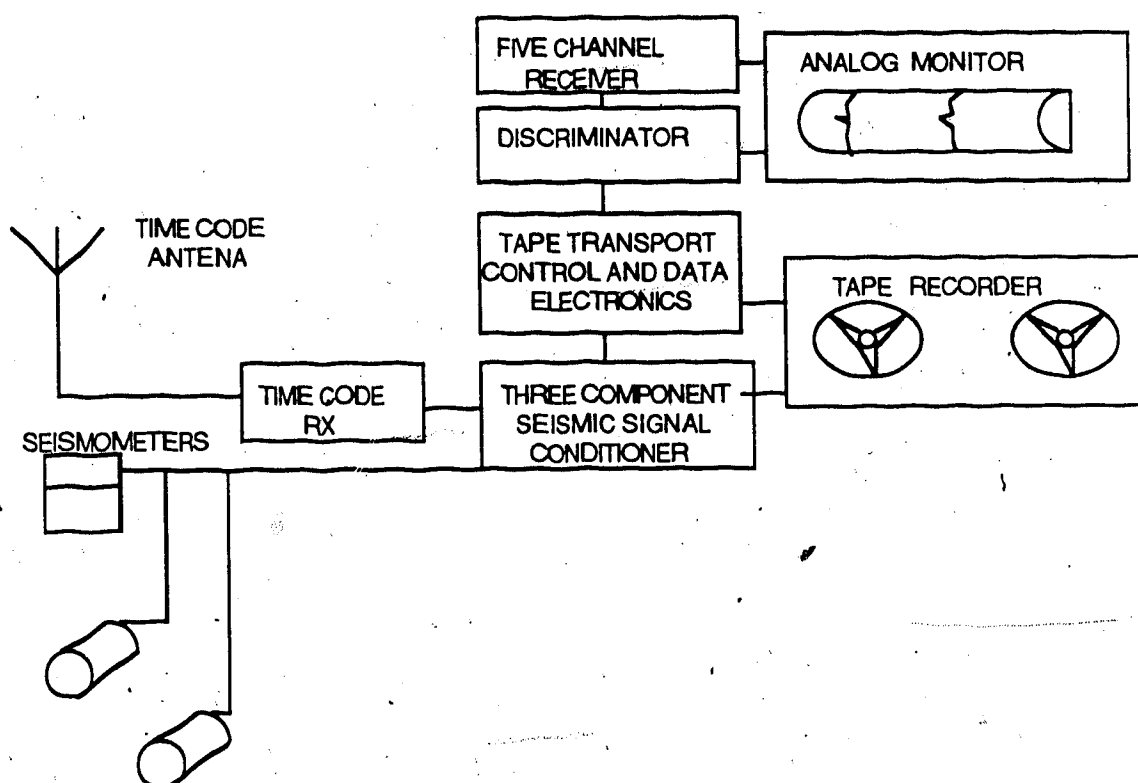


Figure 4..... Base Station ELE configuration and operation.  
Modified from Druid Electronics Design.

Courier Service to the Cold Lake Processing Center at the University of Alberta. Approximately 800 tapes are collected per year. This represents nearly  $200 \times 10^9$  bits of digital data. The station performance on a daily basis is shown in Figure 5.

The playback system in the Physics Building at the University of Alberta consists of two Kennedy 9000 read-write tape transports, a TI 990/10 minicomputer with two 8 inch floppy disc drives and a video monitor. In addition there is a low speed digital flatbed pen plotter (Tektronix 4662 Interactive Digital Plotter), a dot matrix printer (Digital Decwriter IV) and a 14-channel Xerox Versatec (V-80) electrostatic plotter. The overall operation of the system is shown in Figure 6.

### 1.5 GEOLOGY AND HYDROGEOLOGY OF THE STUDY AREA

Generally, in terms of geological evolution, in the Alberta Plains and the Foothills, a major depositional hiatus occurred following the Devonian Period and before the renewal of sedimentation in the Cretaceous. This type of erosional surface truncates the Jurassic, Mississippian and Upper Devonian strata. Cretaceous beds were deposited on the Paleozoic erosional surface with a slight angular unconformity. The Lower and Upper Cretaceous are separated by the Fish Scales marker zone. During Tertiary time only minor deposition occurred (Gold, in prep.).

# Digital Performance

■ 100 Availability  
 - 50 + Availability  
 x 50 Availability  
 - 50 - Availability  
 N/A Availability

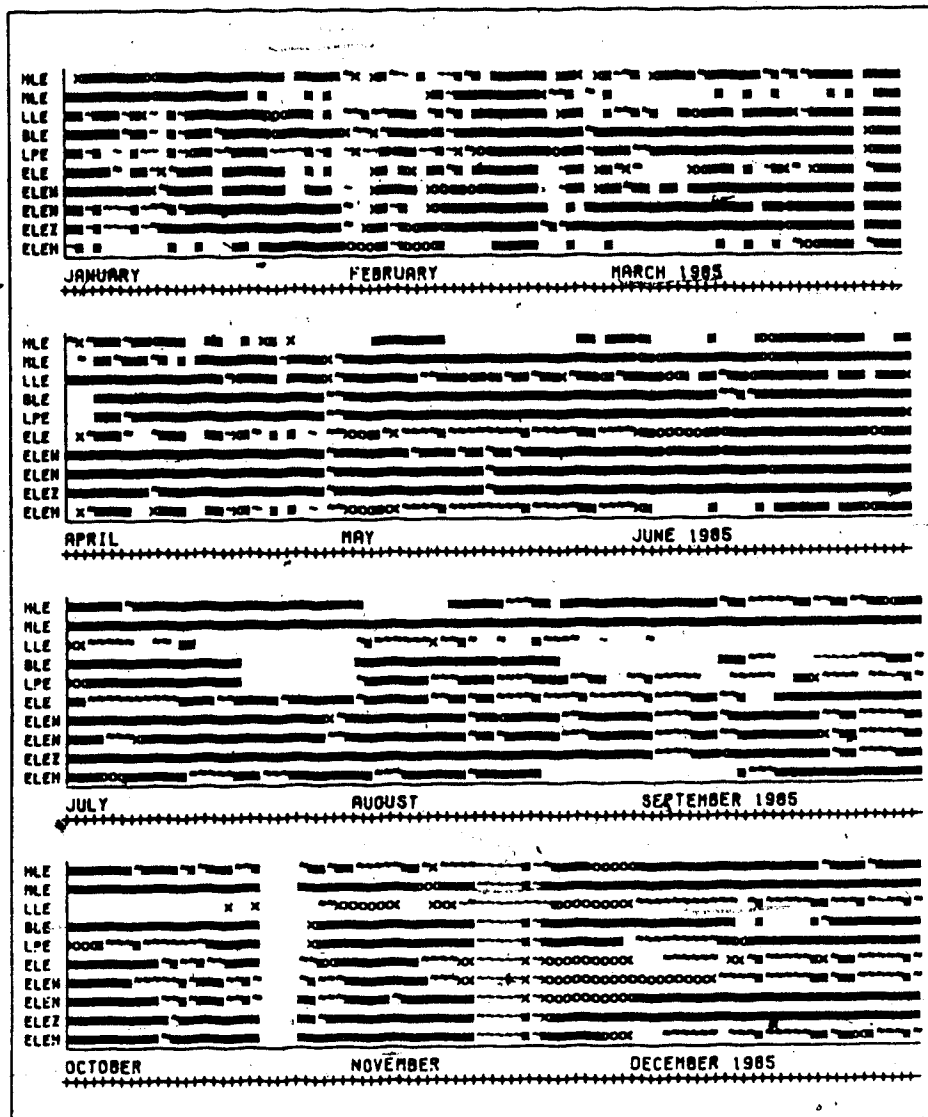


Figure 5..... Daily digital recording performance on the Cold Lake Seismic Array for 1985.



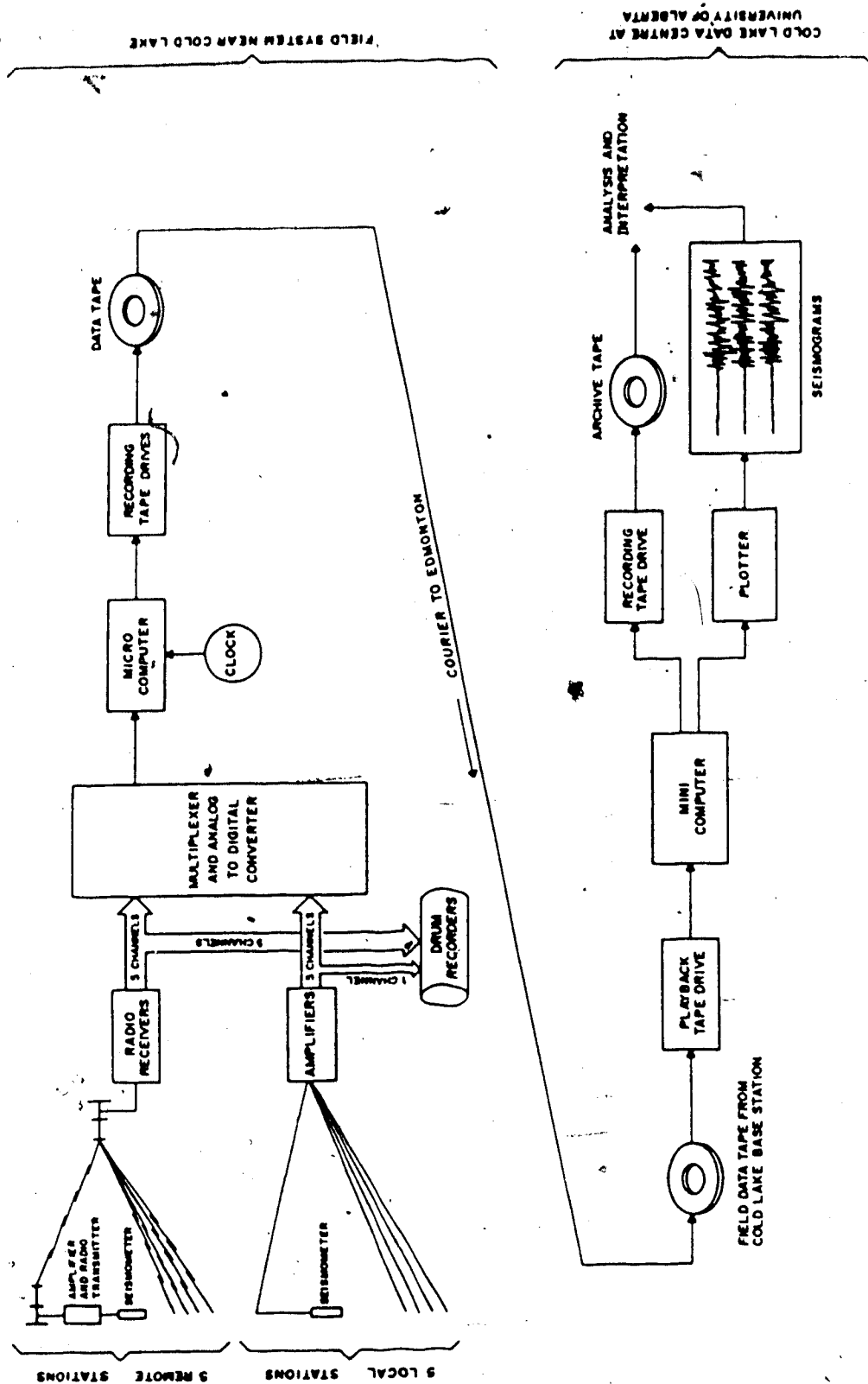


Figure 6.... Block diagram of the instrumentation at the field sites, the base station near Cold Lake and the Cold Lake Seismic Data Centre at the University of Alberta, Edmonton (After Kanasewich et al., 1984).

The topography of the Cold Lake area varies from 535 to 650 meters above sea level (Figure 7). The surface deposits consist of muskeg, glacial till, and morainal material (Figure 8) which range in thickness from 25 to 150 meters (Andriachek and Fenton, 1983). A geomorphological characteristic of the study area is a number of buried valleys which cut through the Upper Cretaceous sands and shales. Figure 9 illustrates these valleys, using data from Figures 7 and 8. The grid of data points was smoothed with a simple digital filter, and compared to the bedrock map by Gold (in prep.). This Cretaceous erosional surface is of interest to this study because one hypothesis relates the seismic microtremors as originating at this level. Detailed discussion of these features will be presented later in this study.

Heavy Oil Production is obtained from the Lower Cretaceous beds which occur below the Base of Fish Scale zone (Figure 10). Oil production is obtained below the Colony Member (Figure 11), mainly from the Clearwater Formation of the Upper Mannville Group, which is of Albian age (100-116 m.y.). Some oil and gas also occurs in two units of the Grand Rapids formation above the Clearwater. Oil also occurs in the McMurray Formation below the Clearwater (Figure 12) (Strom and Dunbar, 1979). All these horizons can be seen from the figures to have a gentle dip to the southwest.

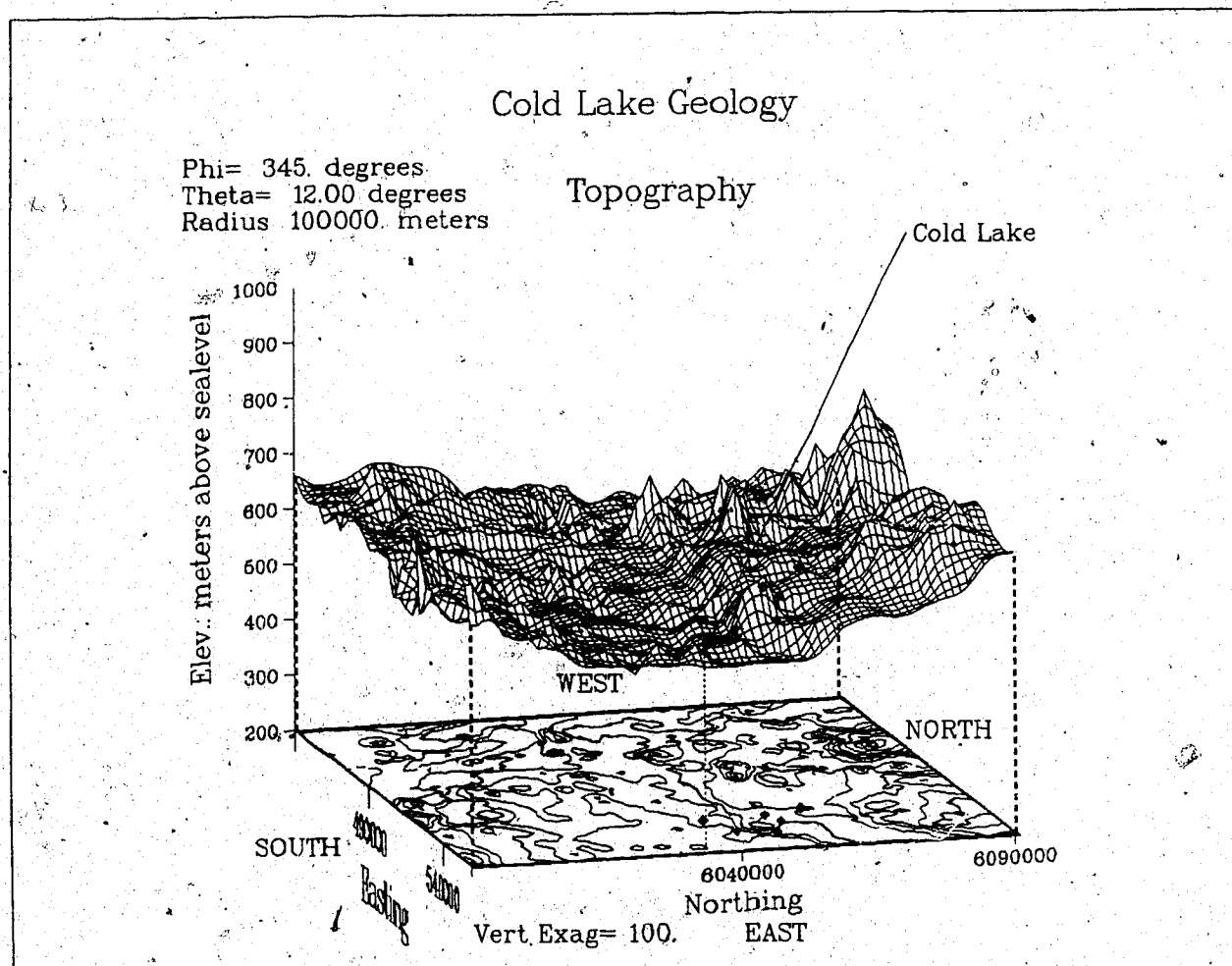


Figure 7.... 3D representation of Cold Lake area Topography.

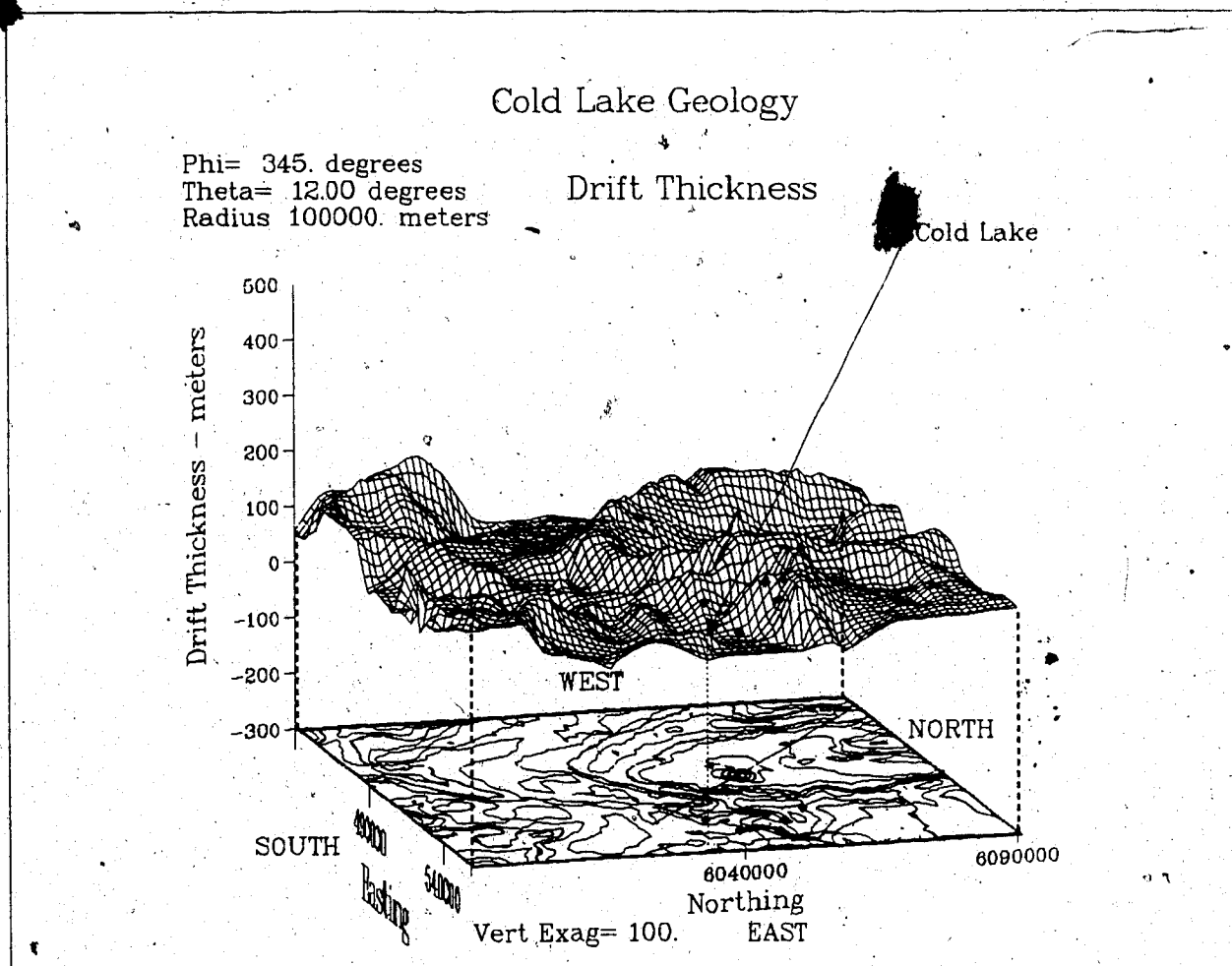


Figure 8.... 3D - Thickness of drift cover, Cold Lake area.

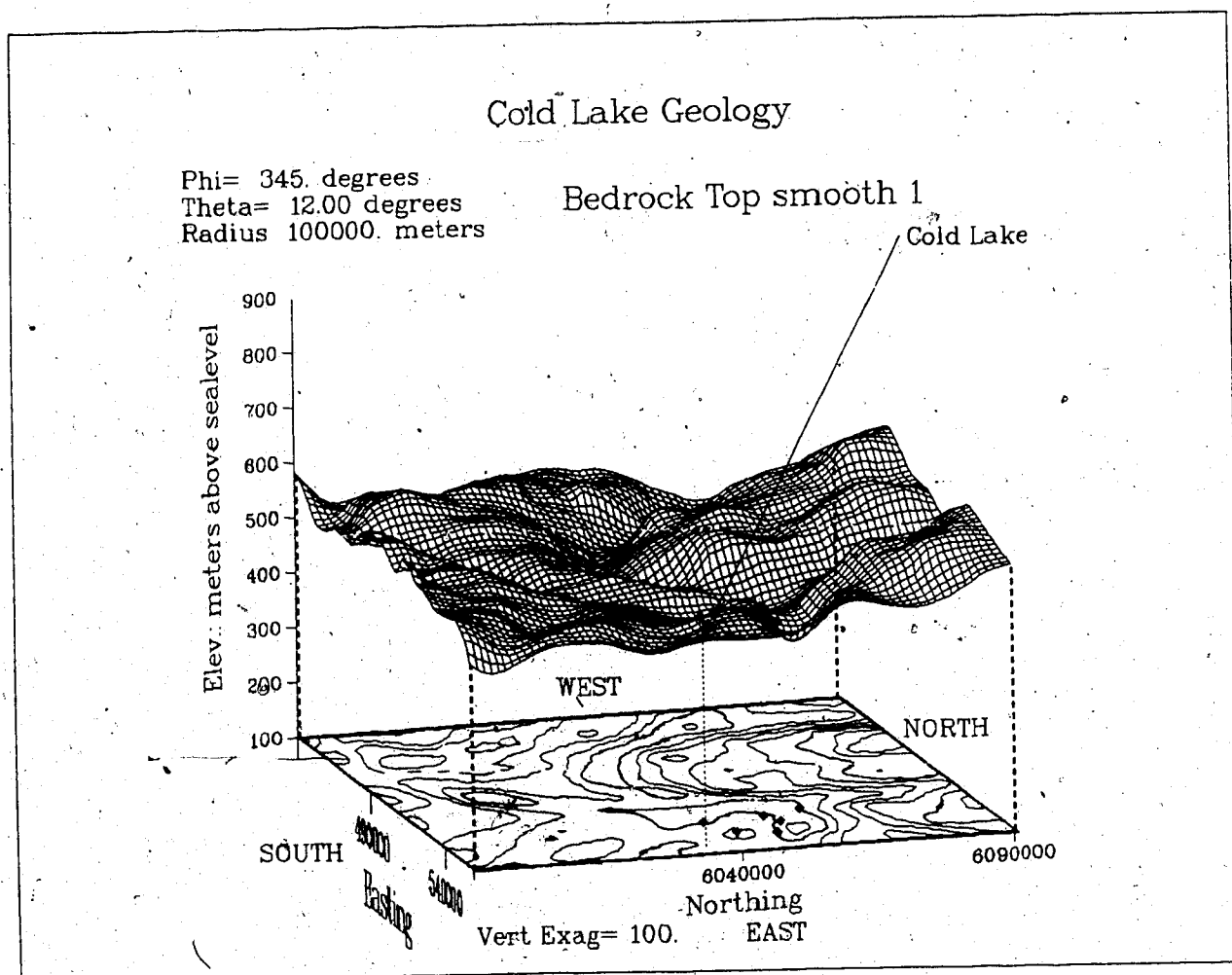


Figure 9.... 3D - Top of smoothed bedrock in the Cold Lake area.

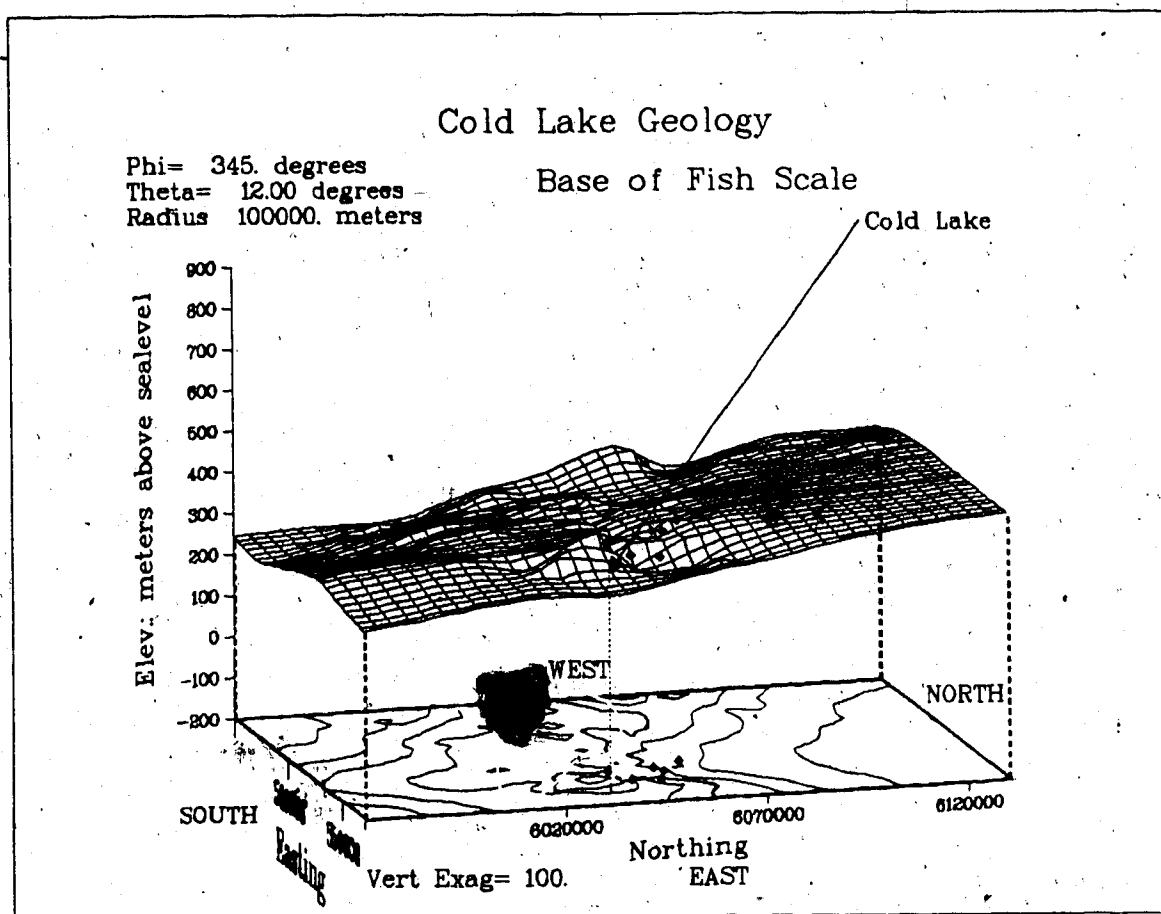


Figure 10.... 3D representation of the elevation of Base of Fish Scales.

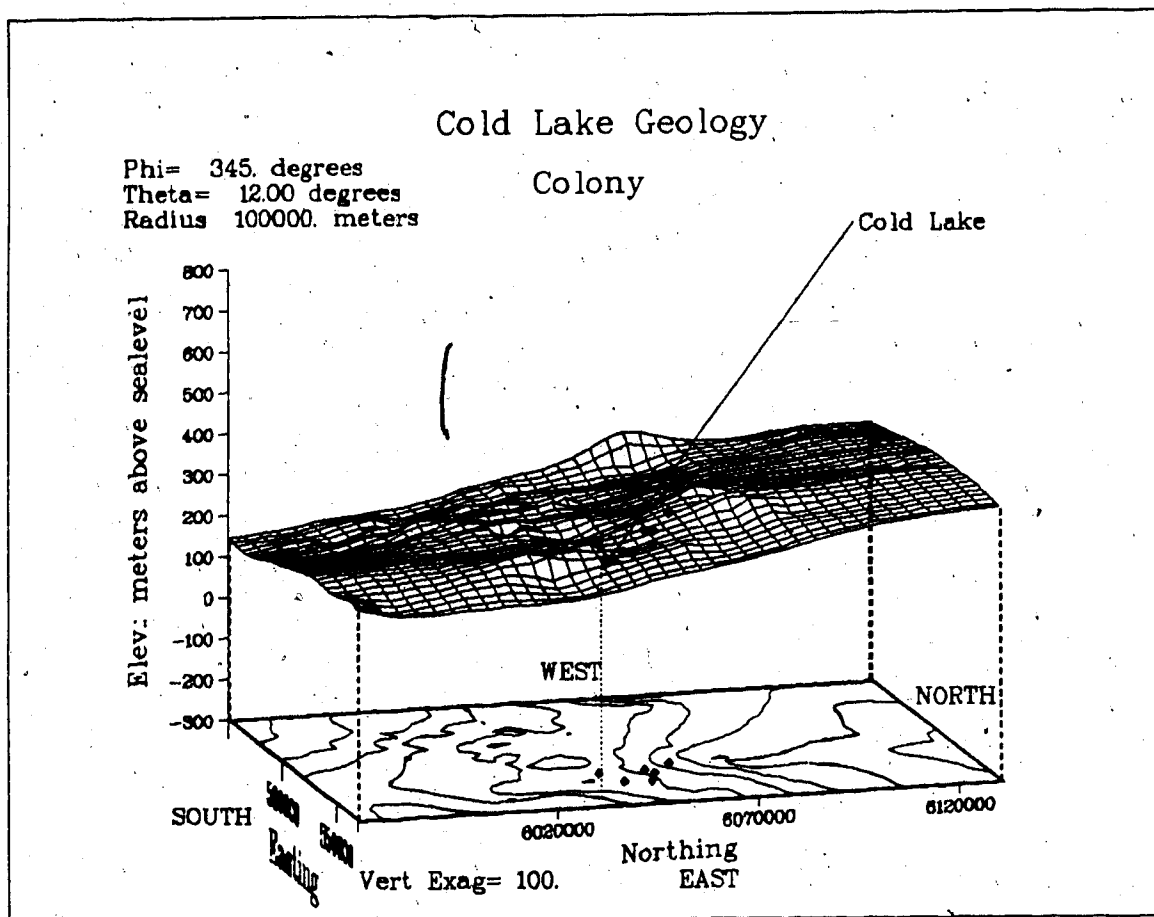


Figure 11.... 3D representation of the top of Colony Member.

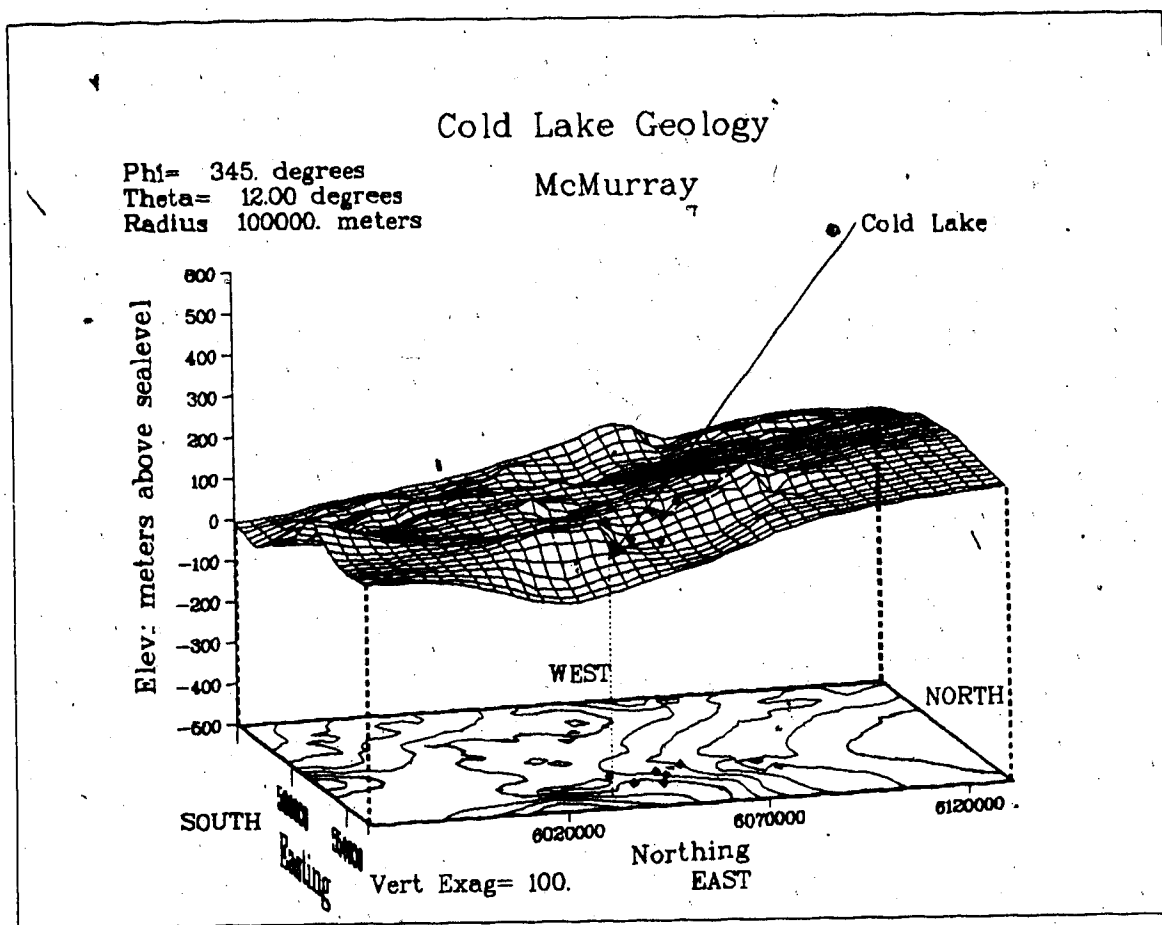


Figure 12.... 3D representation - elevations of McMurray.



There is only a small amount of information from a few wells drilled into Paleozoic sediments (Figure 13). Figure 14 shows that the Precambrian crystalline basement rocks have been highly eroded so that this surface is a smooth plane with no extreme variations.

In the figures above, all the information was obtained from well information. The three-dimensional plots obtained from wells represent the horizons shown in Table 5.

As mentioned above, the two zones of particular interest in this study are the Lower Cretaceous Period, and the period involving the glacial and preglacial history.

#### 1.5.1 Lower Cretaceous

In most of Western Canada's sedimentary basin, Lower Cretaceous rocks are thick in the Foothills area and thin out to the east. These rocks have been divided into three units; the Lower Mannville, the Upper Mannville, and the Lower Colorado.

The Lower Mannville is a basal fill deposit and is the first sedimentation after a long period of erosion. These rocks are dominantly non-marine in origin. The topographic setting of the Early Cretaceous time was similar to the Arctic MacKenzie delta, with uplifted mountains ranges in the Cordillera to the west, but the present day Rocky Mountains had not yet been formed.

The Lower Mannville deposits were a product of erosion of the Cordillera, and continental deposition towards the

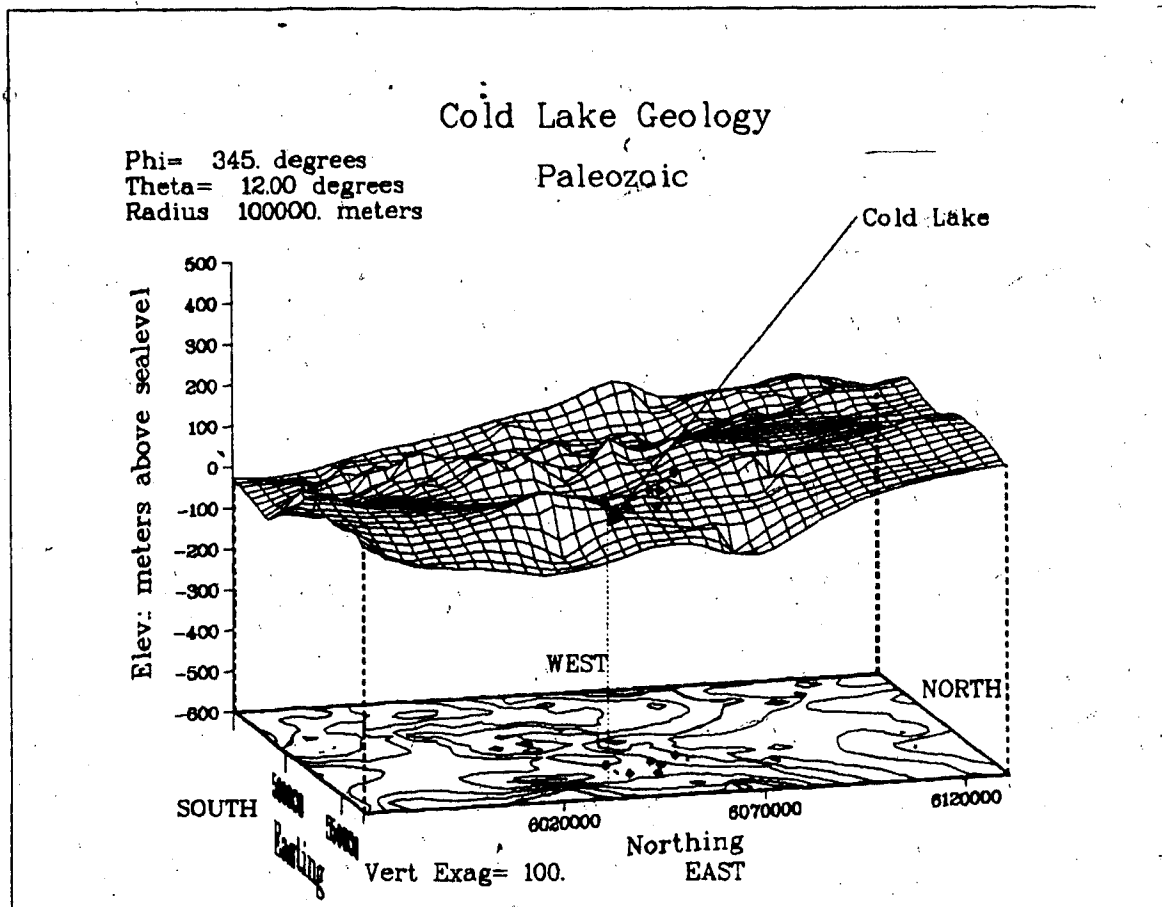


Figure 13.... 3D representation - elevations of Paleozoic.

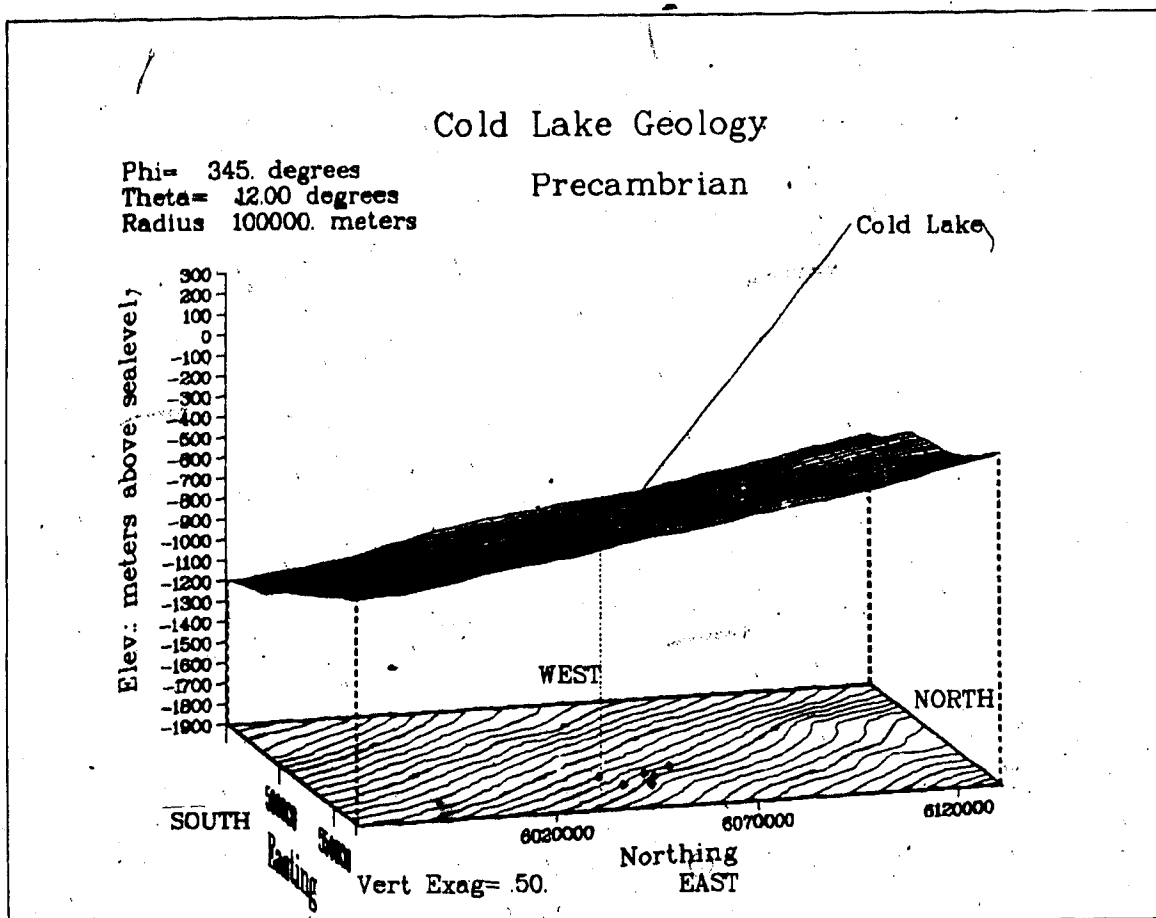


Figure 14.... 3D representation - elevations of Precambrian

| ERA OR PERIOD | GROUP | FORMATION OR MARKER |
|---------------|-------|---------------------|
|---------------|-------|---------------------|

|                |              |                                  |
|----------------|--------------|----------------------------------|
| Recent         | ---          | Topography                       |
| Tertiary       | ---          | Paskapoo                         |
| Up. Cretaceous | Post         | Wapiti                           |
| "              | Colorado     | Second White<br>Speckled Shale   |
| L. Cretaceous  | Colorado     | Base Fish Scales                 |
|                | U. Mannville | Top of Colony Mem.<br>Clearwater |
|                | L. Mannville | Top of McMurray                  |
| Paleozoic      | -----        | -----                            |
| Precambrian    | -----        | -----                            |

Table 5.... Geological Horizons used for the analysis of  
microseismicity in Cold Lake area.

east. The McMurray formation is within this group. At the end of Lower Mannville time, a brief marine invasion from the north appears to have penetrated as far south as central Alberta ( Gold, in prep.).

The Upper Mannville represents marine transgression. In general, in the south-central Plains these beds are non-marine, becoming more marine to the north-east and entirely marine in the northern Plains and Foothills. The Upper Mannville were non-marine, consisting of grey shales, siltstones, argillaceous sandstones and a few coal beds. The thickness is about 140 m around the Cold Lake area.

The Clearwater formation consists of shales, siltstones and sandstones, occasionally glauconitic, and is considered to be of mixed marine and non-marine origin. The Wabiskaw member near its base is well-sorted glauconitic sandstone, mainly marine in origin. The Grand Rapids formation, overlying the Clearwater formation has a higher sandstone content than the Clearwater. Both the Clearwater and Grand Rapids are mainly deltaic deposits with periods of marine transgression.

The Lower Colorado unit represents a time of marine deposition over all the Western Canada Basin except in the extreme southern Foothills. This unit lies at the top of the Lower Cretaceous and contains the Joli-Fou and Viking Formations of marine origin. The Joli-Fou is dark grey shale overlying Upper Mannville. The Viking is mainly sandstone, fine-grained and shaly to the east and northeast until it

becomes silty shale. In general, Lower Colorado sandstones thin to the east, indicating Cordilleran uplift as the sediment source.

### 1.5.2 Upper Cretaceous

The Upper Cretaceous rocks throughout the plains show uninterrupted deposition, consisting of marine shales at the base to continental sandstone at the top. They are subdivided into two units: the "Upper Colorado Group" and the "Post-Colorado Supergroup".

The Upper Colorado Group is undivided in most of the Cold Lake area. Its base is the "Base of Fish Scales" marker, and it includes two other markers called the "Second White Specks" and the "First White Specks". It consists of uniform dark grey shale. In east-central Alberta this group is represented by dark marine shale, originally called the LaBiche Formation. The Upper Colorado Group is terminated by the First White Specks marker bed.

The Post-Colorado Supergroup forms most of the bedrock throughout the Plains. Sandstone is the predominant rock, related to non-marine depositional conditions that occurred in the Western Canada sedimentary basin at the time. The lower part of the Lea Park formation within the group is mainly light grey and glauconitic shale with abundant ironstone concretions. The upper part is dark grey bentonitic shale. The Belly River formation is made up of a sequence of marine and continental to marine deltaic

deposits. It forms the bedrock surface in central Alberta and either outcrops, or subcrops below the drift cover.

The Bearpaw formation overlies the Belly River formation and consists of dark grey marine shales. It has been dated at approximately 75 million years. Finally there is the Horseshoe Canyon Formation, a series of predominantly non-marine beds of later Cretaceous age, marking the end of Cretaceous deposition. This formation along with the Eastend and Whitemud formations, form the Edmonton Group in central and southern Alberta.

### 1.5.3 Tectonic History

A broad shallow sea covered the western Canadian Plains at the beginning of the Late Cretaceous period, connecting the Arctic Ocean and the Gulf of Mexico, with a western margin confined by the western Cordillera. Dark grey Colorado Group shales were deposited at this time. Uplift to the northwest and erosion and transportation in the southeast deposited the Dunvegan delta complex in northwestern Alberta while shale was still being deposited to the southeast (Gold, in prep.).

Major tectonism in the Cordillera afterwards produced erosion, transportation to the east and deposition of clastics as delta complexes. At the beginning the Milk River sandstone in southwestern Alberta was deposited, marine transgression took place and again a major regression from deposition of the Belly River delta occurred due to uplift of

the Cordillera.

As the tectonic activity continued in the Cordillera the St. Mary River, Edmonton and Wapiti sandstones were deposited, filling the interior sea and forcing it to withdraw to the southeast at the end of the Cretaceous period.

Continental deposition continued into Tertiary Period, being responsible for the Paskapoo Formation adjacent to Foothills and the Ravenscrag Formation in Saskatchewan. In the Tertiary epoch, major uplift and deformation took place, forming the Rocky Mountains during the Laramide Orogeny. As a result the Interior Plains were uplifted and differentially warped in places. Then a period of erosion and minor crustal movement continued during this period. Only a few deposits from this epoch remain in Alberta, possibly due to Oligocene uplift that caused their removal.

At the present time, there is no indication that any tectonic activity still takes place in the Cold Lake area.

#### 1.5.4 Bedrock Topography and Buried Valleys

Figure 9 in Section 1.5 indicates that we know a great deal about the upper surface of the Cretaceous deposits from many logged boreholes. These deposits consist basically of the Lea Park and the Belly River Formations. The Lea Park shale subcrops throughout most of the area, and the Belly River sandstone overlies in higher ground in the southwest part of the Cold Lake area.



In Figure 9 the highest topographic points are between approximately 625 to 650 m , dissected by several valleys that are products of subaerial erosion, either during preglacial or glacial time. The data for examination of this bedrock surface was obtained from many wells drilled in the area by Alberta Environment Alberta Research Council, the Oil Industry for structural and geological mapping and oil and gas exploration, and by water well drillers for domestic and industrial water supply.

Subsequent glacial activity in the area has filled the earlier valleys as can be seen by the drift thickness shown in Figure 8. The mechanisms for the creation of these valleys were examined by Gold (in prep.) in detail.

In Table 6 we can see the width, depth and gradient of each channel in the area, as indicated by Gold (in prep.). These results are topographically dependent and hence only represent average values. The main valleys, Helina, Beverly, Imperial Mills and Kikino, have typical preglacial Empress Member One sands and gravel at their base derived from the mountains or local bedrock.

On the basis of Tertiary fill and channel morphology, Gold (in prep.), separated the valleys into three categories; The first group are wide, low gradient preglacial valleys with gently sloping walls. This includes Helina Valley of interest to this study. The second group consists of narrower, low-to-medium gradient preglacial valleys with steeper walls. This includes the Beverly

# **Bedrock Valley Dimensions**

|             | Width(km) | Thickness(m) | Gradient(m/km) |
|-------------|-----------|--------------|----------------|
| Helina      | 8-12      | 35-36        | .4             |
| Beverly     | 5-8       | 45-60        | .6             |
| Imperial M. | 15        | 60           | .8             |
| Kikino      | 3-8       | 30-45        | .5             |
| Bronson L.  | 1.5-3     | 30-43        | 1.3            |
| Vegreville  | 2.5-6     | 30           | 1.3            |
| Vermilion   | 3-5       | 35           | 1.7            |
| Sinclair    | 8-10      | 40-70        | 2.3            |
| St. Paul    | 1-1.5     | 25           | 2.9            |
| Holyoke     | 1-2       | 15-20        |                |
| Big Meadow  | 1-1.5     | 14-23        |                |

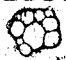
Table 6.... Bedrock Valley Dimensions ( after Gold, in prep.).

Valley. The third category consists of narrow, medium-to-high gradient valleys without preglacial deposits that appear to be of entirely glacial origin.

Based on these categories one may discuss briefly the preglacial history of the area and its relation to the channel configuration. As mentioned, the preglacial channels, defined on the basis of the bedrock topography and Tertiary deposition, delineate a drainage system which could be related directly to this study.

Figure 15 shows the drainage system and it is reasonable to expect that preglacial topography could have shown the results of multiple stages of drainage and downcutting, influenced by the various orogenic activities that took place in the Tertiary period. Mention is made only of the characteristics of the Helina and Beverly Valleys which are thought to be related to this study.

The Helina valley appears to be part of the southeast-trending collector system and probably carried the ancestral Athabasca and Peace Rivers. Also, within the area of interest, the Helina Valley is approximately 15 km wide, with gently slopping valley walls. The Beverly Valley forms part of the regional Tertiary radial feeder system. It possesses extensive upstream networks to the southwest of the area. This extensive upstream system is considered to be the ancestral North Saskatchewan River. Both valleys are important water collectors in the area and a number of aquifers have been drilled to their surface in order to





obtain water for the area. The water withdrawal and the changes of pore pressure at that level will be considered later in this thesis.

## 1.6 HEAVY OIL RECOVERY

The term "Heavy Oil" denotes crude oil having an API gravity of 25°, or less, ( a standard used to indentify the specific gravity of oil ), and viscosity up to several thousand centipoises. This particular type of oil is not very mobile at reservoir conditions. Enormous heavy oil resources occur in Canada, Venezuela, and the United States.

In Canada, the principal heavy oil deposits from which production is obtained are located at Lloydminster, Chauvin, and Wainwright, of approximately 12 billion barrels of production capability. In Cold Lake heavy oil deposits total about 165 billion barrels. The viscosity of the Cold Lake crude varies from 50,000 to 100,000 centipoise. In Northern Alberta are the Athabasca, Wabasca, Peace River, and Buffalo Head Hills oil sand deposits, totalling 730 billion barrels ( Farouq A., 1982).

Based on certain reservoir parameters Heavy Oil deposits have been classified into three categories:

### Category 1.

*This type of heavy oil has rock and fluid parameters most desirable for thermal recovery operations.*

These parameters according to Farouq Ali (1982), are  
1) sandstone reservoirs at depths of 3000 feet or less, 2) oil-saturated sands having net thickness of 10 feet or greater, 3) stock tank oil saturations of 1750 barrels per acre-ft or greater, and 4) viscosity of reservoir oil-sufficient for oil to be mobile in its present state.

*Category 2.*

*This includes heavy oil contained in reservoirs having some of the above basic parameters.*

*Category 3.*

*This applies to heavy oil reservoirs having only few of the necessary parameters.*

In order to recover heavy oil thermal methods must be employed. Any successful recovery technique must involve a reduction in the viscosity of the crude in order that its mobility may be increased. A wide variety of thermal methods has been used in Heavy Oil reservoirs. Basically, these include the use of hot fluid or underground combustion. Some of the methods are: (Farouq Ali, 1982)

*Cyclic steam stimulation*

*Steam flooding*

*Forward in situ combustion*

*Reverse combustion*

### *Wellbore heating*

### *Conduction heating*

Due to the fact that Cyclic Steam stimulation is one of the major strategies used for Heavy Oil recovery in Cold Lake area, a detailed analysis of the technique will be introduced here.

#### 1.6.1 Cyclic Steam Stimulation

One of the most widely used methods for oil recovery is cyclic steam stimulation. Cyclic steaming was first applied in 1957, by Shell Oil Company in Venezuela. This technique has great advantages such as quick payout, flexibility of operation, and applicability in very viscous oil formations. However, large quantities of oil remain unrecovered even after many steam injection cycles. The percentage variation of oil recovery using this method goes from 10% to about 40%.

The basic mechanisms of this method are:

Steam is injected in a well for several weeks at the highest possible rate to reduce heat losses. The reason for the need of high injection rates is the minimization of heat losses. Then the injected steam heats the rocks and the fluids around the wellbore. Due to gravity segregation, steam changes permeability and viscosity and the fluid fingers into the formation.

When the desired volume of steam has been injected, usually the well is shut for about 2 weeks in a so called "soak" period, Esso wells do not have a soak period since the advantages of soaking are questionable due to the low thermal diffusivity of oil sand, ( McDougall, 1987). This causes partial condensation of steam, which in turn heats the rock and the fluids, and achieves even distribution of injected heat. As time progresses after steam injection and the soak period, the original viscosity of the reservoir may be lowered by a few hundred centipoise within the steam zone. At this point thermal expansion of oil and water occurs.

Before the well is placed into production, the heated sand contains highly mobile oil, steam and water. Due to lowering of the face pressure of the sand by production, several driving forces help in expelling the oil and other fluids into the wellbore, where it is pumped off.

The well produces for an extended period of time at a rate many times higher than the cold production rate. Due to heat losses the steam heated sand cools down as time advances, which results in reduction of oil production. Then the whole cycle is repeated again, injecting steam, soaking the well, and producing again. Figure 16 shows such stimulation steps for only 3 cycles. The number of cycles in some cases has reached about 15 to 20 times. The process is called the "huff and puff" method.



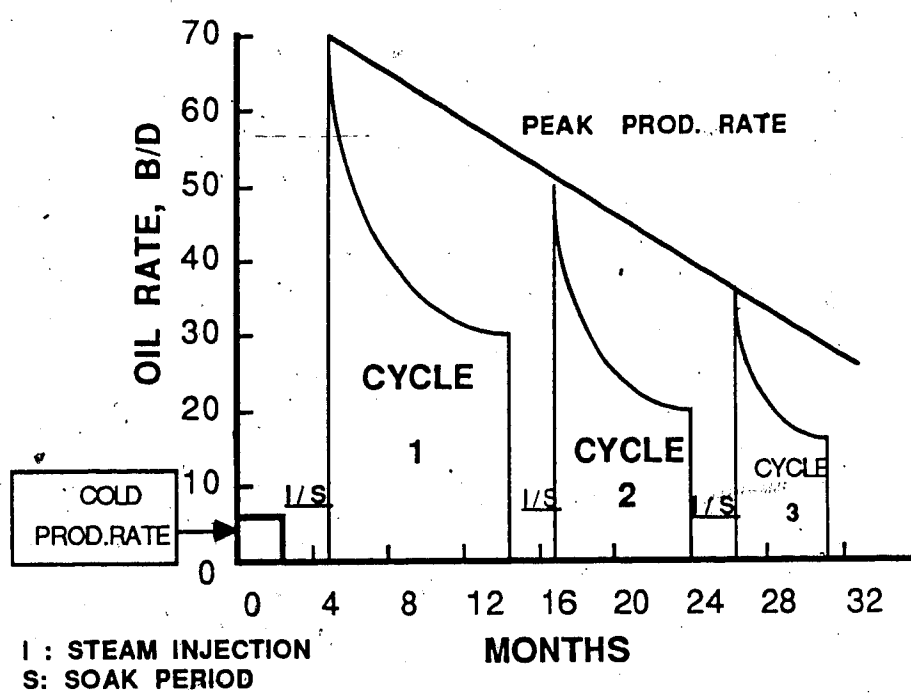


Figure 16.... Cyclic Steam Stimulation Performance.

### 1.6.2 Heavy Oil Recovery in Cold Lake

Heavy Oil Recovery and industrial activity in the Cold Lake area was initiated in the early seventies. One of the major early plants in the area operated by Esso Resources Ltd. is Leming Pilot Plant.

The Leming Plant originally began operation in 1975 as an experimental pilot designed primarily to investigate steam stimulation in a type of reservoir being considered for commercial development. Experimental operations have since branched out to cover a wide range of recovery configurations. Some of these include hot water and steam bank floods, chemical injection, a horizontal well, varying well casings and completions. Also, investigations in reservoir fracturing, steam pressure and quality, optimum handling of well-to-well pressure response, infill well operation, and well casing failure mechanisms and prevention have been carried out.

Steam stimulation is a very important aspect of oil recovery in Cold Lake. Operating strategies by Esso Resources include the development of well pads, each one containing several wells. Other strategies, not now used by Esso, of recovery have been applied in the area such as sequential row steaming, which reduces the time of the "soak" period of production wells, using a main steaming well for injection. This method has been tested but communication problems between wells are present.

Until the end of 1985, there were 28 wellpads in the Leming Pilot Plant. The older pads surround the area of the Plant and as industrial activity increased, new pads were developed with a north-western trend, covering an area of the well and pad locations as shown in Figure 17.

Most of the wells in the plant are drilled to the Clearwater formation, where most of the oil is present. There are several wells used for waste water disposal purposes which are drilled to the top of the Cambrian.

Detailed analysis of the operation of these pads has been obtained from Esso Resources but some of the material is confidential and it will not be presented here. Oil production and steam injection volumes have been included in this material as they are to be used for interpretation purposes. Relative steam injection rates, steam injection, and oil production volumes are shown in Figure 18, Figure 19 and Figure 20.

Page 51 has been removed due to poor print quality of the information.

Figure 17: Cold Lake Leming Pilot Pad & Well Locations.

Modified from Esso Resources Canada Ltd. 1985

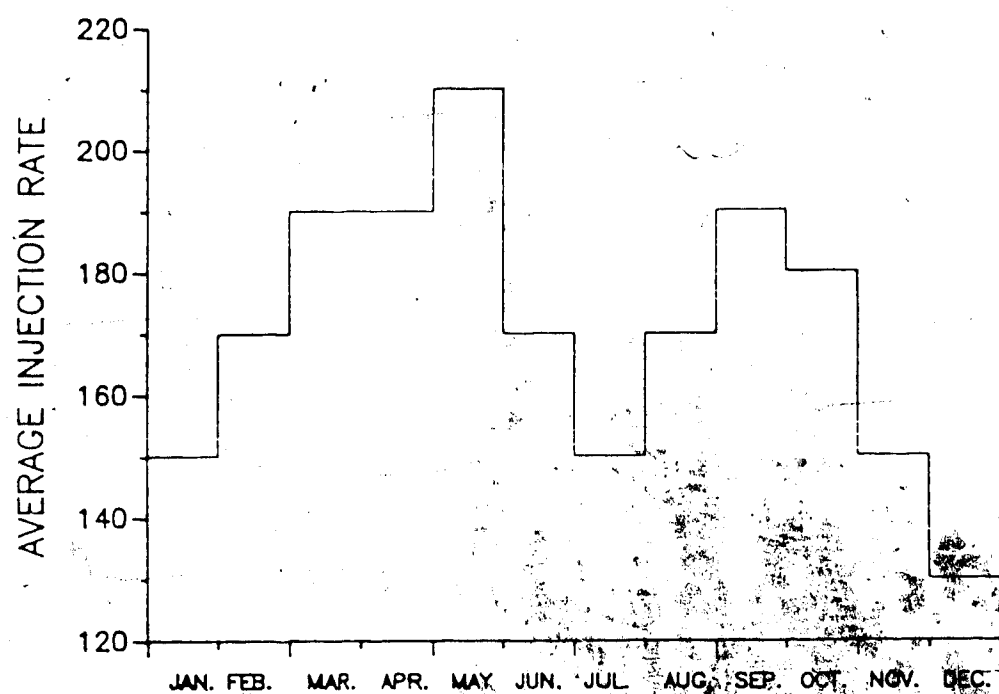


Figure 18.... Average Steam Injection rate for Leming Pilot Plant during 1983

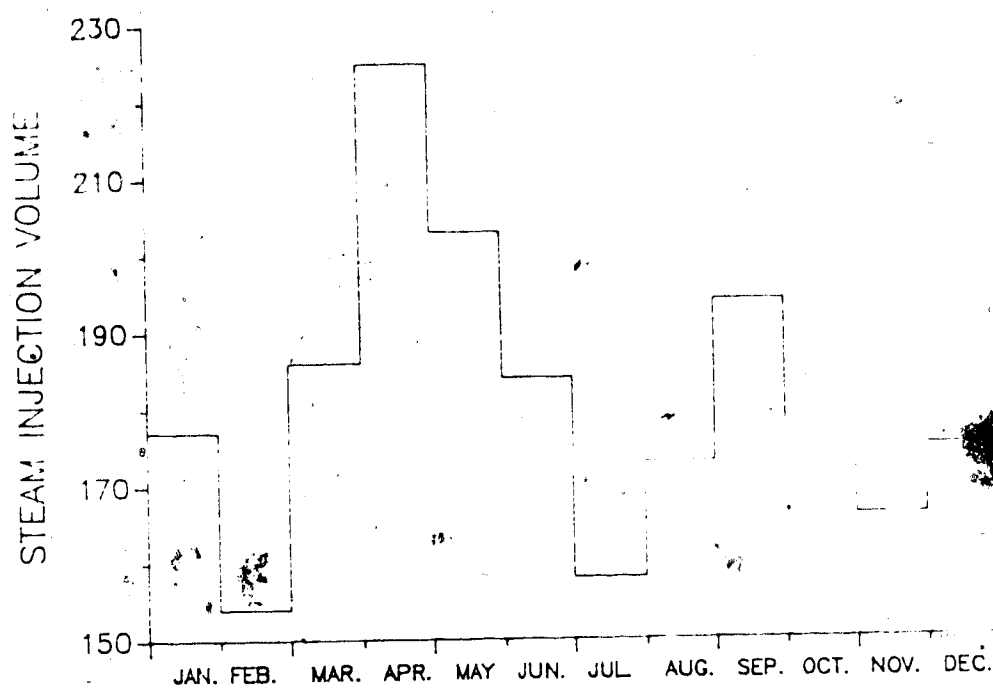


Figure 19.... Average Steam Injection Volume for Leming Pilot Plant during 1983

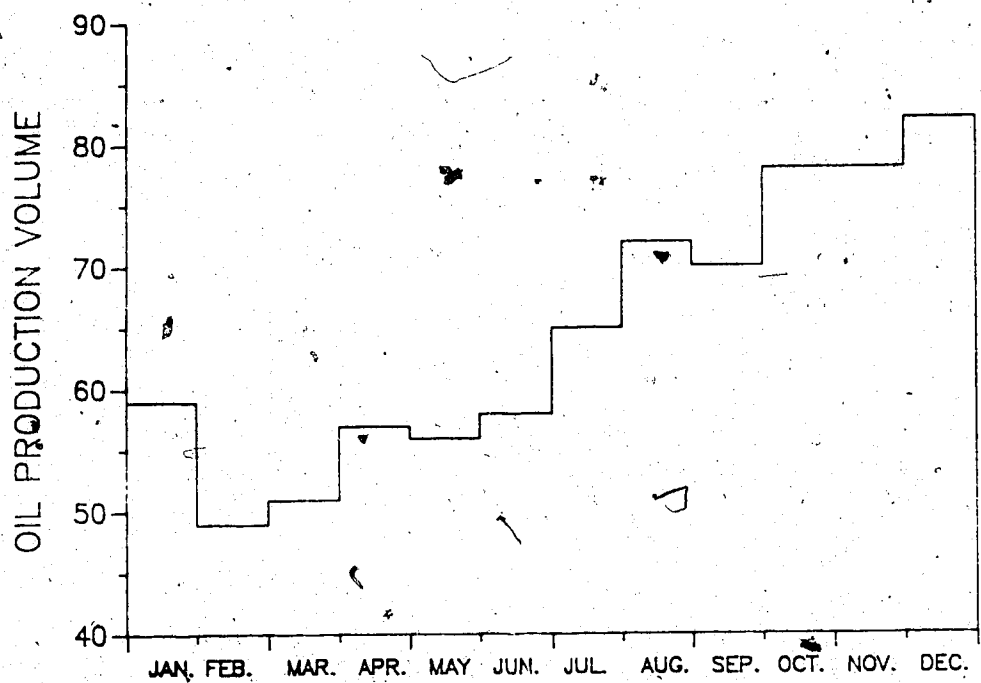


Figure 20.... Average Oil Production Volume for Leming Pilot Plant during 1983

## 2. PROCESSING PROCEDURES

### 2.1 DATA PROCESSING

Data processing and interpretation is carried out in the Cold Lake Seismic Data Centre in the Physics Department of the University of Alberta. The operations of the Center are supervised by Charles McCloughan and directed by E. R. Kanasewich from the University of Alberta. Druid Electronics provides the maintenance under contract to Earth Sciences Division of the Alberta Environment. Supervision for the entire Cold Lake seismicity project is under Dr. D. Bingham from the Earth Sciences Division.

Tapes and analog recordings are received in the data center twice a week from the field operations. Any impulsive events common to three or more stations are identified by Carole Holt from Alberta Environment on the Helicorder records. A histogram of daily event transfers is shown in Figure 21. The number of events transferred increased as array performance improved and as more efficient software for data transfer became available.

All the events identified, are transferred using the TI 900 system from the "Field Tape" to a "First Scratch Tape" using a software package provided by Druid Electronics. A custom program transfers the compressed data from the "First Scratch Tape" to a "Second Scratch Tape" in an IBM compatible format, from which writing anomalies (0 and 1 length blocks) are eliminated. The Output of the Second



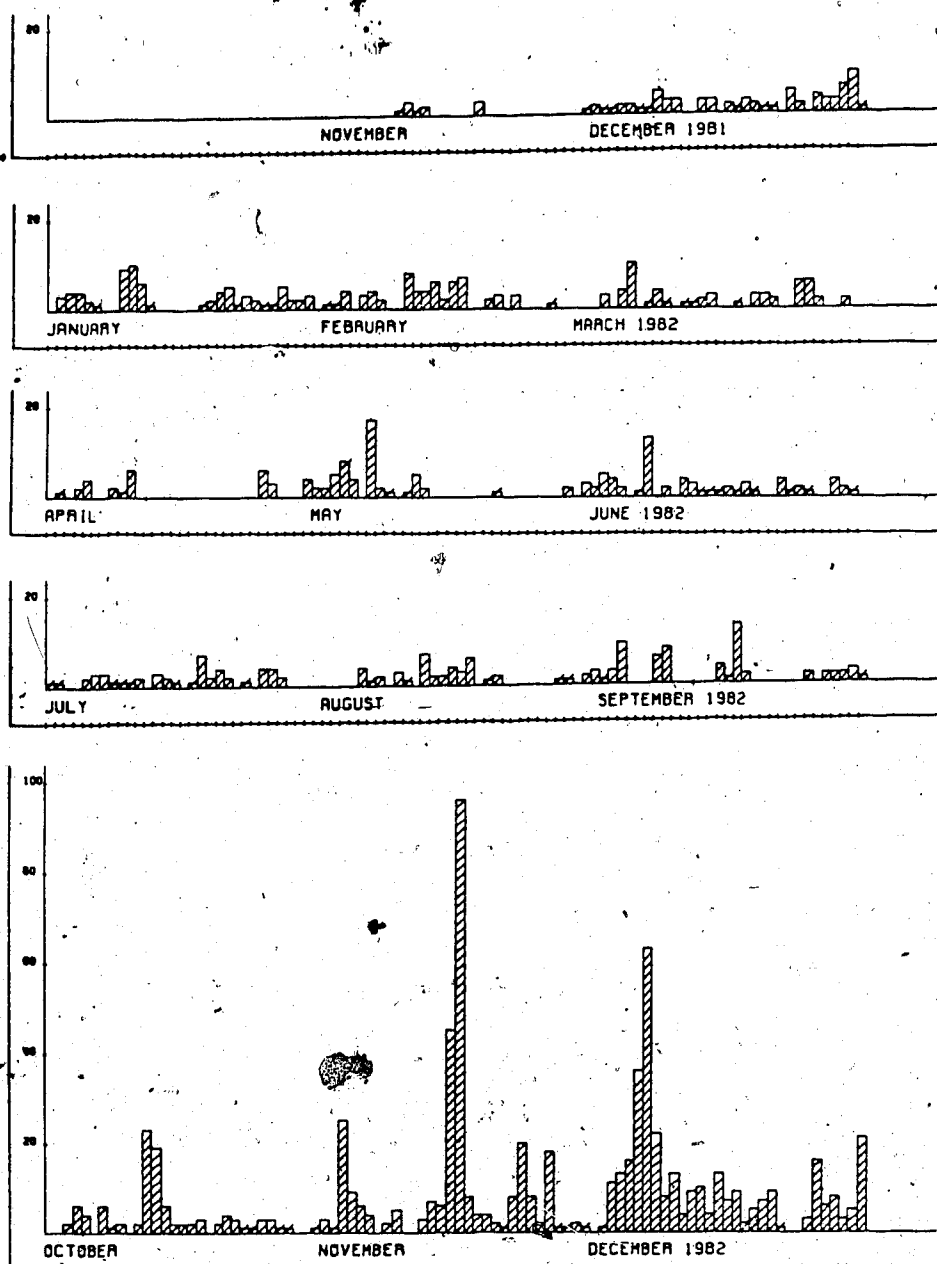


Figure 21.... Histogram showing the number of events transferred from a Field Tape to a Scratch Tape.

Scratch Tape is still readable at either the Cold Lake Center on the TI 990 or in the University Computing Center on the Amdahl 5680 system. The field tape stores data in frames that contain 90 milliseconds of seismic information per frame. Since ELEH is sampled 15 times per frame and the WWVB time code (channel 11) is only sampled once, the following channel order is used in each frame.

1,2,3,4,5,6,7,8,9,10,11,1,1

1,2,3,4,5,6,7,8,9,10, 1,1

1,2,3,4,5,6,7,8,9,10, 1,1

1,2,3,4,5,6,7,8,9,10, 1,1

1,2,3,4,5,6,7,8,9,10, 1,1

Depending on the degree of compression, 10 blocks of data will normally contain 50 to 70 seconds of real time information. Desired portions of the Field Tape are transferred in 10 block units to the Scratch Tapes. Typically 10 to 100 blocks are saved from each seismic event.

A "Study Tape" with data in a more standard uncompressed format is created at the University of Alberta Computing Center using a program written by C. McCloughan. The header on each block contains 30 1\*2 words with information on the year, day, hour, minute, second and millisecond of the block start. It also contains the number of complete frames of data in the block and 22 words for

information on channel gains, etc. The data themselves are contained in units of a fifth of a frame with signals 1 to 13 representing the following field sensors.

1=ELEH 2=ELEH 3=ELEH

4=ELEZ 5=ELEN 6=ELEW

7=ELE 8=LPE 9=BLE

10=LLE 11=MLE 12=HLE

13=WWVB

Each block contains 77 frames so that there are  $30 + (5 \times 13 \times 77) = 5035$  words or 10070 bytes per block. Unused locations at the end of blocks containing less than 77 frames are padded with zeros. Several plotting formats are used for displaying the digital data.

The location and name of the stations and sensors are indicated by a three- or four-letter code in accordance with international seismic convention. The first two letters is an abbreviation for a local feature such as a lake. The third letter is always E and indicates that is an Alberta Environment station. The fourth letter, if present, indicates the direction (Z,W,N) of the sensors as vertical (+ = UP), north-south, or east-west, respectively, or it is H, indicating a high sampling rate. On a graphic display the positive or upward direction is either north or east. The trace labeled WWVB is the time signal, which contains the

day, hour, minute, and second in a digital code. Our graphics display shows a 10-sec marker below the WWVB signal. The block start time for the field data is shown at the top of the graph, and a graph is always plotted for this time. Figure 22 shows a graphical display of an event.

## 2.2 EVENT DETECTION - CATEGORIZATION

In most microearthquake networks, event detection is a procedure for recording the approximate time of occurrence of a microearthquake within the network, recognize it and separate it from other events such as teleseisms, sonic booms, and explosions. Some laboratories use either automated, semiautomated or visual methods for detecting such events on seismograms. In the Cold Lake microseismic network visual methods are used for event detection. Paper seismograms from helicorders are examined in order to separate the events, and in turn, to be stored on magnetic tape, with the correct time code for further analysis.

Separation of different events recorded by the Cold Lake array is based upon frequency, amplitude and signal duration variations. The classification of the events which have been detected by this array has been separated into four categories:

Type "A" events (Figure 23) are local earth tremors with epicenters within 15km from the center of the

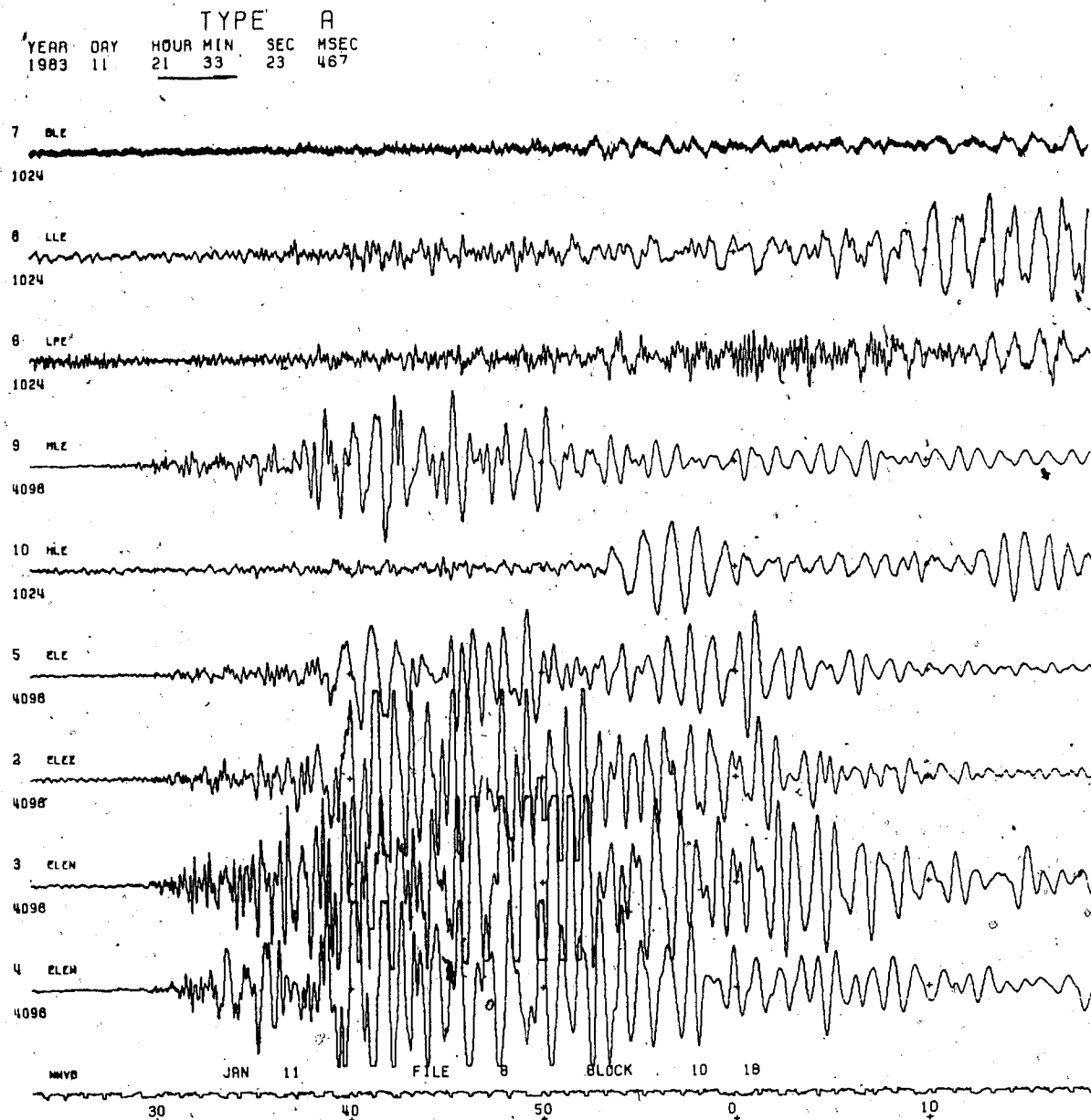


Figure 22.... An event recorded by the Cold Lake Seismic Array and plotted versus WVVB time. Also file and block numbers as well as the date are shown.

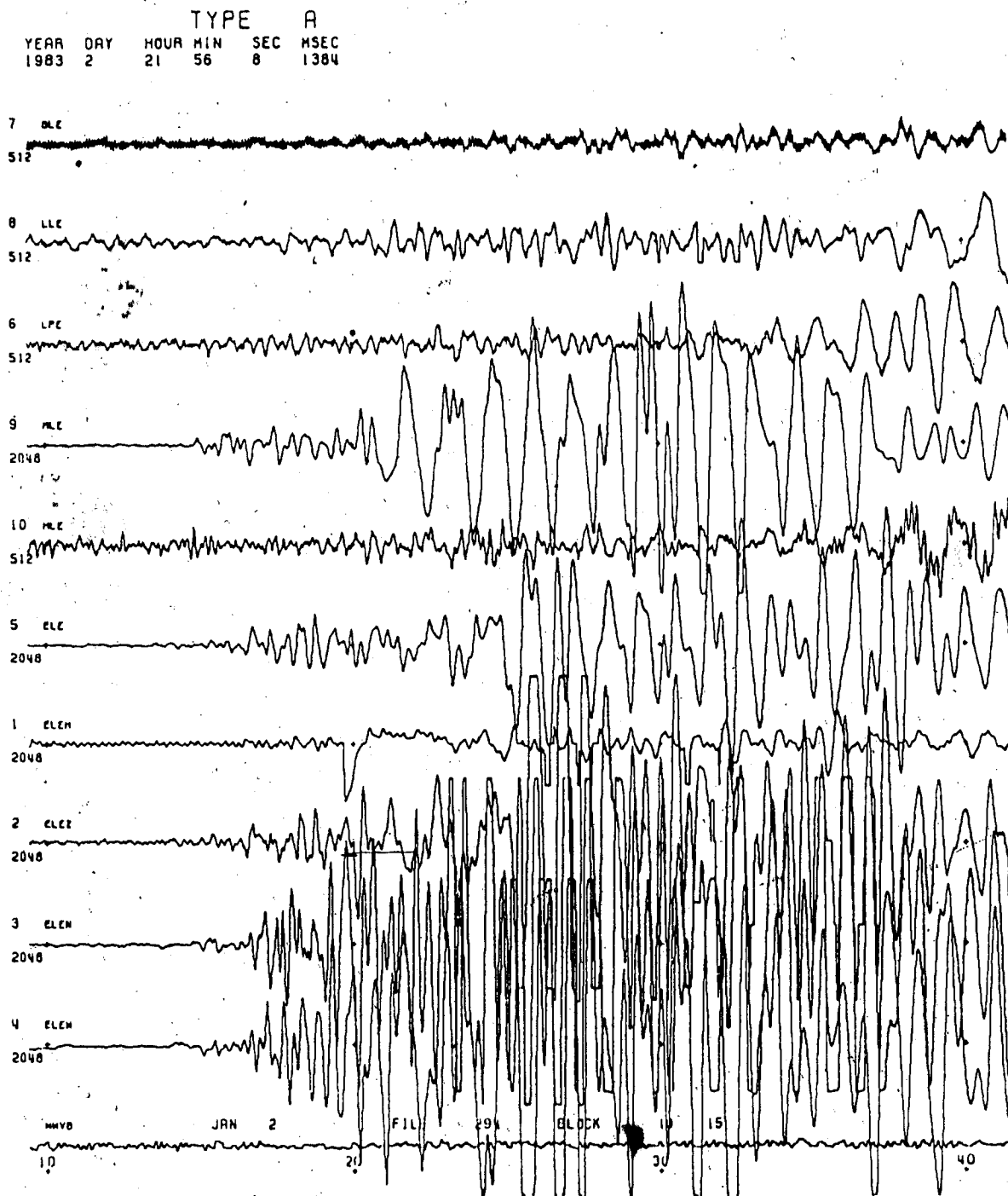


Figure 23.... Type "A" event recorded by the Cold Lake Seismic Array. Note the strong Surface Wave present and short duration of oscillation.

array. These events range from magnitude -2.0 to +1.5. They are characterized by a strong surface wave, emergent P waves, and high frequency content short duration of oscillations;

Type "B" events (Figure 24) are local impulsive earth tremors to the north of the array and some or all of these may be due to chemical explosions by seismic crews or the Canadian Forces on the D.N.D. Weapons Range near Burnt Lake, located north of the study area. Their phase velocity is equal to the speed of sound (approx. 330 m/s) ;

Type "C" events (Figure 25) are sonic arrivals due to supersonic flights, mainly on the weapons range area ( phase velocity approx. 330 m/s);

Type "D" category (Figure 26) are teleseismic events due to are earthquakes taking place in other parts of the world. The apparent velocity of arrival is very high ( more than 8km/s) and the spectrum seldom has energy above 2Hz.

This study will emphasize the analysis of the type "A" events. The other types of events will only be mentioned briefly in this chapter.

1984 B EVENT  
YEAR DAY HOUR MIN SEC MSEC  
1984 6 5 58 9 826

7 BLE  
258

8 LLE  
2048

6 LPE  
512

9 BLE  
64

5 ELE  
64

JAN 6 FILE 197 BLOCK 4 6 FILTERED 0.10 10.0

†  
10

†  
20

Figure 24.... Type "B" event recorded by the Cold Lake Seismic Array. Possible explosion to the NW of the array.



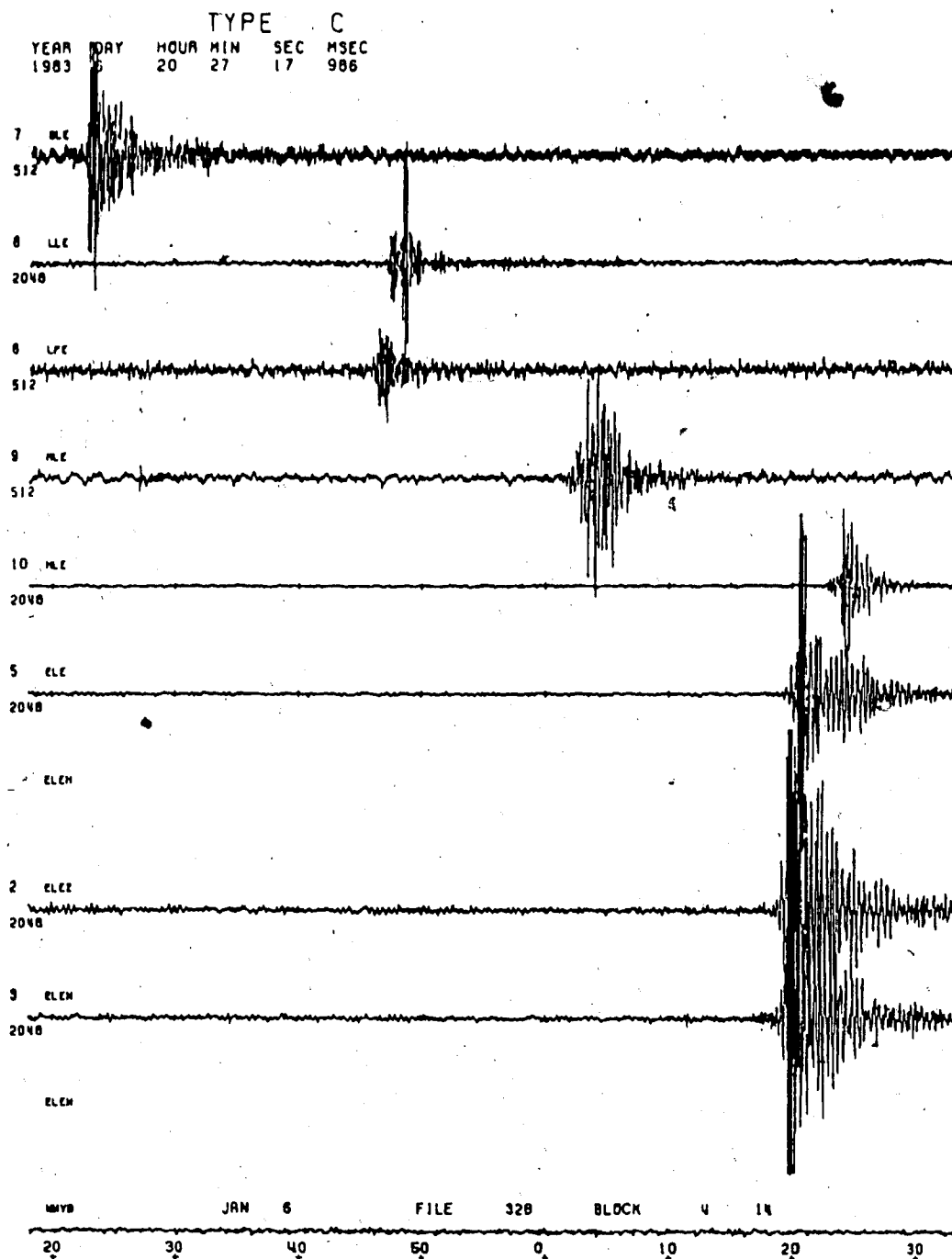


Figure 25.... Type "C" event recorded by the Cold Lake Seismic Array. It is a sonic arrival from aircraft flying.

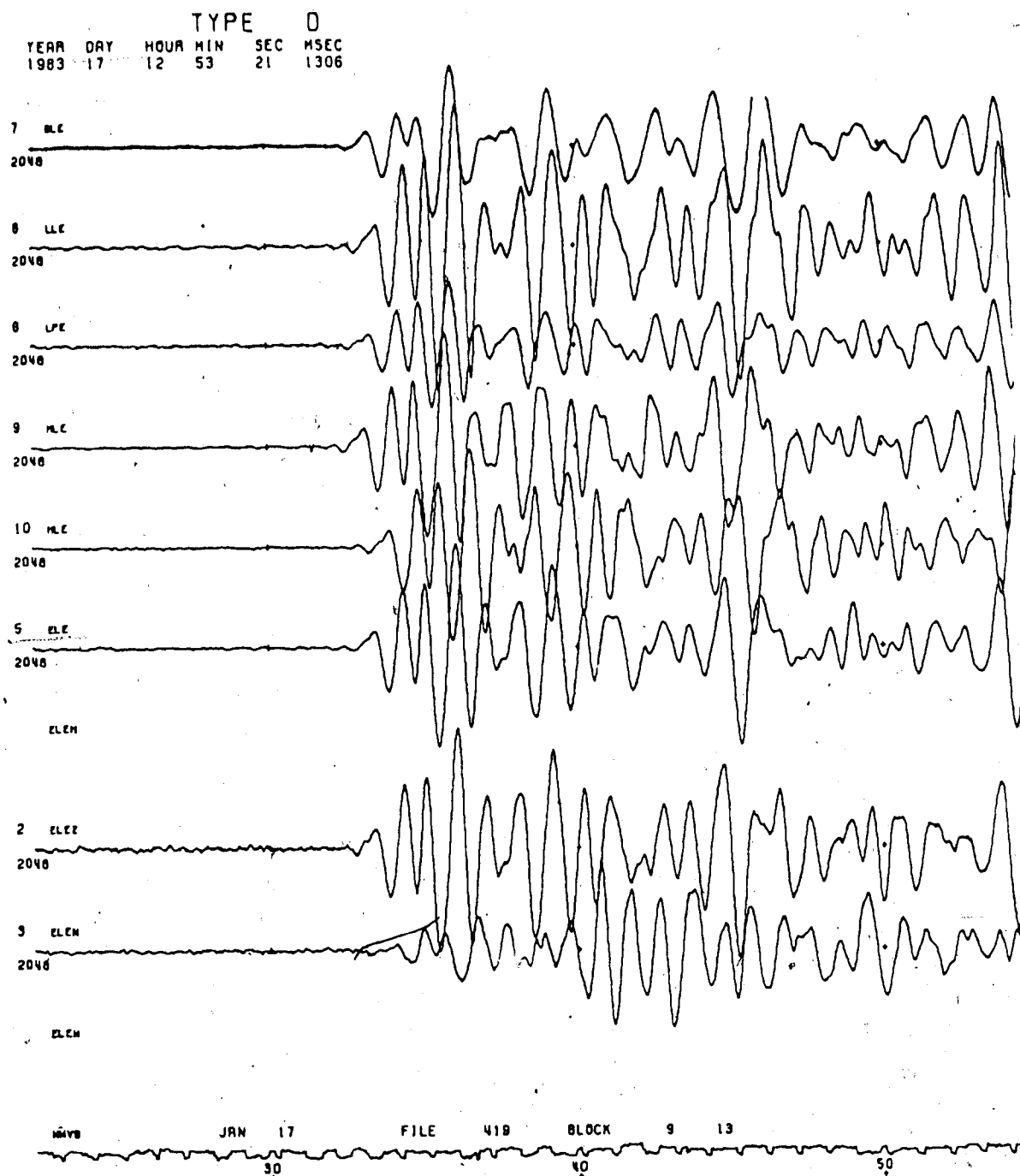


Figure 26.... Type "p" event recorded by the Cold Lake Seismic Array. This is an earthquake of magnitude 6.0 from Greece on 17 January 1983.

## 2.3 EVENT PROCESSING

Event processing is the method used for measuring some basic parameters from the recorded seismic traces that describe the seismic characteristics of the ground motion. Such parameters are known as phase data and are categorized as:

- 1) *Onset time and direction of motion of the first P- arrival.*
- 2) *The onset time for later arrivals, S- arrival (where possible).*
- 3) *The maximum amplitude and its associated period.*  
*and*
- 4) *The signal duration of the seismic event.*

We need to have precise phase data in order to compute origin time, hypocenter, magnitude of the earthquake and also obtain the focal mechanisms. Several visual, semiautomated, automated methods are usually employed for such processing. In this study in order to present the data in an appropriate form for phase picking, revised methods of display such as, direct plotting, filtering, tapering and also an automatic method, have been employed.

### 2.3.1 Direct Plotting

One of the basic methods for preliminary examination of a seismic event is a direct plot of such event over all its

time of oscillation as shown in Figure 27. Plotting is done using a PLOTLIB routine from the main frame system at the University of Alberta after, reading the appropriate file number, block number, date and time, from a magnetic tape where the type "A" events are stored. In this manner an unfiltered plot with no gain modification has been made of the entire wave arrival for each "A" event. Usually this procedure does not yield reliable graphs for timing and phase identification, because the amplitude scale is inappropriate for an analog display of the first breaks. This is because the direct P arrivals are emergent.

Basically, using this type of plot one can measure the total duration of oscillation for a particular station to be used for magnitude determination. This procedure will be discussed in section 2.4. Also, the graph allows one to choose the appropriate block interval for an event containing the necessary phase data to be used for further processing.

### 2.3.2 Spectral Analysis and Filtering

Before applying any kind of filtering to a time series, one should obtain the amplitude spectrum of the event. There are several methods in existence for making spectral estimates. In this study a spectral estimate will be made using a Daniel window.

The power spectrum of  $f(t)$  is given by,

TYPE A  
 YEAR DAY HOUR MIN SEC MSEC  
 1986 1 5 48 42 577

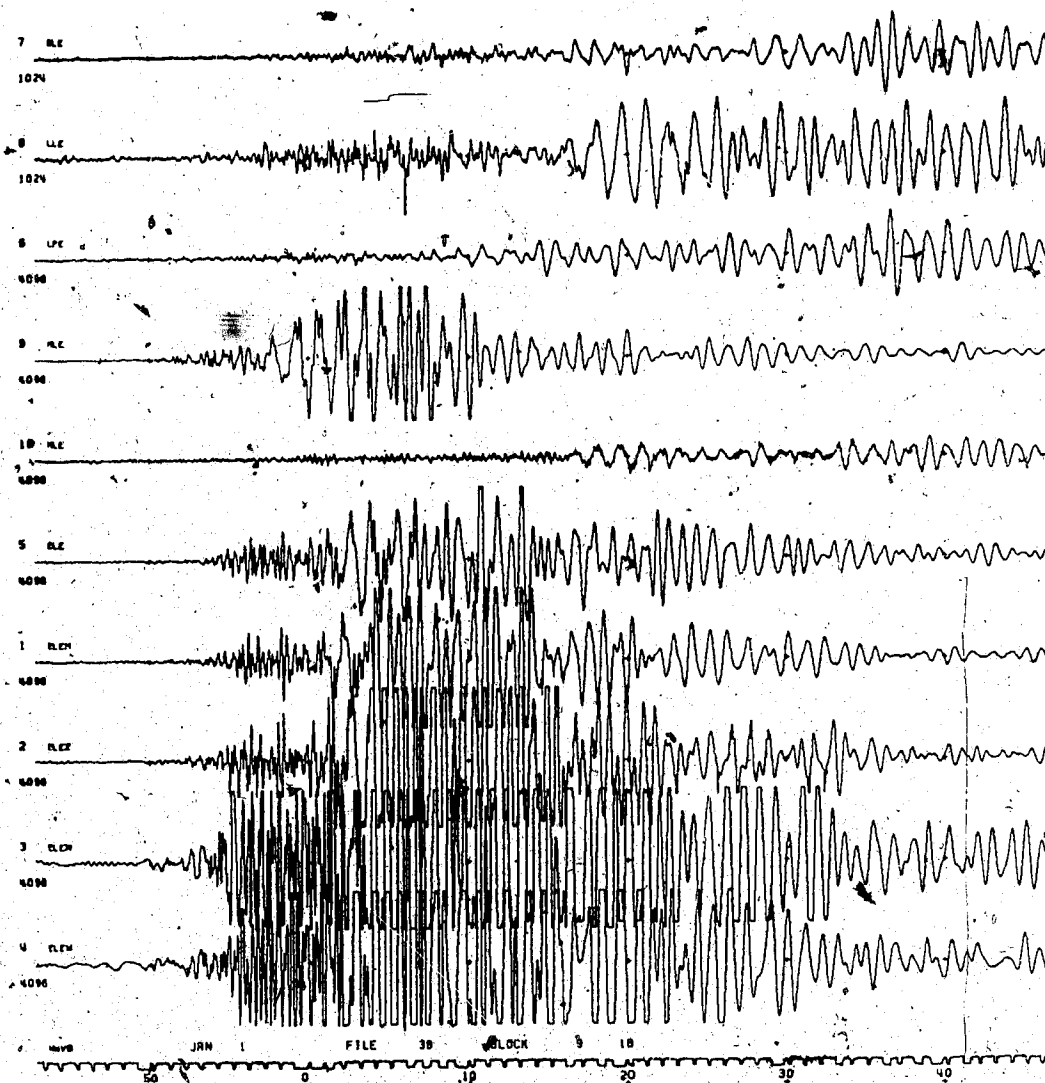


Figure 27.... Direct plot of an "A" type event as it is saved at the magnetic tape. The characteristics of such an event are clearly present.

$$P_s(W) = (N'/N) (1/2m+1) \sum F(W+j)F^*(W-j)$$

where

$$W=0,1,\dots,N/2$$

the sum goes over  $j$  from  $-m$  to  $m$  ( $m$  length of time window), and  $F^*$  is the complex conjugate of  $F$ . A discrete Fourier transform is used to obtain  $F(W)$  for the time series  $f(t)$  as:

$$F(W) = \sum f(t)\exp(-2\pi i W T/N)$$

where  $N$  is the number of samples of data,  $T=0,1,\dots,N-1$ , and additional zeroes  $T=N,\dots,N'-1$ , are given to make  $N'$  a power of 2; the summation goes from 0 to  $N'-1$ .

Spectral estimates calculated from station MLE are shown in Figure 28 (noise), and Figure 29 (P - phase). These estimates have been calculated using an algorithm written by Mark Baxter and Dr. E.R. Kanasewich, 1983.

As indicated in Figure 29, most of the energy is concentrated is between 1.0 to 8.0 Hz, a frequency band which can be isolated by filtering for further data analysis. Since, at some stations the signal to noise ratio is about 1.0, an application of bandpass filtering lead to some enhancement. However, the spectral pattern for both noise and signal is different so the improvement is, usually great.

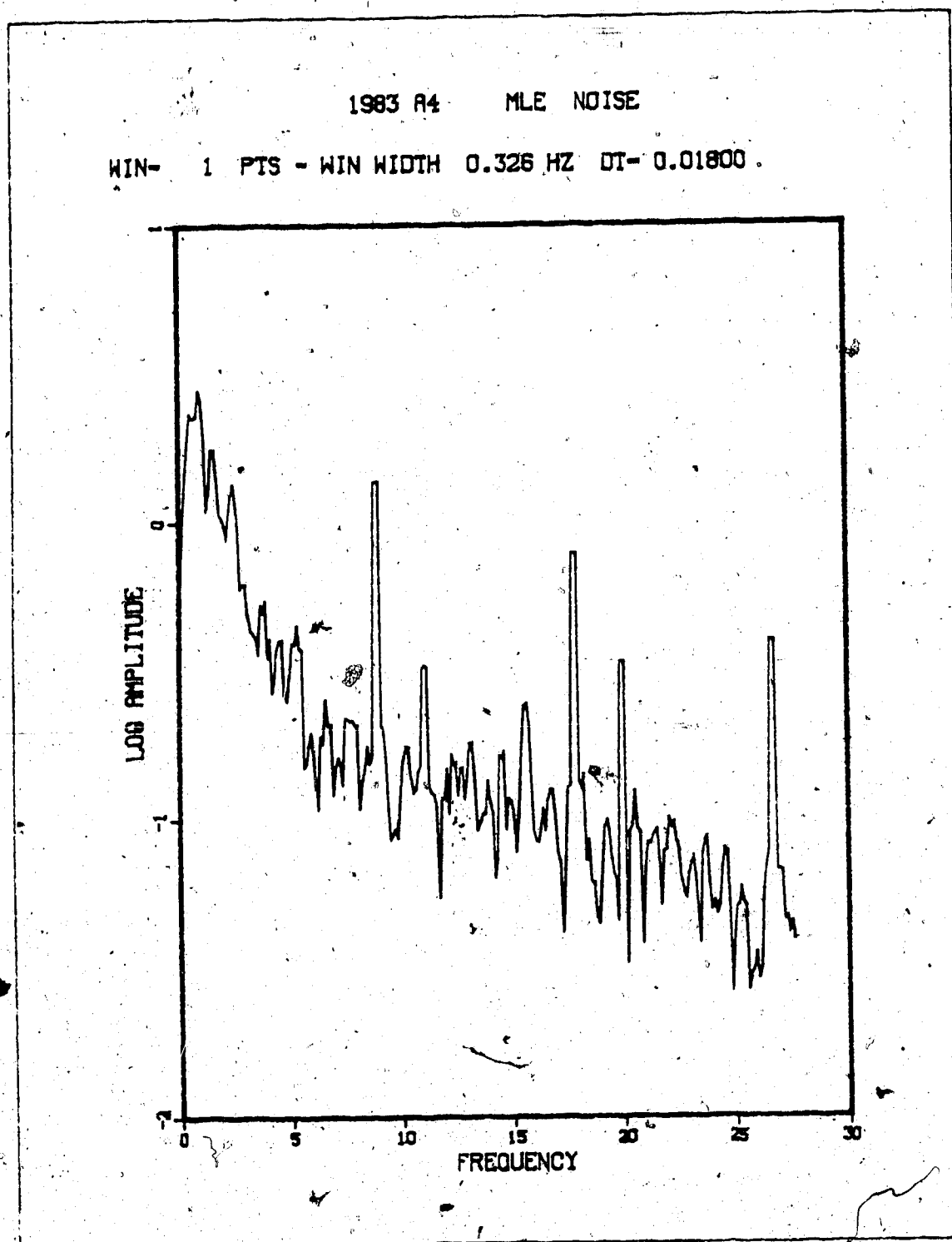


Figure 28.... Amplitude Spectrum of 10 sec noise signal before a P- arrival from station MLE. It is clear that only a small amount of energy is present at low frequencies.

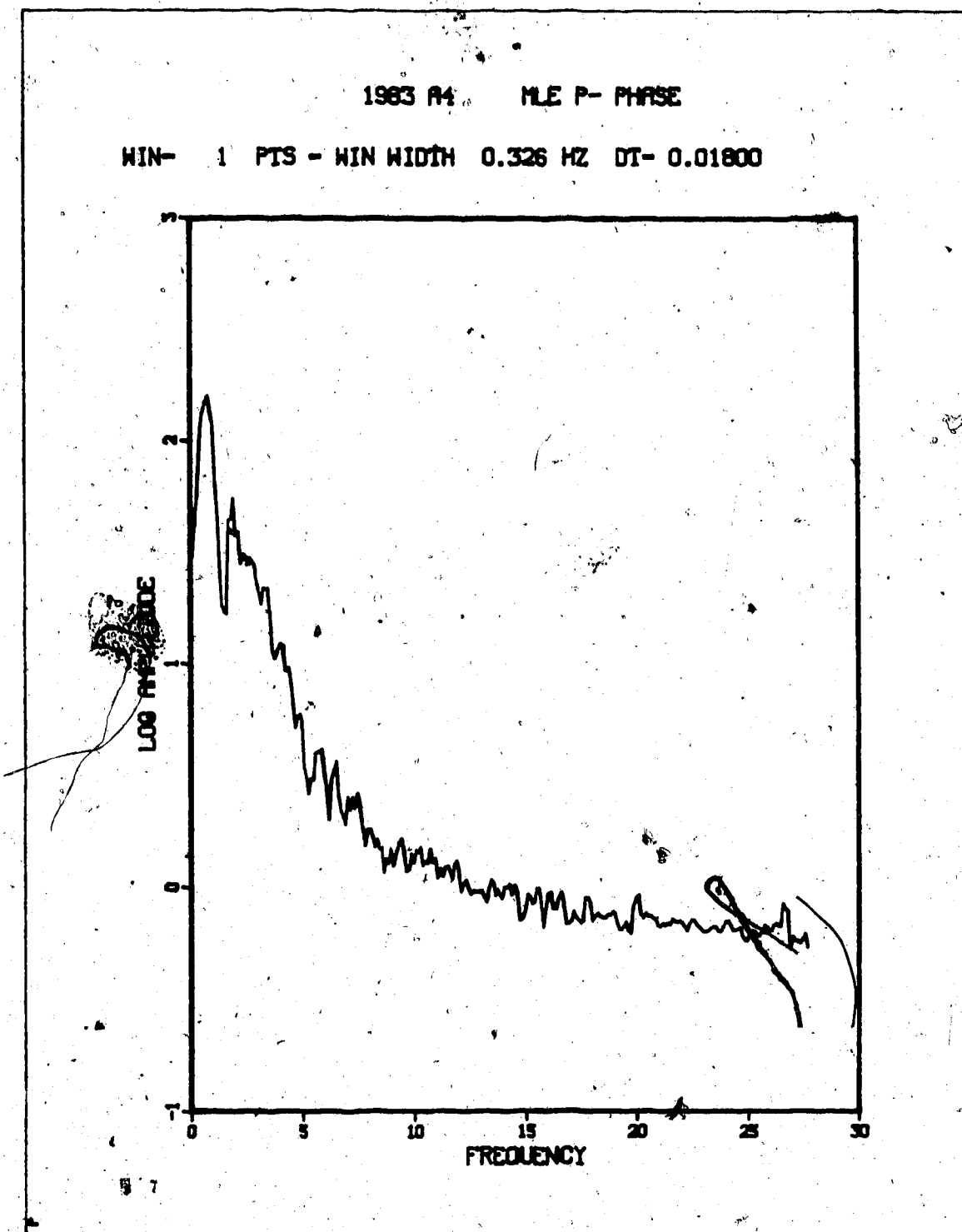


Figure 29.... Amplitude Spectrum of a P- arrival from station MLE.



In order to reduce noise levels in a seismic signal filtering application is necessary. A filter operator,  $W=(W_1, \dots, W_n)$  when convolved with a series  $x(t)$  gives an output  $y(t)$ :

$$y(t) = W * x(t)$$

The characteristics of this filter are such that signals with the desired frequencies are passed through and the remaining harmonics are reduced or rejected. In this study a routine written by David Ganley in 1977 is applied to the data in order to perform the necessary filtering. The algorithm uses a recursive Butterworth band-pass filter. The filter has eight poles in the  $s$ -plane and may be applied in the forward and reverse direction in order to have zero phase shift.

Using this routine and pass-bands appropriate from spectral estimates, application to raw data gives satisfactory results as can be seen in Figure 30 and Figure 31 where band-pass filtered signals of 1.0-8.0 Hz and 0.4-5.0 Hz have been obtained respectively. Also spectral estimates of these events show clearly the rejection of the unwanted frequencies.

Getting the data in this form and choosing an appropriate window, one can visually pick P-phase arrivals quite easily unless the signal is very weak. Figure 32 shows

1984 A7 EVENT  
YEAR DAY HOUR MIN SEC MSEC  
1984 22 20 35 49 1278

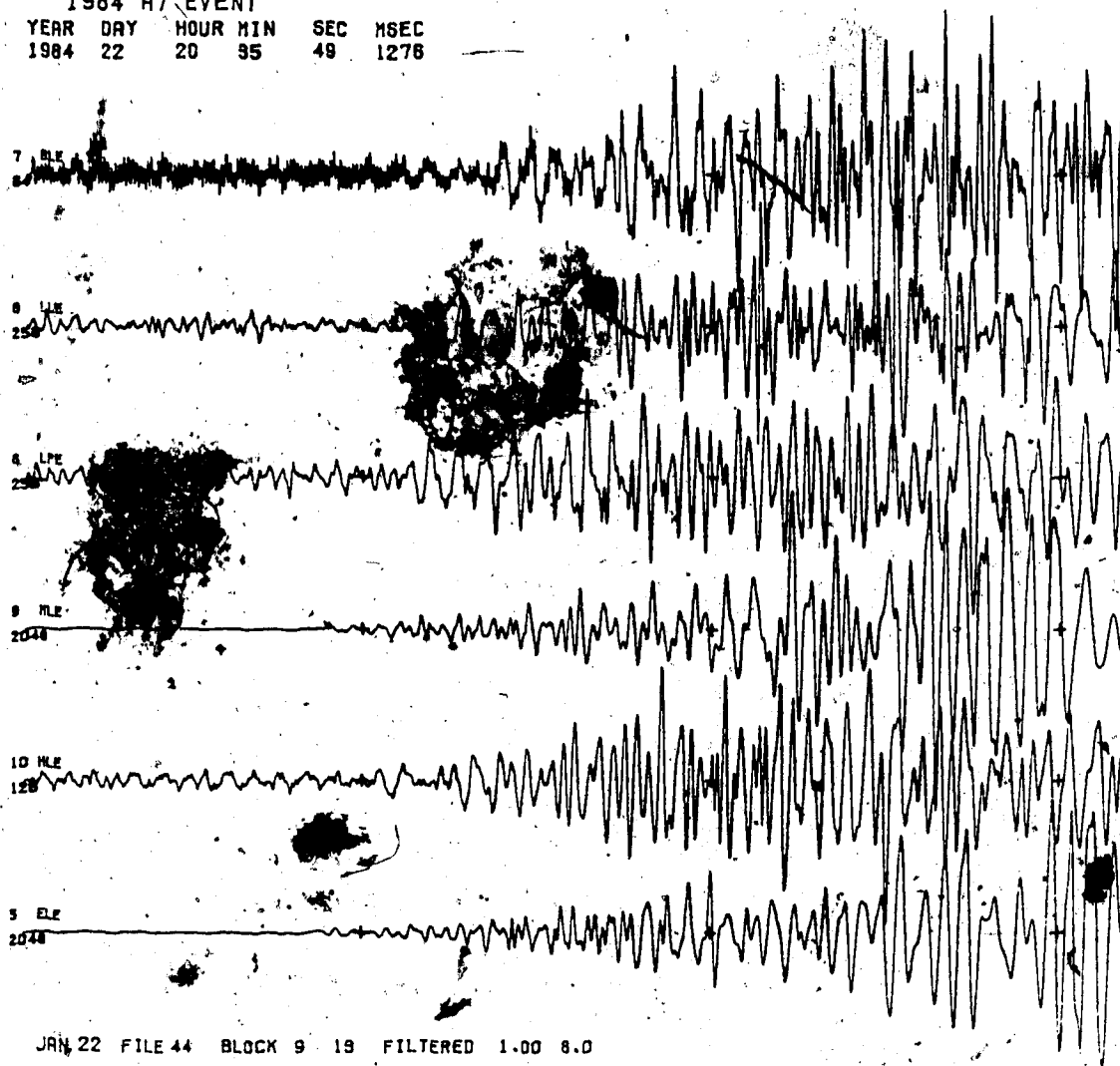


Figure 30.... Band Pass filtered "A" type event between 1.0 and 8.0 Hz. A significant improvement in signal quality is evident.

1989 A19 EVENT  
 YEAR DAY HOUR MIN SEC HSEC  
 1989 89 0 55 14 746

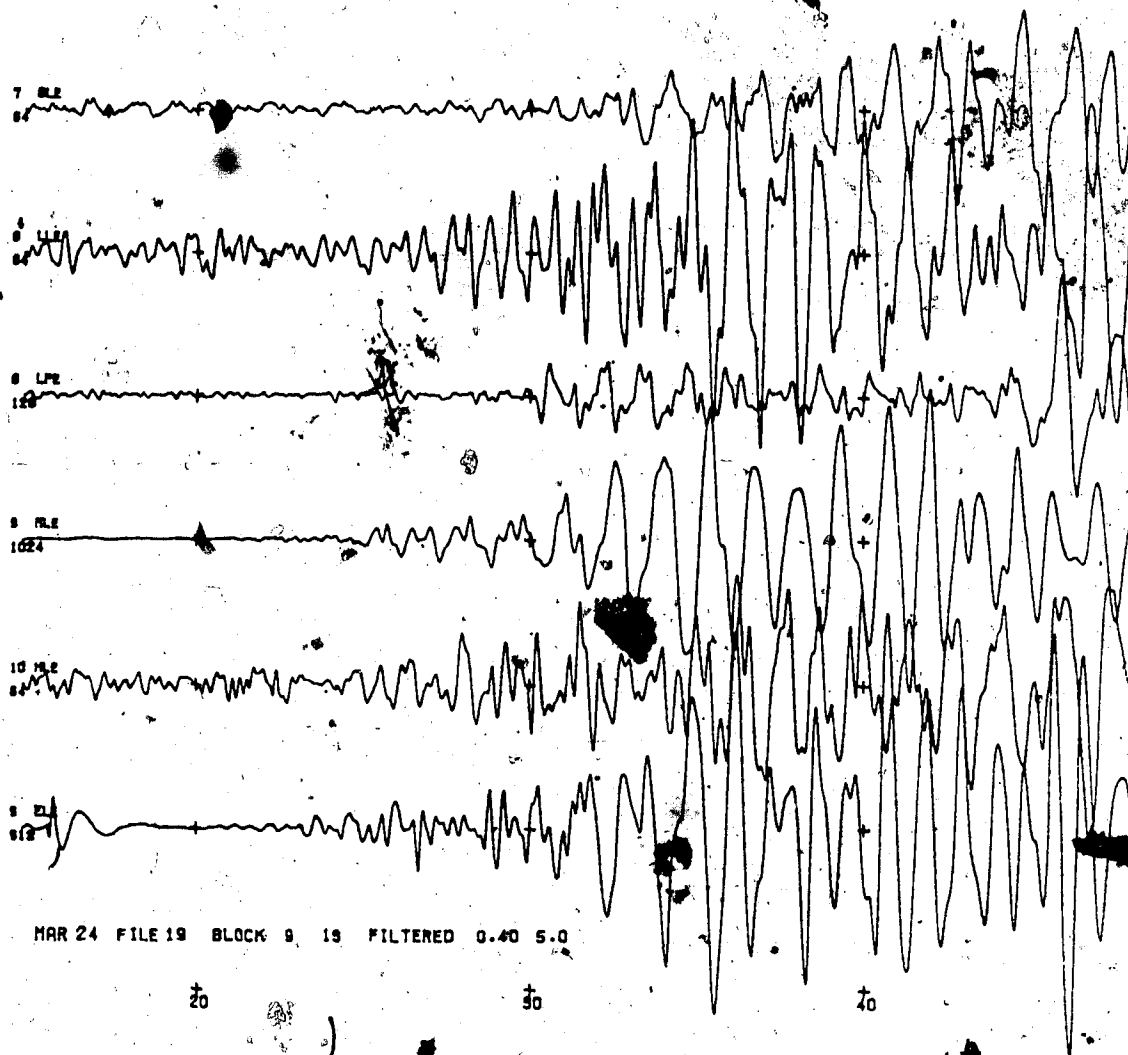


Figure 31.... Band Pass filtered "A" type event between 0.4 and 5.0 Hz. The signal appearance is quite satisfactory for analysis.

1983 A4 EVE.

| YEAR | DAY | HOUR | MIN | SEC | MSEC |
|------|-----|------|-----|-----|------|
| 1983 | 2   | 21   | 56  | 0   | 1384 |

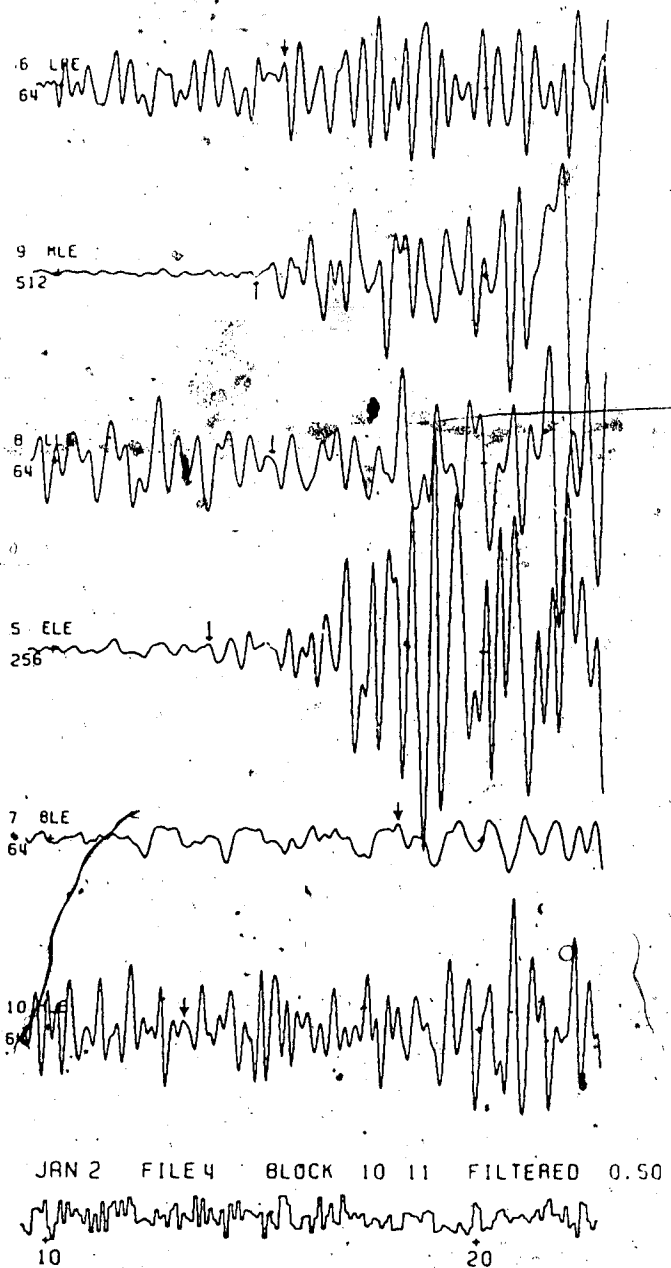


Figure 32.... Band Pass filtered "A" type event between 0.4 and 5.0 Hz. The hand picked P- wave arrivals are indicated with arrows.

such hand picked arrivals for a particular event as well as the observed arrival times for each station and directions of motion.

### 2.3.3 Tapering

Another method used in this study is to modify the data by tapering the signal levels so as to view both large and small amplitude phases. Some times the wave energy at any station is a number of times larger than the others. This creates difficulties in analog displays of the P- arrivals. The method gradually tapers the high amplitudes in order to get a scale ratio which allows a clear picture of first arrival. The algorithm has been developed by C. McCloughan under the direction of Dr. Kanasewich. At first it is applied a desired filter band, then the operator instructs where to start tapering and for how many points. The tapering function is a linear decrease with time. The program ignores stations with small amplitude ratios and only activates for the higher ones. Once tapering is done, a graphical plot of the event is obtained indicating the scale factor for amplitude reduction. Figure 33 shows such an application for a particular event. The method can be used to pick P- arrivals at a particular station where high amplitudes of later phases occur.

1983 A18 FILE 18 MAR 23 POINT 304 BLOCK 9 12  
 YEAR DAY HOUR MIN SEC MSEC  
 1983 82 22 13 1 211

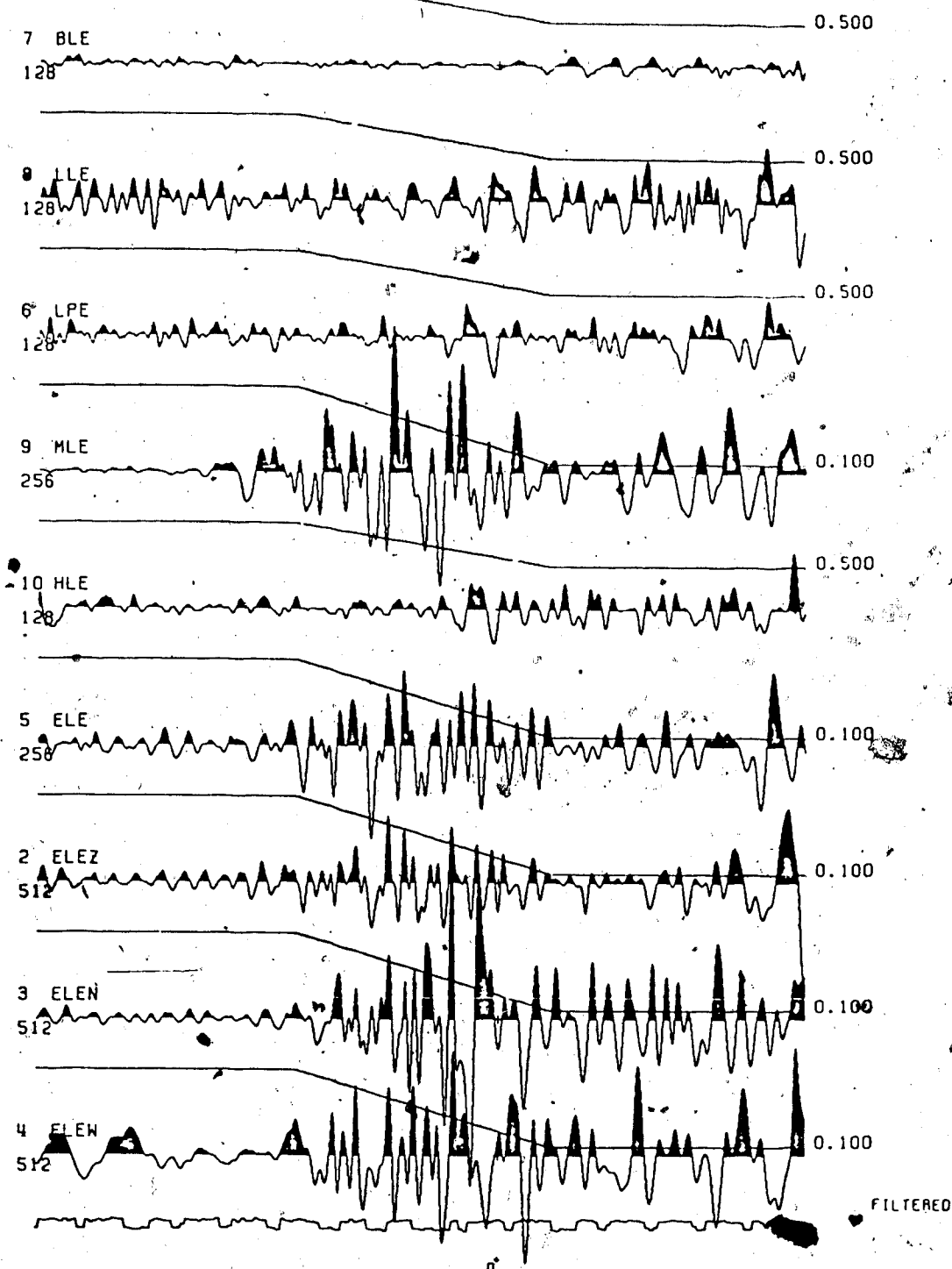


Figure 33.... A plot of a 'tapered "A" type event. High amplitudes linearly decrease with time by a factor indicated to the right of the signal.

### 2.3.4 Automatic processing

Because automation of data processing is attractive, in this study an algorithm was developed which does automatic phase picking, timing and first motion direction for single traces. A detailed description of this algorithm with results is presented in Chapter 3 of this thesis.

## 2.4 DATA ANALYSIS

For the operation of a microearthquake array it is necessary to determine the basic parameters of the recorded events. Such parameters are origin time, hypocenter location, magnitude, focal mechanism. In section 2.3 several techniques were introduced to process seismic data in order to obtain arrival times, first motions, amplitudes and periods, and signal durations. Once these data are known one can proceed with further analysis. Some basic steps before any analysis are the knowledge of station location, which is shown in Table 4, a realistic velocity structure model that characterizes the area, and at least four arrival times to the stations.

The velocity structure of the area has been obtained as follows. A pair of test shots were detonated on the 14th of February 1984, to calibrate the velocity model used to locate the Cold Lake events. The seismograms for this pair are shown in Figure 34. The charge size of B3 was 11 kg. and our estimate of the local magnitude from recorded seismograms is 0.0. Event B4 was from a total of 34 kg. of

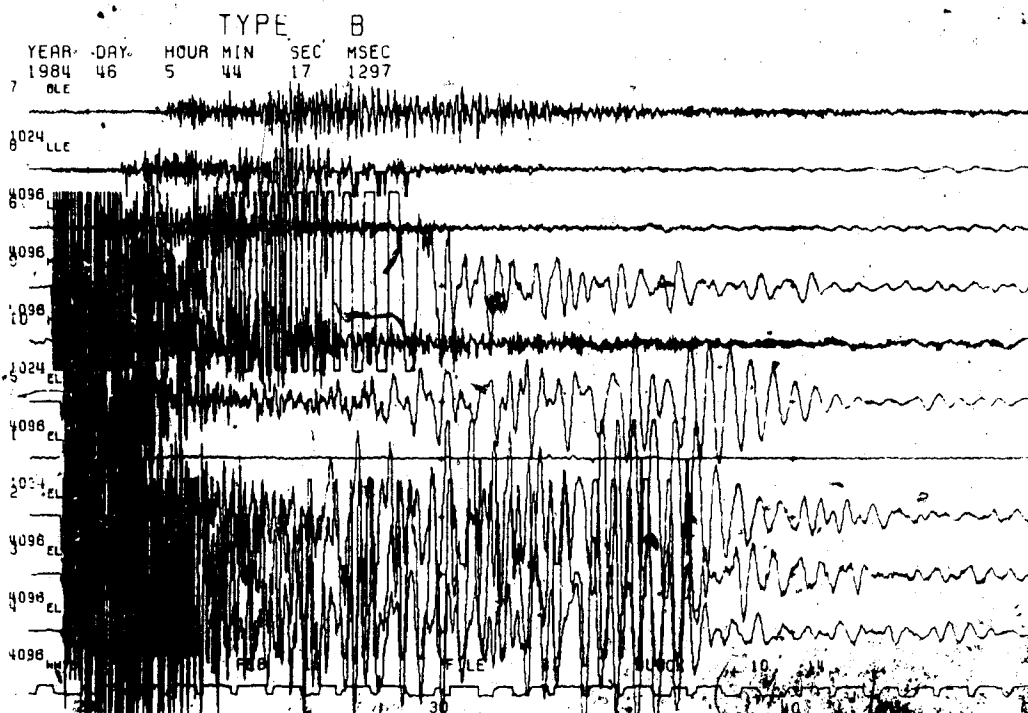
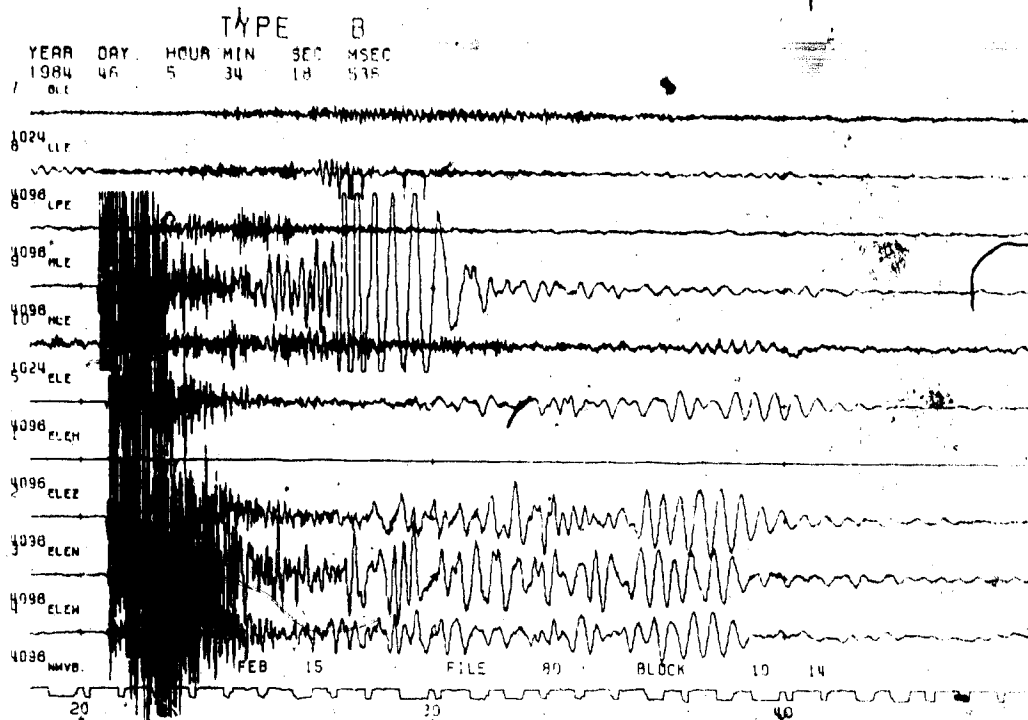


Figure 34.... Seismograms of B 3 and B 4. Event B3 is 11 kg. of explosives detonated in a single bore at a depth of 20m.. Event B4 is a 34 kg. total charge at depth of 20m.



charge in 3 shallow ( 20m) holes distributed over a distance of 50 m. Location of the events using HYP071 algorithm ( Lee and Lahr, 1975) was within 70 meters of the surveyed location. It is considered that the velocity function ( Table 7), obtained from sonic logs and refraction data, and the plane layered model are adequate for the present configuration of the array.

In terms of arrival time data in this study, we use P-arrival times. Arrival time data for other phases is difficult to obtain due to limited number of stations making correlation ambiguous. Using P- arrival times for locating earthquakes inside a network is not a very difficult problem. The major draw-back, with our inability to obtain later phase data, is the limited confidence in focal mechanism solutions. The magnitude of the event, following Japanese experience with earthquakes, is sometimes obtained from signal duration; this method has been used in our study and will be presented later on this thesis.

In order to obtain the necessary parameters, usage of a digital computer is necessary. As has been mentioned above, we use the HYP071 algorithm, a program which calculates hypocenter locations and focal mechanism solutions for a given set of arrival times, velocity structure and directions of motion. The methods of location, magnitude calculation and focal mechanism solutions will be discussed in detail here.

## CRUSTAL MODEL COLD LAKE

| P-VELOCITY<br>km/sec | DEPTH<br>km |
|----------------------|-------------|
| 0.700                | 0.00        |
| 1.200                | 0.10        |
| 2.100                | 0.18        |
| 2.400                | 0.33        |
| 2.600                | 0.48        |
| 4.500                | 0.55        |
| 5.800                | 1.20        |
| 6.500                | 3.00        |

Table 7.... Crustal model for Cold Lake as determined by two test explosions and verification with HYP071.

#### 2.4.1 Hypocenter determination

Upon the occurrence of an earthquake one can obtain a set of arrival times for a particular array. Using this data one needs to find the origin time and hypocenter of the earthquake. This procedure is called the earthquake location problem. Hypocenter refers to the projection on the surface of the earth directly above the focus or epicenter. In this study we used an earthquake location algorithm HYPO71 (Lee and Lahr, 1975) which uses Geiger's method for obtaining the location. A brief analysis on the basic implementation of the method is given here.

The earthquake location problem considers a four dimensional space, the spatial coordinates  $x, y, z$  and the time,  $t$ . A vector in such space is denoted as:

$$x = (x, y, z, t) \quad (2.1)$$

In the case of an earthquake event one has data consisting of arrival times,  $t_k$ , from stations located at  $(x_k, y_k, z_k)$ , where  $k=1, 2, \dots, m$ , is the number indentifying the station involved.

In order to obtain a location solution one must calculate travel times ( $T_k$ ) on the basis of a model which best describes the geophysical characteristics of the area. For a trial hypocenter at  $(x^*, y^*, z^*)$  at a trial origin time  $t^*$ , the trial vector  $x^*$  is given by :

$$x^* = (x^*, y^*, z^*, t^*) \quad (2.2)$$

Then the theoretical arrival time  $t_k$  of the model for  $x^*$  to the  $k$ th station is given by:

$$t_k(x^*) = T_k(x^*) + t^* \quad (2.3)$$

$$k = 1, \dots, m$$

where  $T_k(x^*)$  is the theoretical travel time and  $t^*$  is the trial origin time.

Then the residual travel time at the  $k$ th station,  $r_k$ , between observed and theoretical travel times is:

$$r_k = \tau_k - t_k(x^*)$$

or

$$r_k = \tau_k - T_k(x^*) - t^* \quad (2.4)$$

$$k = 1, \dots, m$$

The objective of the method is to minimize the residuals for particular adjustments of  $x^*$ , in the least square sense, using Geiger's (1912) method, which applies a Gauss-Newton iterative technique for the solution of the adjustment vector. The mathematical steps of the method applied to a microearthquake networks are described in detail in Chapters 5 and 6 of Lee et al. (1981). A summary explanation is given here avoiding details on Generalized Linear Inversion and solutions of linear systems.



$$G = \begin{bmatrix} m \Sigma a_i & \Sigma b_i & \Sigma c_i \\ \Sigma a_i & \Sigma a_i^2 & \Sigma a_i b_i & \Sigma a_i c_i \\ \Sigma b_i & \Sigma a_i b_i & \Sigma b_i^2 & \Sigma b_i c_i \\ \Sigma c_i & \Sigma a_i c_i & \Sigma b_i c_i & \Sigma c_i^2 \end{bmatrix} \quad (2.10)$$

$$\rho = (\Sigma r_k, \Sigma a_k r_k, \Sigma b_k r_k, \Sigma c_k r_k)^t \quad (2.11)$$

in which the  $\Sigma$  goes from  $k = 1, 2, \dots, m$  and

$$\begin{aligned} a_k &= \partial T_k / \partial x \\ b_k &= \partial T_k / \partial y \\ c_k &= \partial T_k / \partial z \end{aligned} \quad (2.12)$$

all evaluated at  $x^*$ .

Then using the system of equations 2.9 we solve the location problem following the steps (Lee et al., 1981)

1. Guess a trial origin time  $t^*$  and a trial hypocenter  $(x^*, y^*, z^*)$ , (usually taken to be at the station with the earliest time).
2. Compute the theoretical travel time  $T_k$ , and its spatial derivatives,  $\partial T_k / \partial x$ ,  $\partial T_k / \partial y$ ,  $\partial T_k / \partial z$ , at  $x^*$ , from the trial hypocenter to the  $k$ th station.
3. Compute the matrix  $G$  in equation (2.10) and the vector  $\rho$  as given in equation (2.11)
4. Solve the system of four linear equations given

in equation 2.9 for the adjustments  $\delta x$ .

5. An improved origin time is then given by  $t + \delta t$  and by  $(x + \delta x, y + \delta y, z + \delta z)$  and used as new trial hypocenter.

6. Repeat steps 2 to 5 until some cutoff criteria are met, and then the solution for the location is set.

As mentioned the above method is used in HYPO71. All the hypocenters calculated for this study have been derived using this program. Table 8 shows the basic parameters inputted in the algorithm and Table 9 shows some results and explanations on the output parameters.

#### 2.4.2 Magnitude Determination

Earthquake intensity variations show that there are different sizes of earthquakes. Based on the intensity effects seismologists thought it necessary to introduce a scale for rating earthquakes in terms of their energy. C. F. Richter proposed a magnitude scale in 1935 based solely on epicentral distance and the amplitudes of ground motion recorded by seismographs. This method is widely accepted and used in most research applications of seismology. The basic relationship for the local magnitude of an earthquake in terms of amplitude, observed at a station is given by

$$M = \log_{10} A - \log_{10} A_0(\Delta)$$

# EPICENTRAL DETERMINATION (HYPO71)

DATE (840106) = Year(1984), Month(01), Day(06).

ORIGIN (558 12.64) = Origin time (hr-min) (seconds).

LAT N: Latitude in degrees and minutes of epicenter.

LONG W: Longitude in degrees and minutes of epicenter.

DEPTH: Depth in km of hypocenter.

DM: Epicentral distance in km to nearest station.

RMS: Root mean square error of time residual in seconds.

ERH: Standard error of epicenter in km.

ERZ: Standard error of focal depth in km.

Q: Solution quality (A,B,C,D=excellent,good,fair,poor).

STN: Stations used in epicentral determination.

DIST: Distance from epicenter in km.

AZM: Azimuthal angle between epicenter and station in degrees.

AIN: Incidence angle measured from downward vertical.

HRMN: Hours and minutes of arrival time.

P-SEC: Second's portion of P-arrival.

TPOBS: Observed P-travel time in seconds.

TPCAL: Calculated travel time in seconds.

P-RES: Residual of P-arrival in seconds.

P-WT: Weight used in hypocenter solution for P-arrival.

Table 8.... Description of the parameters used for epicentral determination using HYPO71.



A1 - JAN 01 05 46 MAG. 1.3

| DATE   | ORIGIN    | LAT N    | LONG W    | DEPTH | MAG | NO | DM | GAP | RMS  |
|--------|-----------|----------|-----------|-------|-----|----|----|-----|------|
| 840101 | 546 48.18 | 54-32.66 | 110-21.11 | 0.00  | 1.3 | 5  | 2  | 106 | 0.32 |

| STN | DIST | AZM | AIN | PRMK | HRMN | P-SEC | TPOBS | TPCAL | P-RES | P-WT |
|-----|------|-----|-----|------|------|-------|-------|-------|-------|------|
| ELE | 2.0  | 134 | 9   | EPC0 | 546  | 49.40 | 1.22  | 1.12  | 0.10  | 1.20 |
| MLE | 6.4  | 31  | 7   | EPC0 | 546  | 50.00 | 1.82  | 2.00  | -0.18 | 1.07 |
| HLE | 9.6  | 239 | 7   | EPC0 | 546  | 50.35 | 2.17  | 2.55  | -0.39 | 0.96 |
| LPE | 9.9  | 329 | 7   | EPC0 | 546  | 50.73 | 2.55  | 2.60  | -0.05 | 1.00 |
| LLE | 12.0 | 306 | 7   | EPC0 | 546  | 51.79 | 3.61  | 2.96  | 0.65  | 0.77 |

A4 JAN 11 21 06 MAG. 1.2

| DATE   | ORIGIN     | LAT N    | LONG W    | DEPTH | MAG | NO | DM | GAP | RMS  |
|--------|------------|----------|-----------|-------|-----|----|----|-----|------|
| 840111 | 21 6 53.79 | 54-33.62 | 110-21.57 | 0.00  | 1.2 | 5  | 4  | 103 | 0.41 |

| STN | DIST | AZM | AIN | PRMK | HRMN | P-SEC | TPOBS | TPCAL | P-RES | P-WT |
|-----|------|-----|-----|------|------|-------|-------|-------|-------|------|
| ELE | 3.7  | 149 | 9   | EPC0 | 21 6 | 54.77 | 0.98  | 1.50  | -0.52 | 1.12 |
| MLE | 5.3  | 46  | 7   | EPC0 | 21 6 | 55.60 | 1.81  | 1.81  | 0.01  | 1.14 |
| LPE | 8.1  | 326 | 7   | EPC0 | 21 6 | 55.82 | 2.03  | 2.29  | -0.26 | 1.05 |
| HLE | 10.3 | 229 | 7   | EPC0 | 21 6 | 57.09 | 3.30  | 2.66  | 0.64  | 0.92 |
| BLE | 19.4 | 312 | 6   | EPC0 | 21 6 | 58.31 | 4.52  | 4.19  | 0.33  | 0.77 |

A7 JAN 22 20 35 MAG 1.5

| DATE   | ORIGIN    | LAT N    | LONG W    | DEPTH | MAG | NO | DM | GAP | RMS  |
|--------|-----------|----------|-----------|-------|-----|----|----|-----|------|
| 840122 | 2035 0.89 | 54-30.10 | 110-14.61 | 0.00  | 1.5 | 5  | 7  | 289 | 0.47 |

| STN | DIST | AZM | AIN | PRMK | HRMN | P-SEC | TPOBS | TPCAL | P-RES | P-WT |
|-----|------|-----|-----|------|------|-------|-------|-------|-------|------|
| ELE | 6.5  | 301 | 7   | EPC0 | 2035 | 2.67  | 1.78  | 2.02  | -0.24 | 1.36 |
| MLE | 10.9 | 340 | 7   | EPC0 | 2035 | 3.51  | 2.62  | 2.77  | -0.15 | 1.27 |
| HLE | 15.3 | 269 | 7   | EPC0 | 2035 | 4.31  | 3.42  | 3.53  | -0.11 | 1.04 |
| LPE | 17.9 | 318 | 6   | EPC0 | 2035 | 4.81  | 3.92  | 3.96  | -0.04 | 0.90 |
| LLE | 20.4 | 305 | 6   | EPC0 | 2035 | 6.77  | 5.88  | 4.35  | 1.53  | 0.43 |

A12 JAN 24 00 53 MAG. 1.2

| DATE   | ORIGIN    | LAT N    | LONG W    | DEPTH | MAG | NO | DM | GAP | RMS  |
|--------|-----------|----------|-----------|-------|-----|----|----|-----|------|
| 840124 | 053 55.22 | 54-36.33 | 110-18.14 | 0.00  | 1.2 | 5  | 1  | 254 | 0.52 |

| STN | DIST | AZM | AIN | PRMK | HRMN | P-SEC | TPOBS | TPCAL | P-RES | P-WT |
|-----|------|-----|-----|------|------|-------|-------|-------|-------|------|
| MLE | 1.3  | 175 | 9   | EPC0 | 053  | 56.75 | 1.53  | 0.98  | 0.55  | 1.20 |
| ELE | 8.4  | 192 | 7   | EPC0 | 053  | 57.00 | 1.78  | 2.33  | -0.55 | 1.03 |
| LPE | 8.4  | 282 | 7   | EPC0 | 053  | 57.72 | 2.50  | 2.35  | 0.15  | 1.06 |
| LLE | 12.9 | 271 | 7   | EPC0 | 053  | 57.60 | 2.38  | 3.11  | -0.73 | 0.88 |
| HLE | 16.4 | 224 | 7   | EPC0 | 053  | 59.41 | 4.19  | 3.72  | 0.47  | 0.84 |

Table 9.... Trial results of hypocenter determination produced from HYPO71.

where  $A$  is the maximum amplitude in millimeters by a seismogram at epicentral distance  $\Delta$  km, and  $A_0(\Delta)$  is the maximum amplitude at  $\Delta$  km for a standard earthquake.

In the case of nearby events recorded by a microearthquake array the amplitude is too dependent on local geological variations so another method is necessary. Many ideas were introduced for such estimations. Some researchers (Brune and Allen, 1967, Bakun et al., 1978a, Thatcher, 1973) used the maximum amplitude of ground displacement but were unsuccessful in relating this magnitude to the original Richter scale.

Bisztricsany (1958) introduced the idea of signal duration instead of maximum amplitude for magnitude estimations. He determined the relationship between earthquakes with magnitudes 5 to 8 and duration of their surface waves. Later on Solov'ev (1965) applied this technique using total signal duration. Other authors (Tsumura, 1967, Lee et al., 1972, Crosson, 1972) used total signal duration to make local magnitude estimation formulas for a particular microearthquake network. In general, the duration magnitude for a given station is given by

$$M_d = a_1 + a_2 \log_{10} r + a_3 \Delta + a_4 h$$

(Lee et al., 1981), where  $r$  is signal duration in seconds,  $\Delta$  is epicentral distance in kilometers,  $h$  is focal depth in kilometers, and  $a_1, a_2, a_3, a_4$  are empirical constants.

These constants are determined by correlating signal duration with Richter magnitude for a set of selected earthquakes. Also, it should be noted that the definition of duration magnitude varies from author to author.

In the Cold Lake microearthquake array an empirical formula has been obtained based on signal duration and amplitude response of the instruments. The relationship is

$$M_s = A + B \log_{10} r$$

where  $A = -4.5$  related to instrument response and  $B = 2.85$  obtained empirically from teleseismic events and the two trial explosions used to test the velocity structure (section 2.4). The signal duration is  $r$  in seconds.

Table 10 shows some magnitude calculations for various events throughout the study period. Also, Figure 35 shows microseism magnitudes plotted over a period of 5 years. As can be seen the magnitude variation for the Cold Lake array is from  $-2.0$  to  $+1.5$ , emphasizing the classification of the events as microearthquakes.

#### 2.4.3 Focal mechanisms - Fault plane solutions

The terms focal mechanism and fault-plane solution are synonymous because the earthquake focus, or source, is usually assumed to be a point dislocation (fracture), simulating a fault. The movement of the earth on the opposite sides of the fault plane is considered to be under

| EVENT | DATE   | ORIGIN     | DURATION(sec.) | MAGNITUDE |
|-------|--------|------------|----------------|-----------|
| A92   | 821225 | 21 6 0.78  | 108.41         | 1.30      |
| A101  | 821226 | 1457 24.41 | 61.58          | 0.60      |
| A105  | 821226 | 1825 6.04  | 61.58          | 0.60      |
| A109  | 821228 | 550 32.34  | 72.38          | 0.80      |
| A110  | 821228 | 1111 27.22 | 100.00         | 1.20      |
| A115  | 821229 | 1712 9.96  | 61.58          | 0.60      |
| A116  | 821229 | 1822 34.74 | 85.08          | 1.00      |
| A4    | 830102 | 2156 12.42 | 100.00         | 1.20      |
| A8    | 830111 | 2133 27.61 | 92.24          | 1.10      |
| A12   | 830113 | 1528 2.69  | 108.41         | 1.30      |
| A16   | 830206 | 2149 31.18 | 117.54         | 1.40      |
| A17   | 830207 | 035 8.26   | 117.54         | 1.40      |
| A18   | 830322 | 2212 3.74  | 100.00         | 1.20      |
| A19   | 830323 | 055 19.55  | 108.41         | 1.30      |
| A1    | 840101 | 546 48.52  | 108.41         | 1.30      |
| A4    | 840111 | 21 6 53.76 | 100.00         | 1.20      |
| A7    | 840122 | 2035 56.71 | 127.43         | 1.50      |
| A12   | 840124 | 053 55.84  | 100.00         | 1.20      |
| A17   | 840616 | 336 15.68  | 19.87          | -0.80     |
| A19   | 841101 | 21 4 21.11 | 29.76          | -0.30     |
| A20   | 841101 | 23 6 22.43 | 25.32          | -0.50     |
| A1    | 850101 | 1054 6.92  | 37.93          | 0.0       |
| A4    | 850101 | 1926 16.04 | 117.54         | 1.40      |
| A5    | 850102 | 810 57.97  | 108.41         | 1.30      |
| A7    | 850102 | 1526 56.96 | 61.58          | 0.60      |
| A30   | 850116 | 233 15.27  | 78.48          | 0.90      |
| A43   | 850608 | 1711 33.90 | 19.87          | -0.80     |
| A44   | 850612 | 1122 37.88 | 14.38          | -1.20     |
| A45   | 851203 | 1932 2.04  | 25.32          | -0.50     |
| A2    | 860103 | 152 17.35  | 72.38          | 0.80      |
| A3    | 860109 | 0 2 39.34  | 108.41         | 1.30      |
| A7    | 860114 | 2138 14.28 | 78.48          | 0.90      |
| A9    | 860117 | 23 3 37.76 | 78.48          | 0.90      |
| A15   | 861210 | 637 36.10  | 78.48          | 0.90      |

Table 10.... Local Magnitude estimates for "A" type events recorded by the Cold Lake seismic array.

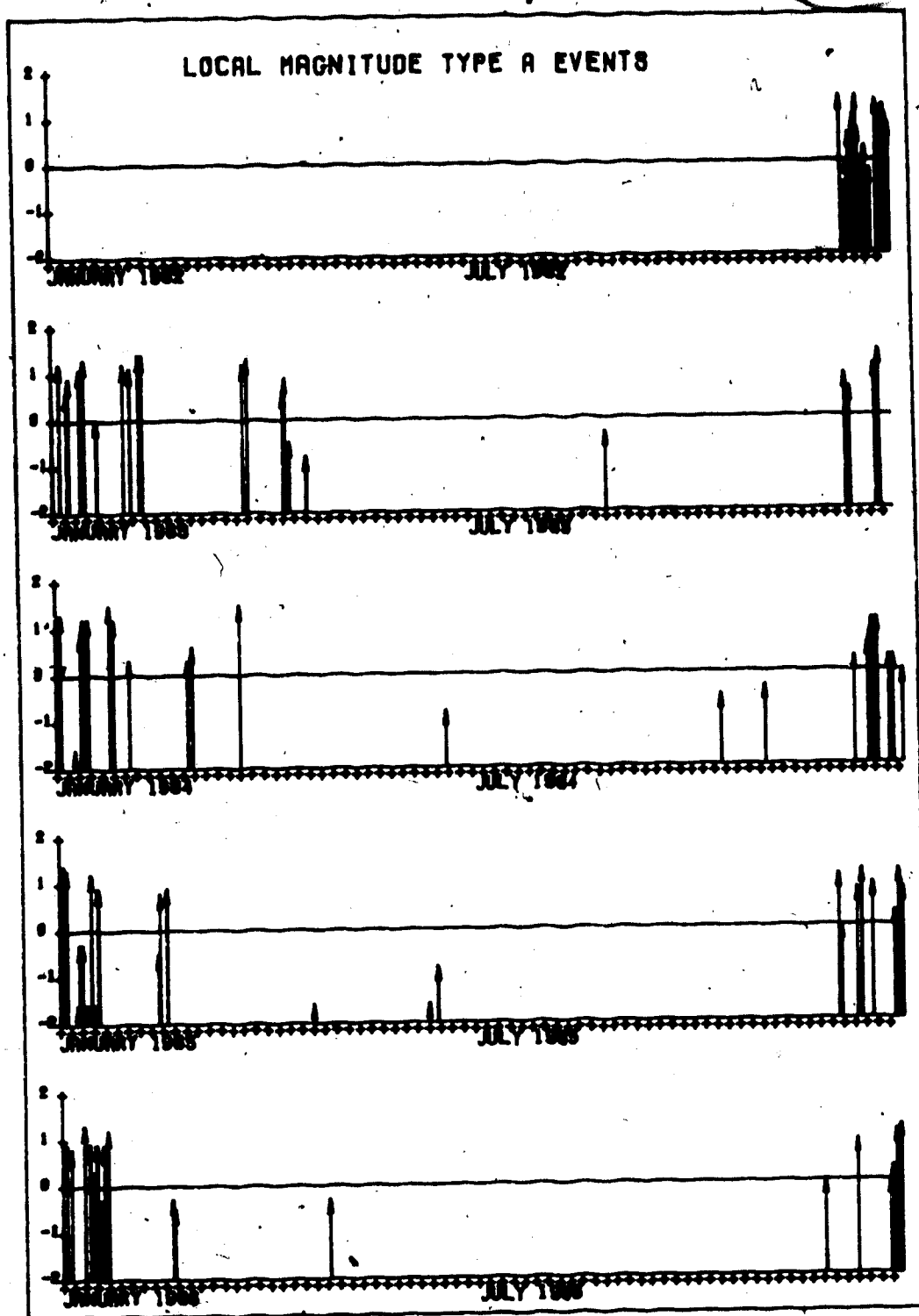


Figure 35.... Local Magnitude of "A" type events for a period starting in January 1982 to December 1986.

the action of a couple, the members of which act on opposite sides of the fault plane. As faulting takes place an elastic wave field is radiated from the earthquake focus.

For most microearthquake networks, focal mechanism solutions are based on first motion of P-waves. Later phases are difficult to identify because only vertical motion is recorded. P-waves can be separated by their first motion into a compression or a dilatation. The space around the focus is divided into four quadrants which receive initial compressions and initial dilatations (Figure 36). The orthogonal planes separating the quarter spaces are called nodal planes. One is the fault plane and the other the auxiliary plane. S-wave first motions are required to resolve the ambiguity of which is the fault plane.

Usually in focal mechanism studies the focus is modelled by point sources. A single form of combined forces is taken to represent the action at the focus. The common models are single couple and double couple. The radiation patterns for both P and S waves corresponding to these models are illustrated in Figure 37.

The axes that bisect the quadrants of compressional and dilatational initial motion are axes of maximum tensile (T) and maximum compressive stresses (P). Basic examples of fault orientation and the relation to these axes is shown in Figure 38. The directions and the nodal planes are shown on a stereographic projection on an equal-area sphere. These examples are used to correlate results for fault

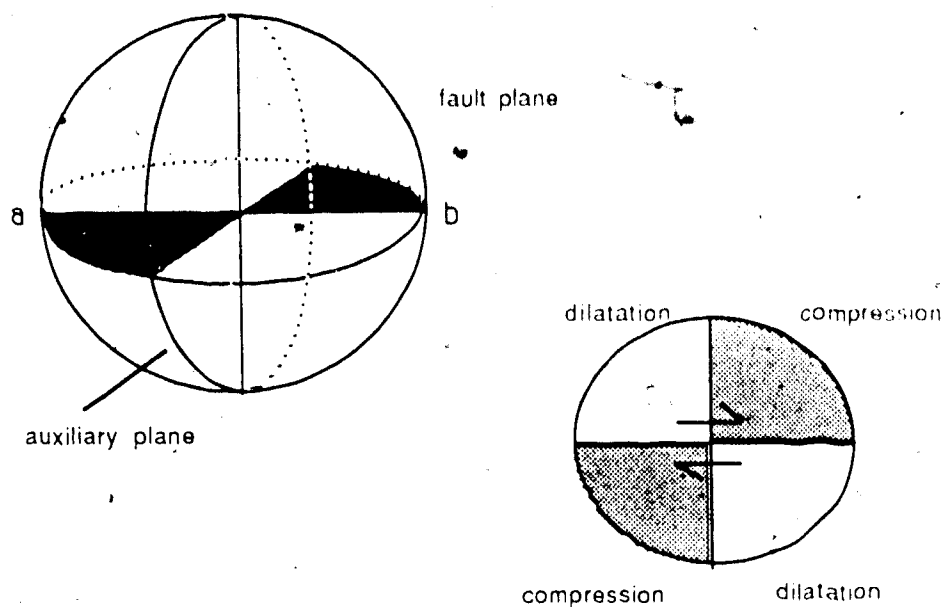


Figure 36.... Focal Mechanisms of an earthquake: first motion study. A small sphere is drawn around the focus of the earthquake resulting to a movement along the segment a-b. This results in compression and dilatation in opposite quadrants.

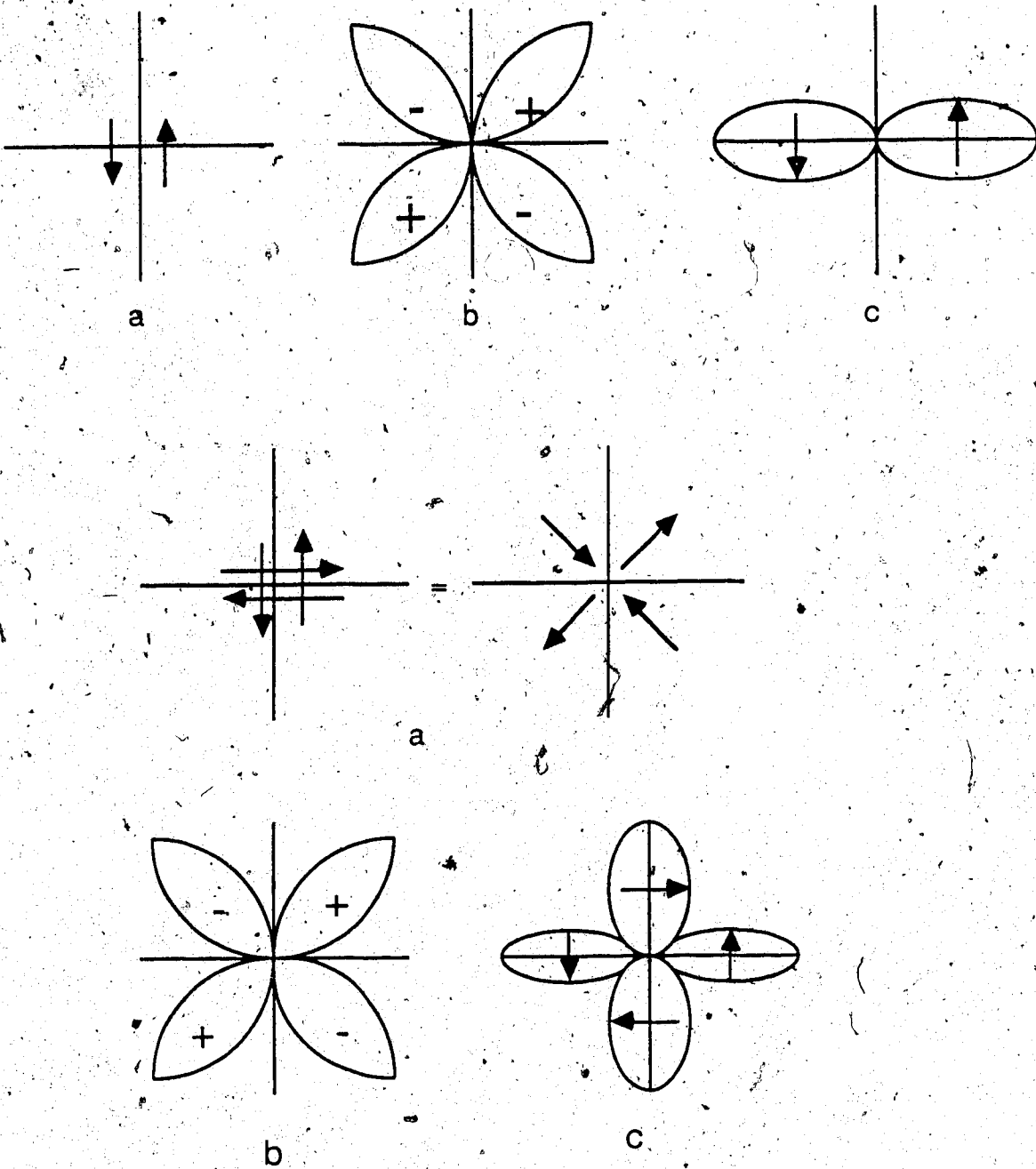


Figure 37.... Single couple (Top) and double couple fault mechanisms, with their radiation pattern of first motions for P- waves (b) and S- waves (c).



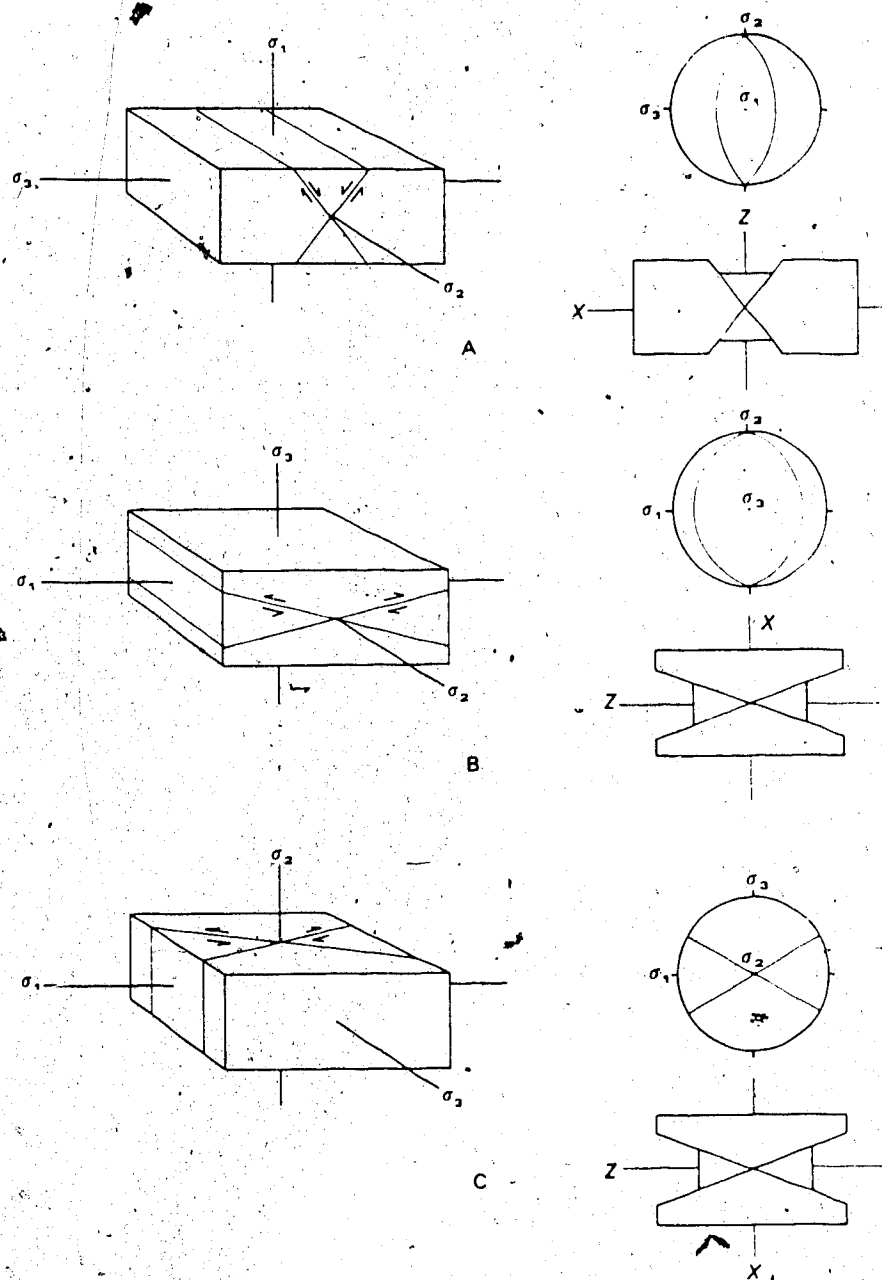


Figure 38.... Fault orientation in relation to principal stress and strain axis. A. Normal fault, B. Thrust fault and C. Strike-slip fault. (Modified from Park, 1983).

plane-solutions from first motion data.

In order to obtain focal mechanism solutions from our data we used the initial motion of P-waves. The solution consists of gathering data concerning the initial motion and plotting the data on an appropriate map and drawing orthogonal planes which separate the compressions from dilatations. In order to draw the planes we need to trace the observed data on the focal sphere (a hypothetical small sphere enclosing the focus).

The position of a given seismic station on the surface of the focal sphere is determined by two angles  $\alpha$  and  $\beta$ .  $\alpha$  is the azimuthal angle from the earthquake epicenter to the given station.  $\beta$  is the take-off angle of the seismic ray from the hypocenter to the given station. In the case of the focal sphere a point can be specified by  $(R, \alpha, \beta)$ , where  $R$  is the radius,  $\alpha$  the azimuthal angle and  $\beta$  the take-off angle. In case where we use an equal area projection, as I have mentioned above, these parameters are transformed into plane polar coordinates  $(r, \theta)$  by

$$r = \sqrt{2} R \sin(\beta/2), \quad \theta = \alpha$$

Since  $R$  is immaterial and the maximum value of  $r$  is taken as unity, the equation is modified to

$$r = \sqrt{2} \sin(\beta/2), \quad \theta = \alpha$$

( Lee et al, 1981, pp. 141-142). This formula is used in HYP071 to plot first motion data on the lower hemisphere of the focal sphere. Figure 39 and Figure 40 show examples of focal mechanism solutions for two events at depths 150m and 470m respectively.

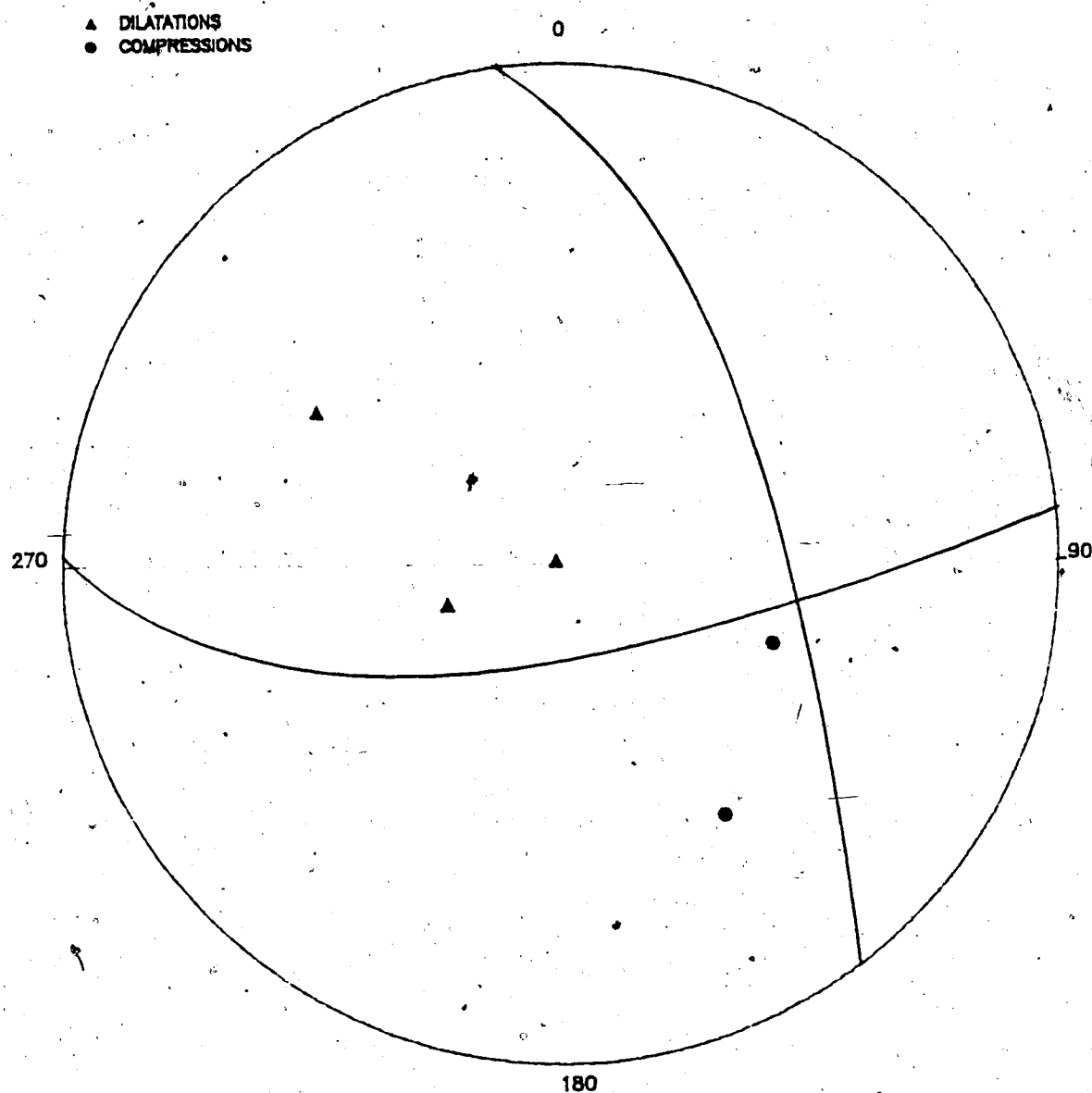


Figure 39.... Focal mechanism solution for an event at depth 150m. There is ambiguity with is the fault and auxiliary plane, As seen there is a dip of  $40^\circ$  NE with a stike  $7^\circ$  NW.

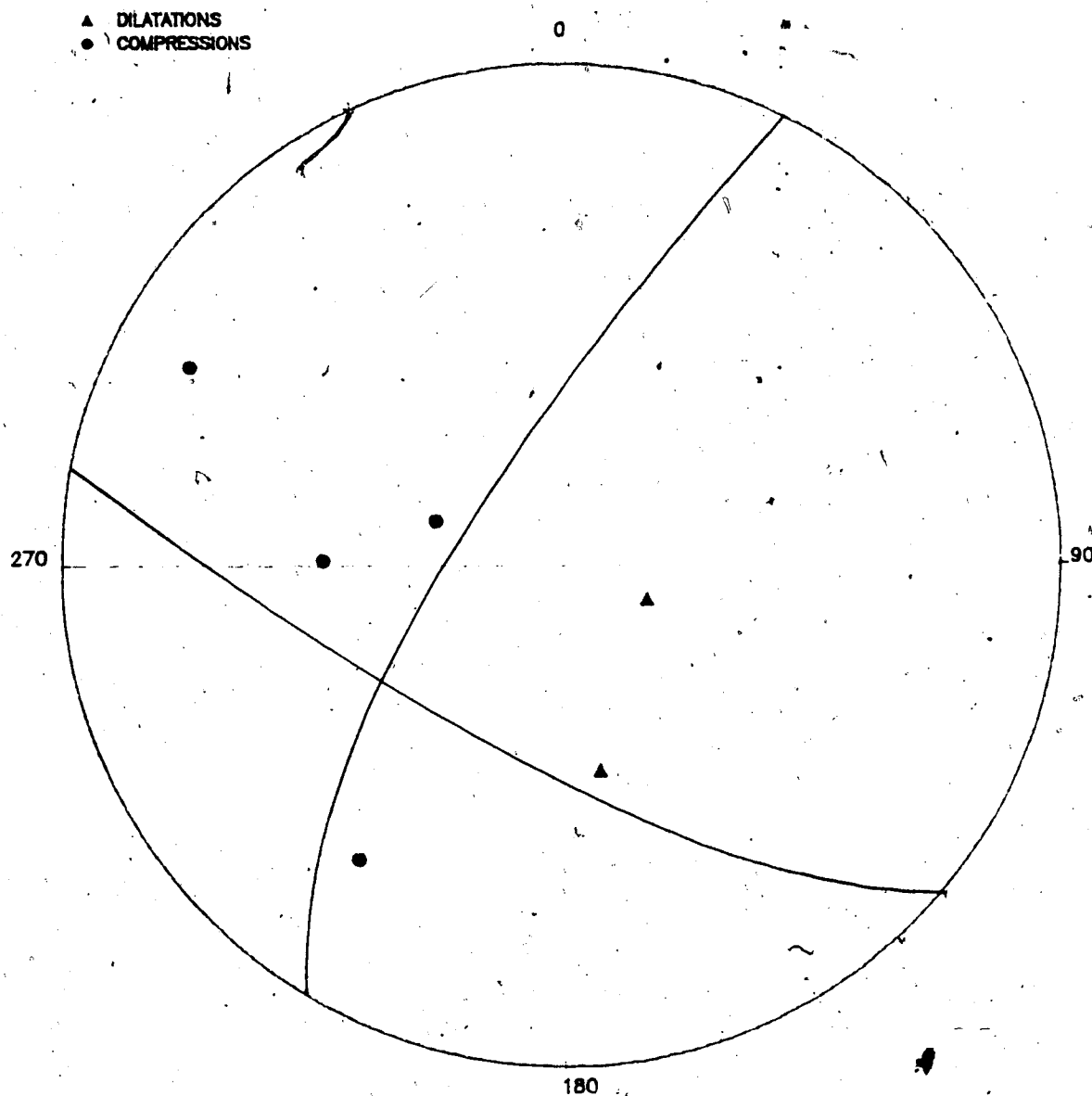


Figure 40.... Focal mechanism solution for an event at depth 470m. It has a dip of  $80^{\circ}$  NW with a strike  $32^{\circ}$  NE.

### 3. AUTOMATIC SEISMIC ANALYSIS

#### 3.1 INTRODUCTION

Computer technology and introduction of artificial intelligence have already been applied to seismic studies (Anderson 1982, Gaby and Anderson 1983, Allen 1978, Stewart 1977, Stevenson 1976). In many microearthquake networks automated approaches have been developed for data analysis. Because most microearthquake arrays are designed for precise determination of hypocenters, it is necessary to have a system that detects first P- arrival times accurately. The automatic system must be capable of analyzing an event logically discarding noise spikes and also later phases in an earthquake.

One of the basic problems in this analysis is that the waveforms recorded at each station in the array have been observed to be dissimilar. This implies that the automatic detection system should be designed to operate independently on single station records before considering the ensemble of data from all stations. A short discussion will be given here for the various methods used.

Most authors use the concept of the characteristic function in their design of algorithms to detect first P- arrival on a single trace. The incoming signal is usually transformed into one or more time series for P- arrival detection. The transformed series, in some cases, is the characteristic function  $C(k)$ , where  $k$  is a time index.

Various such functions have been used, Stewart et al. (1971) used the following

$$C_1(k) = |X_k - X_{k-1}|, k=2,3,\dots \quad (3.1)$$

where  $X_k$  is the amplitude of the incoming signal at time  $t_k$  and  $k$  is an index for counting data points. This type of function works well if the incoming signal contains impulsive high-frequency seismic waves. Along the same lines, Crampin and Fyfe (1974) used equation (3.1) calling it a one sample mechanism, and also introduced four- and eight- sample mechanism functions as

$$C_4(k) = |X_k - X_{k-4}|, k=5,6,\dots \quad (3.2)$$

$$C_8(k) = |X_k - X_{k-8}|, k=9,10,\dots \quad (3.3)$$

These functions are then checked against a threshold level, to see if any one exceeds the level in which case an event is declared. In order to declare an event the condition is that at least three channels should be triggered within a short time window. Then the P- arrival is taken as the time of the first trigger in the time window.

Allen (1978) introduced a characteristic function sensitive to amplitude variations and its first derivative. He defined the modified signal amplitude as

$$A_k = W_1 A_{k-1} + (X_k - X_{k-1}) \quad (3.4)$$

where  $W_1$  is a weighting constant and then the characteristic function is

$$C(k) = A_k^2 + W_2 (X_k - X_{k-1})^2 \quad (3.5)$$

where  $W_2$  is also a weighting constant. Then he calculates the short-term and the long-term average of  $C(k)$ ,  $\alpha(k)$  and  $\beta(k)$  respectively. If  $\alpha(k)/\beta(k)$  exceeds 5 at time index  $k = j$  then an event is declared to have occurred at time  $t_j$ .

Anderson (1978) used another method for calculating a characteristic function. From the input signal,  $X_k$ , the modified amplitude is been obtained as

$$Y(k) = X_k - Z_k \quad (3.6)$$

where  $Z(k)$  is the moving average of the signal given by

$$Z(k) = (n+1)^{-1} \sum |Y(i)| \quad (3.7)$$

for a particular time window (summation). This moving average is used as the threshold criterion for arrival detection.

Numerous methods have been applied to seismic signals for automatic analysis. Each one has its advantages and drawbacks depending on the quality of the recording site,



the instruments used and the signal level. The major benefit from these methods is that it frees the analyst from tedious work. Even though visual methods could be more accurate, automatic methods could be used to process large amounts of events for quick analysis of seismic parameters. A similar type of automatic analysis method has been applied to Cold Lake seismic data.

### 3.2 AUTOPIK

AUTOPIK is a computer based analysis routine designed for seismic signals from the Cold Lake array. The aim of this computer based seismic recognition method is to produce accurate first motion data from single seismic traces. A complete interactive FORTRAN program has been developed to perform the desired steps. The algorithm (which we named AUTOPIK) has been tested with real data and produced good results.

The steps in this automatic analysis are:

- i) Detect arrivals on several stations
- ii) Apply tests to reject false arrivals
- iii) Determine first arrival time and other useful seismic parameters.
- iv) Use results to locate earthquakes and to obtain focal mechanism solutions.

The algorithm at this stage detects first arrival times and checks if they meet certain criteria. The results are being compared to hand picked ones. It should be noted that there is always an ambiguity associated with first arrivals of microtremors, especially due to noise contamination. The algorithm has been tested for events greater than  $M=1.0$ . It has been also applied to events with smaller magnitude.

The basic picking algorithms due to Allen 1978, Anderson 1978, and Stewart 1977, use characteristic functions of the seismic trace  $Y(t)$ , as has been mentioned in section 3.1. I have followed Allen's (1978) approach with some modifications, and a different characteristic function for the seismic trace  $Y(i)$  where  $i=1,2,\dots$  time index. Figure 41 shows the logic blocks (steps) the AUTOPICK routine follows for automatic analysis. The original field data (seismic signal) goes through a filter, then the autopick routine detects the arrivals and if the conditions are met in the criteria routine it stores the results. Figure 42 shows the original field data from station MLE and Figure 43 shows a band passed section of the first arrival from a microseismic event which is used as  $Y(i)$ . Define a modified amplitude  $R(i)$  as:

$$R_i = C_1 R_{i-1} + (Y_i - Y_{i-1}) \quad (3.8)$$

$$C_1 = 0.2 \text{ (weighting constant) and } R_1 = Y_1$$

Figure 44 shows function  $R(i)$  from the example in Figure 42.

## AUTOPICK LOGIC

## BLOCKS

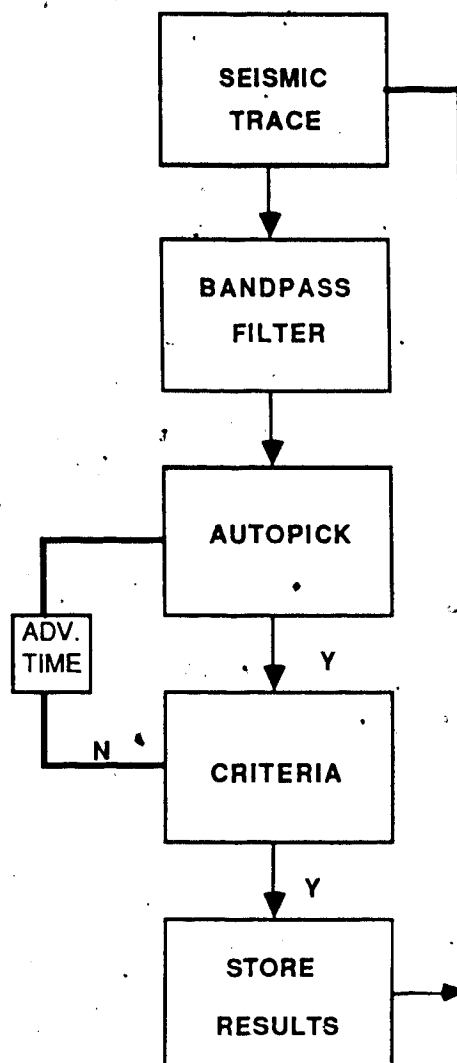


Figure 41.... The logic steps ( blocks ) that the AUTOPICK routine follows in order to perform automatic analysis.

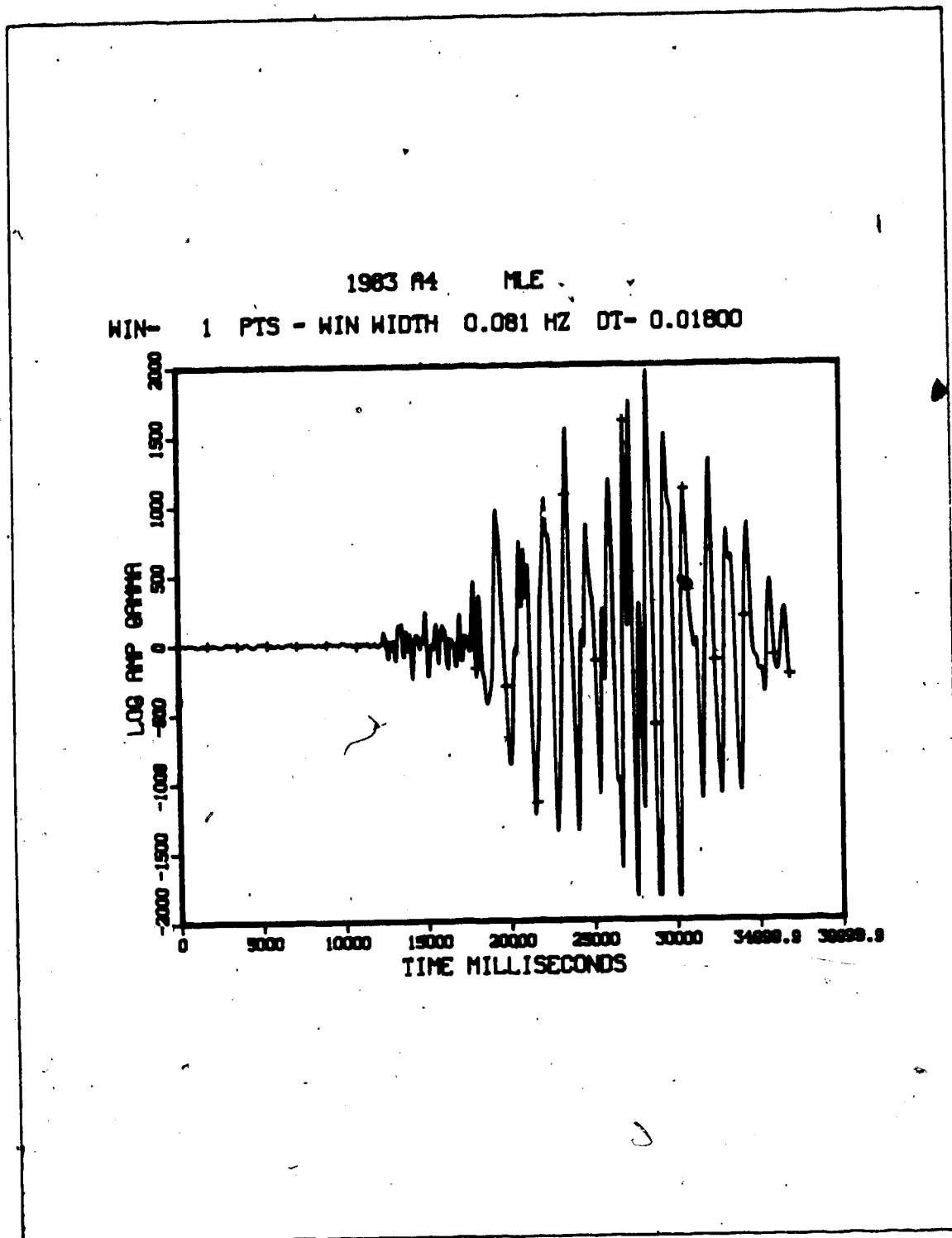


Figure 42.... MLE station raw field data before any analysis from the AUTOPICK has been done.

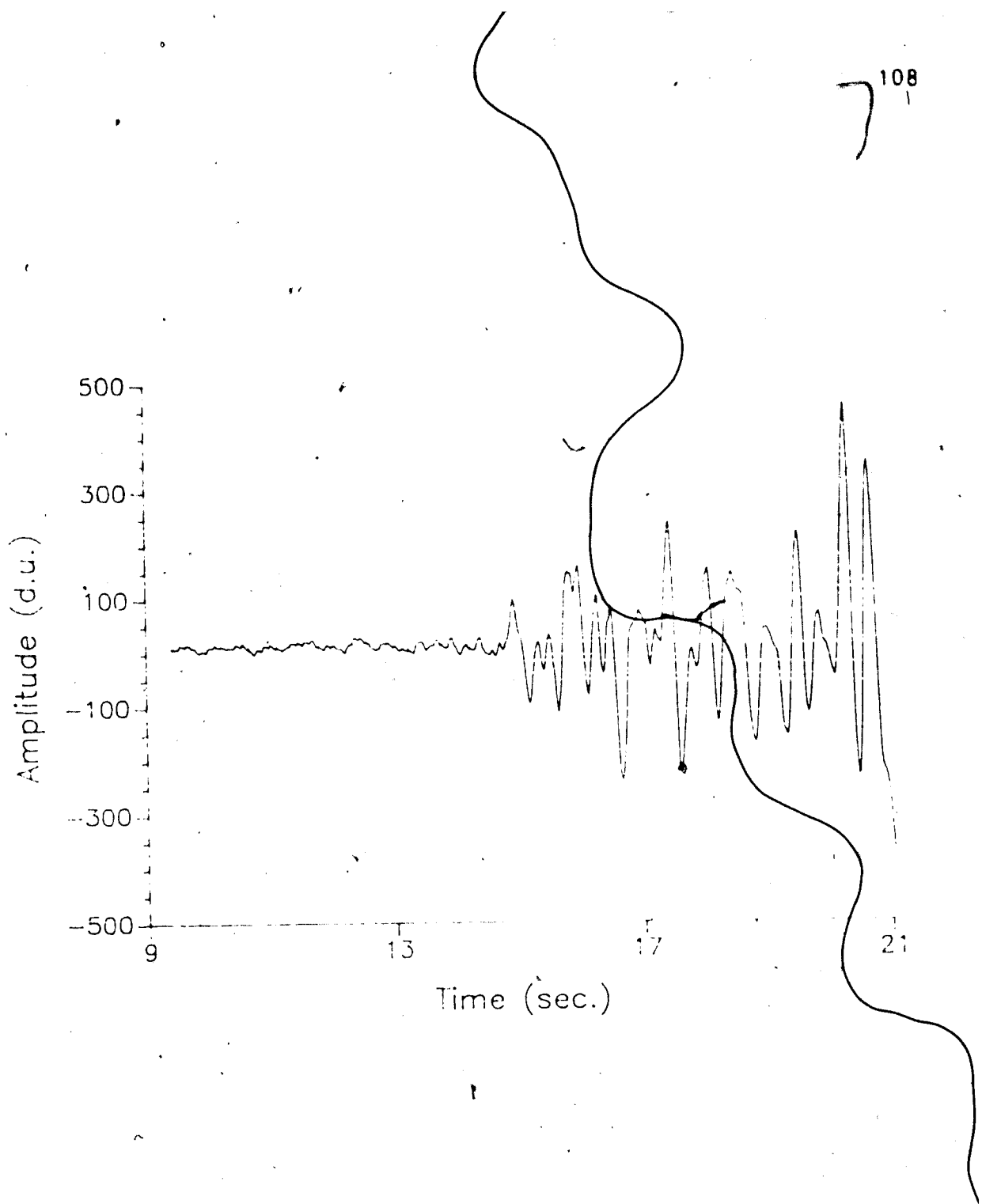


Figure 43.... Band-pass filtered data from station MLE ready to be processed by the automatic seismic recognition routine.

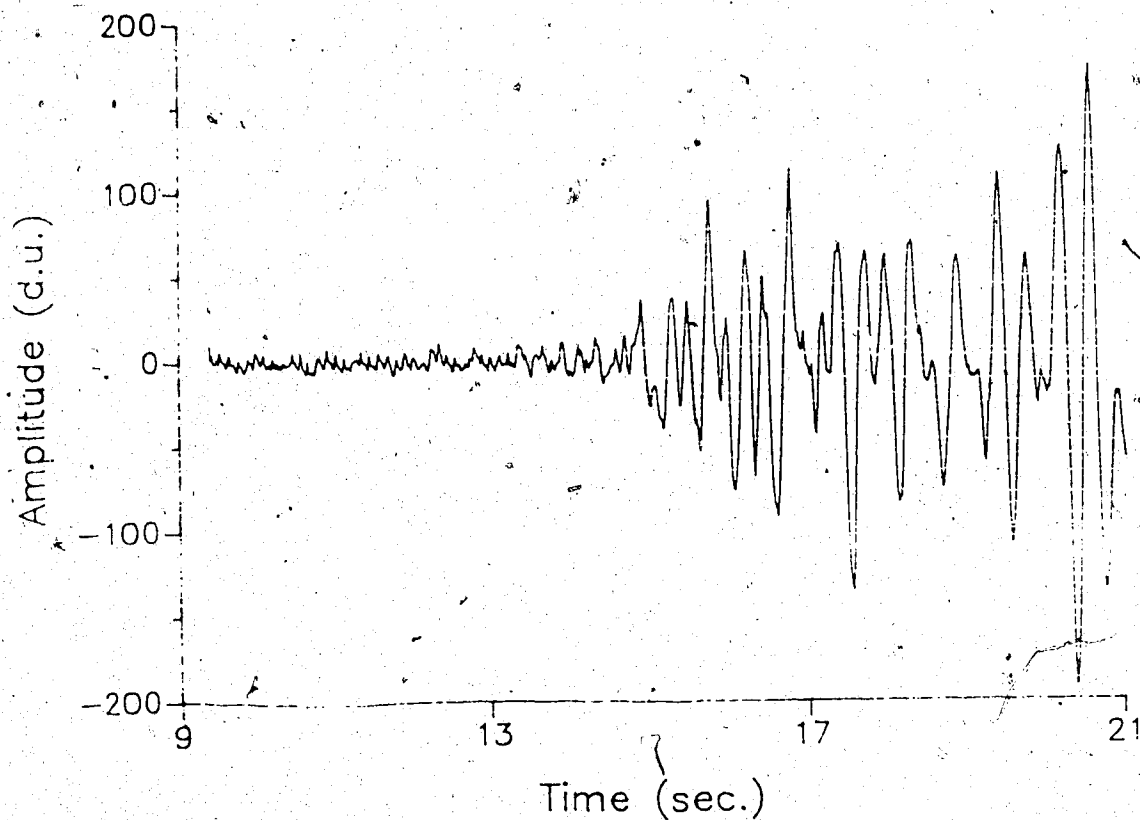


Figure 44.... Modified amplitude signal of an "A" type event using the AUTOPICK routine. Most of the DC component has been removed.

Calculate the first weighted difference

$$\Delta R_1 = C_2 (Y_1 - Y_{1-1}) \quad (3.9)$$

$$C_2 = 0.02 \text{ and } \Delta R_1 = Y_1$$

Next compute the second weighted difference

$$\Delta^2 R_1 = C_3 (Y_{1+1} - 2 Y_1 + Y_{1-1}) \quad (3.10)$$

$$C_3 = 0.002 \text{ and } \Delta^2 R_1 = Y_1$$

Define the characteristic function  $F(i)$  as:

$$F_1 = R_1^2 + (\Delta R_1)^2 + (\Delta^2 R_1)^2 \quad (3.11)$$

The short term average  $a_1$  of  $F(i)$  is defined as,

$$\bar{a}_1 = a_{1-1} + C_4 (F_1 - a_{1-1}) \quad (3.12)$$

$$C_4 = 0.05 \text{ and } a_1 = 0.1$$

the long term average  $\beta_1$  of the characteristic function  $F(i)$  is defined as,

$$\beta_1 = \beta_{1-1} + C_5 (F_1 - \beta_{1-1}) \quad (3.13)$$

$$C_5 = 0.002 \text{ and } \beta_1 = 0.1$$

Define a reference level for the long term average,

$$\gamma_i = C_s \beta_i \quad (3.14)$$

$C_s = 7.0$  (threshold constant)

Before processing the signal we apply bandpass filtering to reduce noise that is outside the frequency range of interest and also eliminate the dc bias level. Figure 45 shows the flow chart (steps) that the AUTOPICK routine follows, before meeting any criteria.

The algorithm checks if  $\alpha$  and  $\beta$  meet certain threshold criteria to detect first arrivals. This is based on the hypothesis that sudden changes of the function  $\alpha$  are more sensitive to signal level variations such as P-arrival. The  $\beta$  function verifies that the pick is an arrival and not noise.

The threshold criteria vary depending on the signal to noise ratio. In our case if  $\gamma \geq 7.0$  and  $\alpha > \gamma$  then a pick is flagged.

Plots of  $\alpha$  and  $\gamma$  (Figure 46 and Figure 47) indicate sharp changes in the first arrival area. This change occurs at the first arrival time but the algorithm has also flagged several wrong arrivals.

In order to avoid false arrivals the program goes through a conditions routine. Figure 48 shows the steps followed by the criteria routine. First when an arrival is triggered by the autopick routine at time  $t_k$  the program checks if  $\alpha > \gamma$  at that time index. If the condition holds the routine finds the first zero crossing of the signal. The



# FLOW CHART AUTOPICK

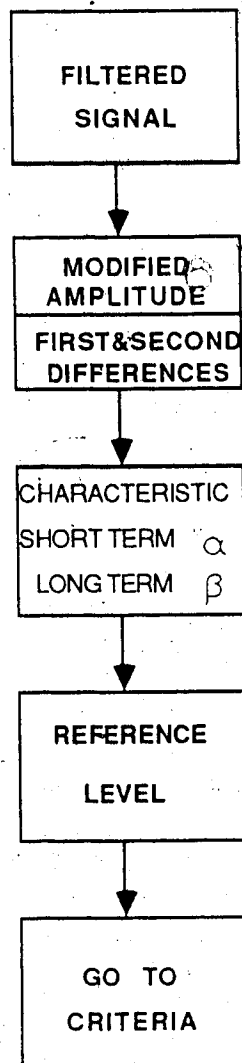


Figure 45.... Flow chart of the AUTOPICK routine steps. These steps are done before the operation goes through the criteria routine.

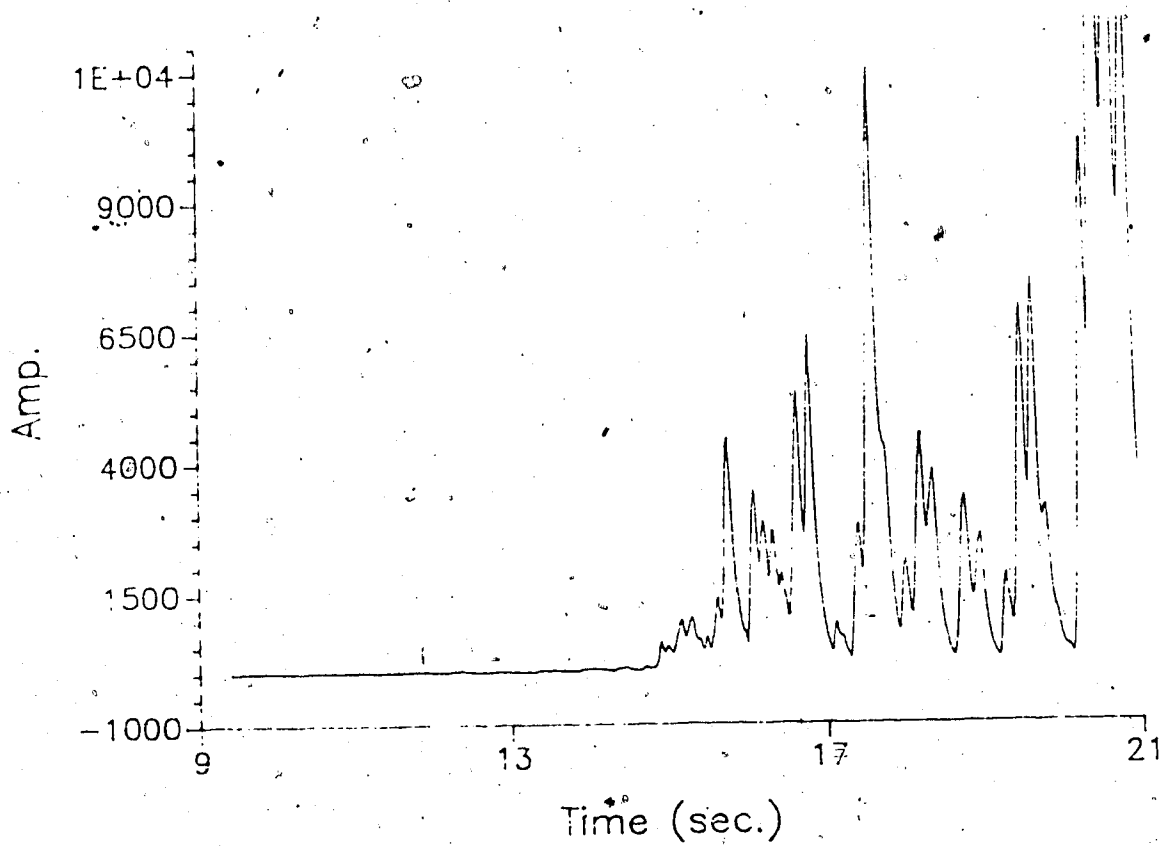


Figure 46.... Short term average of the modified time series used to detect first arrivals. The sharp change at the arrival point is evident.

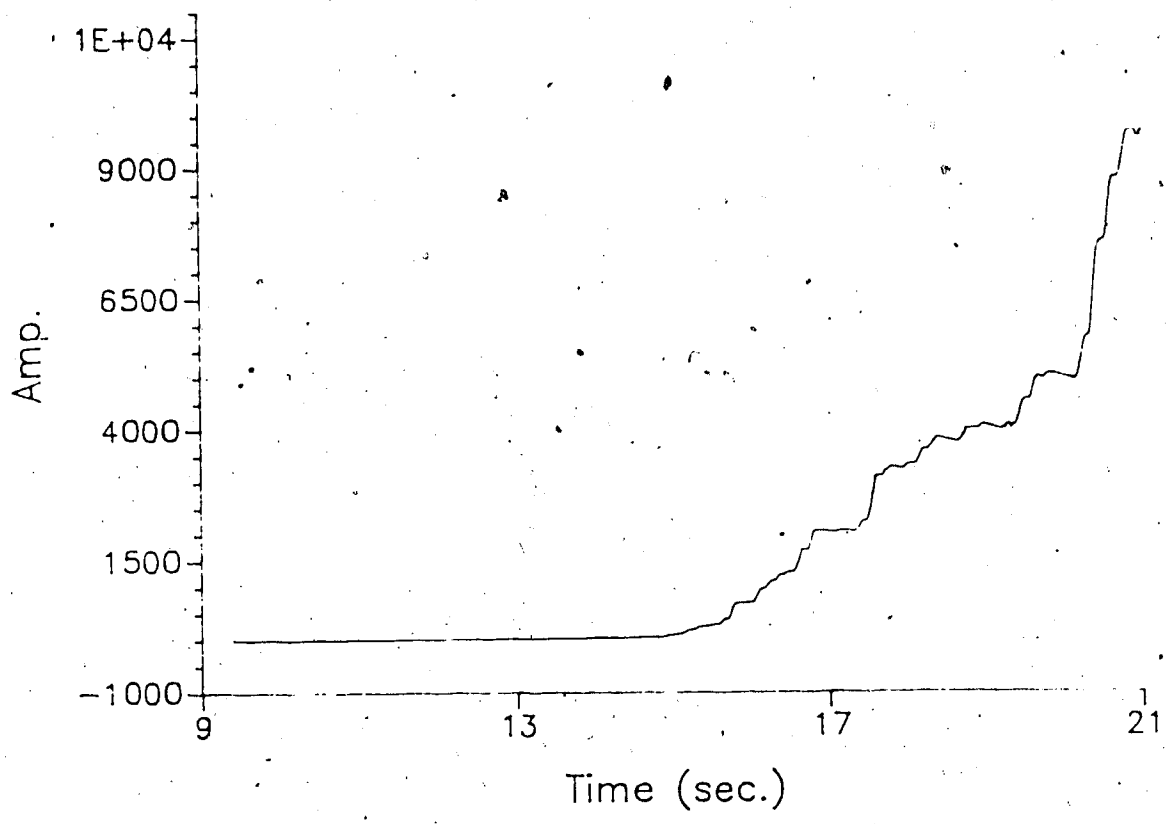


Figure 47.... Long term average of the modified time series. This function is used as a threshold criterion. It also verifies the presence of noise.

## CRITERIA

## ROUTINE

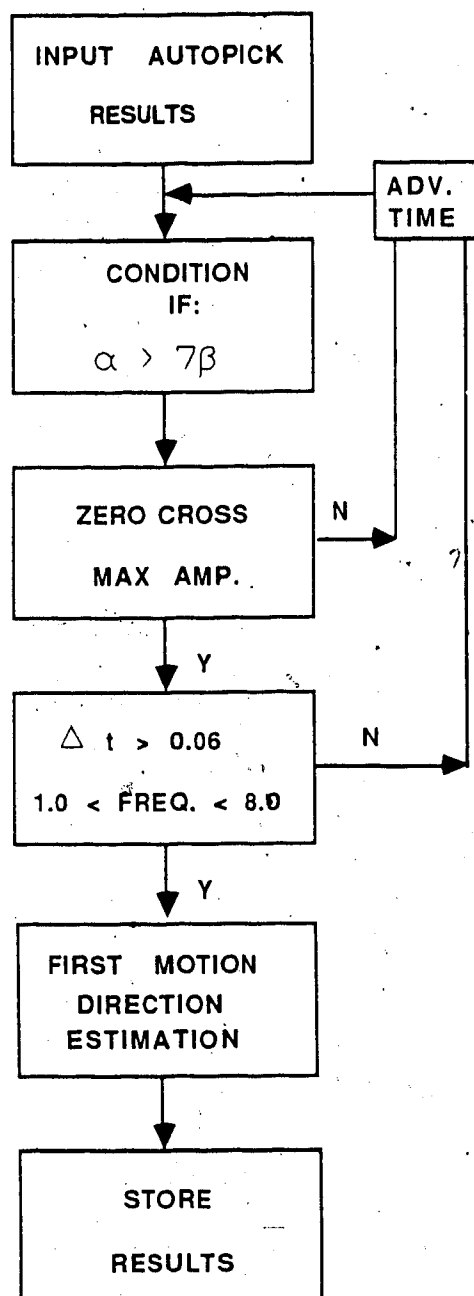


Figure 48.... Logical steps followed by the Criteria routine. If these conditions are met an event is declared and stored.

time of this crossing is taken to be as the time of the first crossing that least deviates from  $t_k$ , the triggered time. Figure 49 shows this operation graphically.

Once one has the first zero crossing, the candidate for first arrival time, one checks for the maximum amplitude criteria in that time interval. If the amplitude falls within the given dynamic range, it should be noted that this criterion varies from station to station in Cold Lake, then the operation continues. If the amplitude condition is false, then the operation advances a time step  $k+1$  and goes through the reference level estimation again.

The next step in the process is the estimation of the time difference between the three consecutive zero crossings starting at the first zero crossing point. If the time difference  $\Delta t$  is less than 0.06 then the phase duration is considered to be correct, otherwise the program goes back to estimate the next triggering level. Upon verification of the phase duration the maximum amplitude of the signal between each zero crossing is checked to meet certain criteria.

If all the above conditions hold, finally the dominant frequency of the time window chosen is checked. The dominant frequency is defined as

$$DF = (1/2) \times 3 \times (1/T_3 - T_1) \quad (3.15)$$

where  $T_1$  is the time of the first zero crossing (first arrival) and  $T_3$  is the time of the third zero crossing

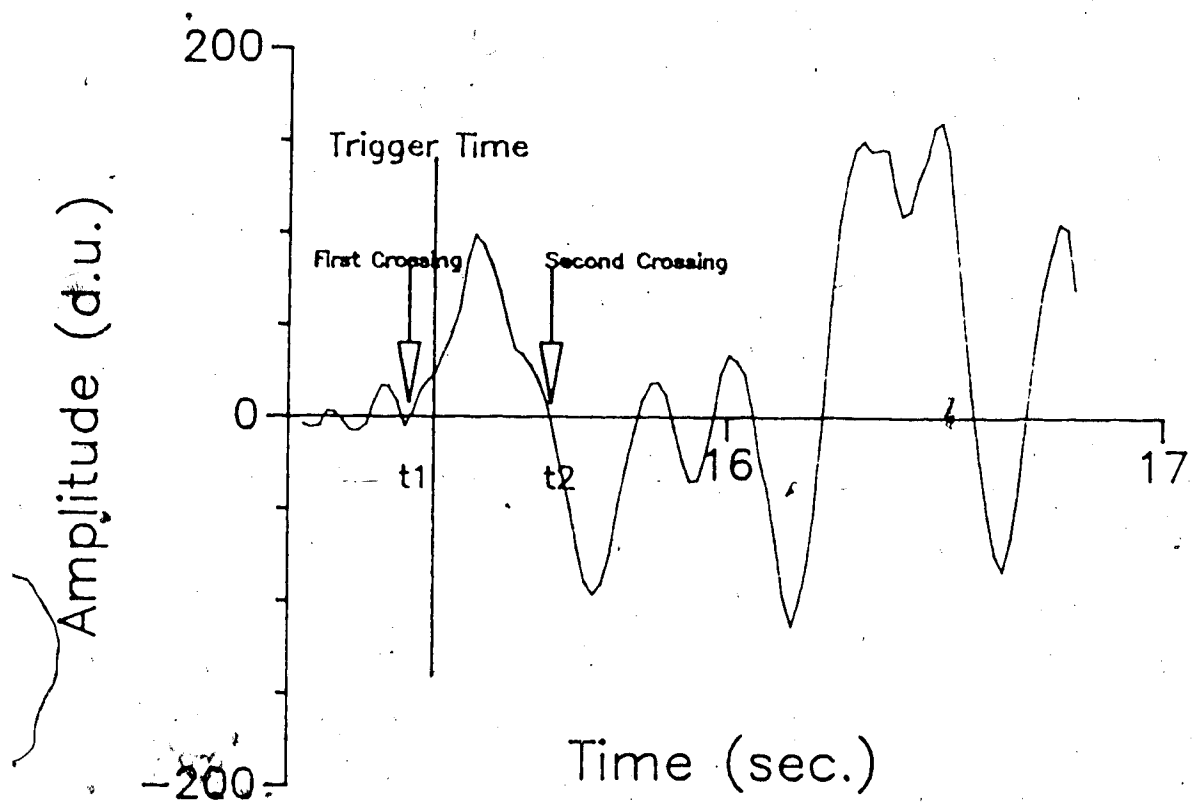


Figure 49.... Graphical representation of the operation used to choose the first zero crossing with respect to triggered time position.

starting at T1. If the dominant frequency is found to be between 1 to 8 Hz then a true first arrival is flagged at T1, otherwise the algorithm advances a time frame to check the conditions again.

At the end the algorithm checks the direction of the first motion. This is obtained by checking the sign of the maximum amplitude value between the first and second zero crossings. If the value is positive the first motion is considered U (up) or + indicating compressions, and if negative is denoted as D (down) or - indicating dilatations.

Finally, the first arrival times for each station, along with directions of motion and dominant frequencies are stored in a file to be used for further analysis.

### 3.3 APPLICATIONS OF AUTOPICK

During completion and testing of the algorithm on many events several problems were observed such as misspicks in events that were impossible to verify visually. No picking was possible on events with small magnitudes and for very noisy signal conditions. All algorithms must fail at some low signal level. The overall performance of the algorithm was satisfactory in those events with large enough magnitude and adequate signal/noise ratio.

Figure 50 and Figure 51 show some results obtained from the AUTOPICK routine. Also Table 11 lists the results of these applications. Comparison of results with hand picked ones is listed in Table 12. We can see that there isn't any

1984 R44 AUTOPICK RESULTS

| YEAR | DAY | HOUR | MIN | SEC | MSEC |
|------|-----|------|-----|-----|------|
| 1984 | 22  | 20   | 35  | 56  | 1207 |

7 BLE  
84

8 LLE  
256

6 LLE  
128

9 HLE  
1024

10 HLE  
128

5 ELE  
1024

JAN 22 FILE 44 BLOCK 10 12 FILTERED 0.40 5.0

†

†

Figure 50.... Autopick results for an "A" type event that occurred on January 22, 1984. The arrows indicate the automatically obtained first break.



## 1982 A92 AUTOPICK RESULTS

| YEAR | DAY | HOUR | MIN | SEC | MSEC |
|------|-----|------|-----|-----|------|
| 1982 | 359 | 21   | 5   | 57  | 488  |

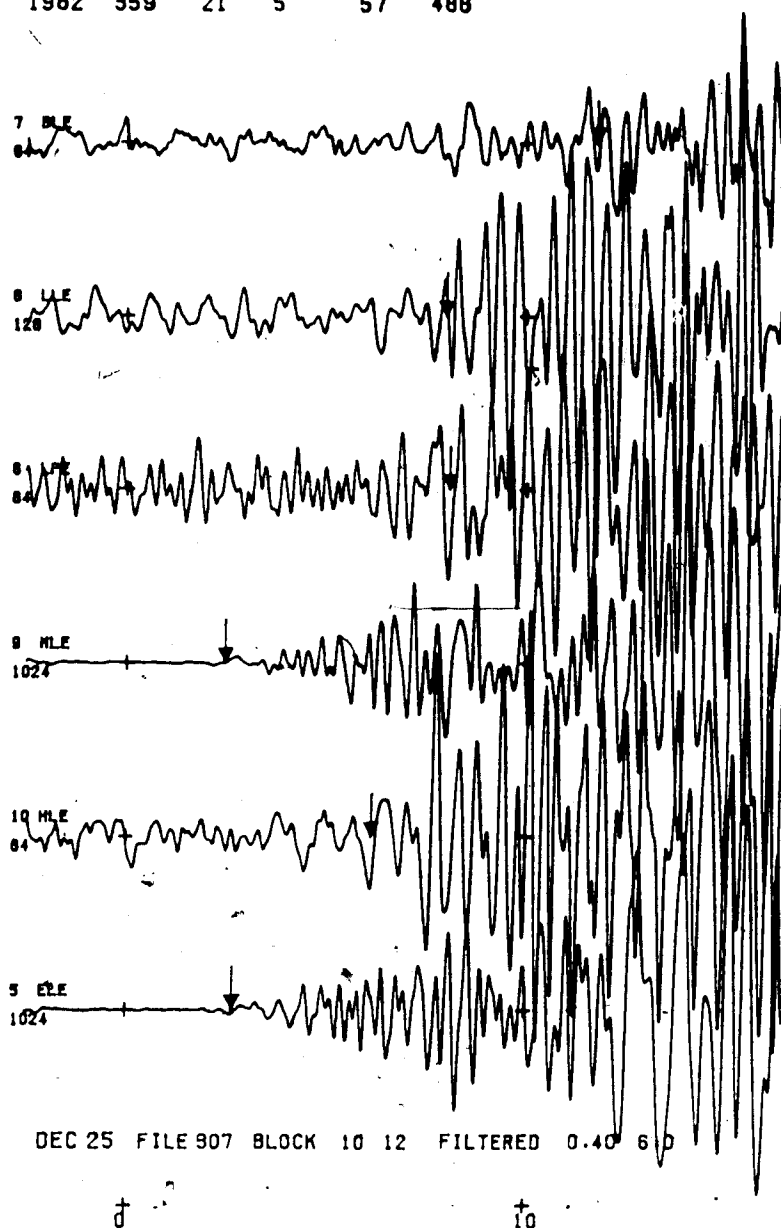


Figure 51.... Autopick results for an "A" type event that occurred on December 25, 1982. The arrows indicate the automatically obtained first break.

## AUTOPICK RESULTS FOR 22/01/1984 EVENT

DOMINANT FREQUENCY IS: 3.0661HZ  
 MAX AMP IS AT T: 67.3714 FIRST MOTION IS "U"  
 FIRST BREAK AT: 67.2614  
 END OF PICKING RESULTS  
 ABOVE RESULTS FOR STATION:BLE  
 DOMINANT FREQUENCY IS: 2.1379HZ  
 MAX AMP IS AT T: 61.7405 FIRST MOTION IS "D"  
 FIRST BREAK AT: 61.6805  
 END OF PICKING RESULTS  
 ABOVE RESULTS FOR STATION:LLE  
 DOMINANT FREQUENCY IS: 3.2069HZ  
 MAX AMP IS AT T: 67.4049 FIRST MOTION IS "D"  
 FIRST BREAK AT: 67.3149  
 END OF PICKING RESULTS  
 ABOVE RESULTS FOR STATION:LPE  
 DOMINANT FREQUENCY IS: 5.2112HZ  
 MAX AMP IS AT T: 68.7078 FIRST MOTION IS "U"  
 FIRST BREAK AT: 68.6177  
 END OF PICKING RESULTS  
 ABOVE RESULTS FOR STATION:MLE  
 DOMINANT FREQUENCY IS: 4.8047HZ  
 MAX AMP IS AT T: 63.8633 FIRST MOTION IS "U"  
 FIRST BREAK AT: 63.8084  
 END OF PICKING RESULTS  
 ABOVE RESULTS FOR STATION:MLE  
 DOMINANT FREQUENCY IS: 2.6496HZ  
 MAX AMP IS AT T: 66.7801 FIRST MOTION IS "U"  
 FIRST BREAK AT: 66.6822  
 END OF PICKING RESULTS  
 ABOVE RESULTS FOR STATION:ELE

## AUTOPICK RESULTS FOR 26/12/1982 EVENT

DOMINANT FREQUENCY IS: 2.8781HZ  
 MAX AMP IS AT T: 66.4183 FIRST MOTION IS "U"  
 FIRST BREAK AT: 66.2904  
 END OF PICKING RESULTS  
 ABOVE RESULTS FOR STATION:BLE  
 DOMINANT FREQUENCY IS: 3.8704HZ  
 MAX AMP IS AT T: 66.3058 FIRST MOTION IS "U"  
 FIRST BREAK AT: 66.2339  
 END OF PICKING RESULTS  
 ABOVE RESULTS FOR STATION:LLE  
 DOMINANT FREQUENCY IS: 3.4741HZ  
 MAX AMP IS AT T: 66.8816 FIRST MOTION IS "U"  
 FIRST BREAK AT: 66.8088  
 END OF PICKING RESULTS  
 ABOVE RESULTS FOR STATION:LPE  
 DOMINANT FREQUENCY IS: 3.7800HZ  
 MAX AMP IS AT T: 66.8178 FIRST MOTION IS "D"  
 FIRST BREAK AT: 66.6459  
 END OF PICKING RESULTS  
 ABOVE RESULTS FOR STATION:MLE  
 DOMINANT FREQUENCY IS: 4.8047HZ  
 MAX AMP IS AT T: 60.1378 FIRST MOTION IS "U"  
 FIRST BREAK AT: 60.0864  
 END OF PICKING RESULTS  
 ABOVE RESULTS FOR STATION:MLE  
 DOMINANT FREQUENCY IS: 4.8047HZ  
 MAX AMP IS AT T: 67.7481 FIRST MOTION IS "D"  
 FIRST BREAK AT: 67.6582  
 END OF PICKING RESULTS  
 ABOVE RESULTS FOR STATION:ELE

Table 11.... Results obtained from AUTOPICK routine used to  
 estimate first arrivals and first motions automatically.  
 Good estimates (top), less reliable (bottom).

---

 AUTOMATIC AND MANUAL COMPARISON

| STATION | DATE/TIME  | VISUAL TIME | AUTOMATIC TIME | DIFFERENCE |
|---------|------------|-------------|----------------|------------|
| MLE     | 8401222035 | 58.95       | 59.61          | 0.60       |
| ELE     | 8401222035 | 58.58       | 58.99          | 0.01       |
| LPE     | 8401222035 | 59.95       | 57.40          | 2.50       |
| LLE     | 8401222035 | 59.98       | 61.65          | 1.67       |
| HLE     | 8401222035 | 60.02?      | 63.80          | 3.50?      |
| BLE     | 8401222035 | 60.90       | 61.60          | 0.70       |

---

## AUTOMATIC AND MANUAL COMPARISON

| STATION | DATE/TIME  | VISUAL TIME | AUTOMATIC TIME | DIFFERENCE |
|---------|------------|-------------|----------------|------------|
| MLE     | 8401240053 | 56.55       | 56.84          | 0.29       |
| ELE     | 8401240053 | 56.80       | 57.65          | 0.80       |
| LPE     | 8401240053 | 57.30       | 56.80          | 0.50       |
| LLE     | 8401240053 | 60.25       | 56.23          | 4.02?      |
| HLE     | 8401240053 | 59.35       | 60.06          | 0.70       |
| BLE     | 8401240053 | 61.45       | 66.29?         | 4.80?      |

Table 12.... Comparison between visually obtained results and the ones obtained from AUTOPICK. Reliable (top), less accurate (bottom).

significant variation between the two methods, and the automatic method can be considered useful at least for these events for which the conditions mentioned above exist.

In case of events with unsatisfactory conditions the algorithm performed at a lower level of accuracy. Figure 52 and Figure 53 show the results of AUTOPICK applied to such events. Table 11 lists the calculated parameters and Table 12 compares automatic and visually hand picked results. A significant agreement between the two exists. The question lies as to which one of the two is more reliable.

In the visual method the analyst only checks emergent P- arrivals and marks them if first motion is well defined without making a quantitative check of amplitude and frequency criteria. The AUTOPICK method not only detects the emergent P- arrival but it checks quantitatively all other possible conditions necessary for this arrival to be considered consistent.

Such an automatic analysis approach can be improved using the notion of affinity and structural grammar recognition techniques. For this particular study this detecting routine is considered more than necessary. Events are timed by analysts and the results of the routine can be checked against the visually obtained ones. If the Cold Lake array keeps operating and the instruments are increased to have a more dense network, then the algorithm could be improved more so that more data could be processed faster in order that quicker analysis of the seismic parameters takes

## 1982 A AUTOPICK RESULTS

| YEAR | DAY | HOUR | MIN | SEC | MSEC |
|------|-----|------|-----|-----|------|
| 1982 | 962 | 11   | 11  | 22  | 985  |

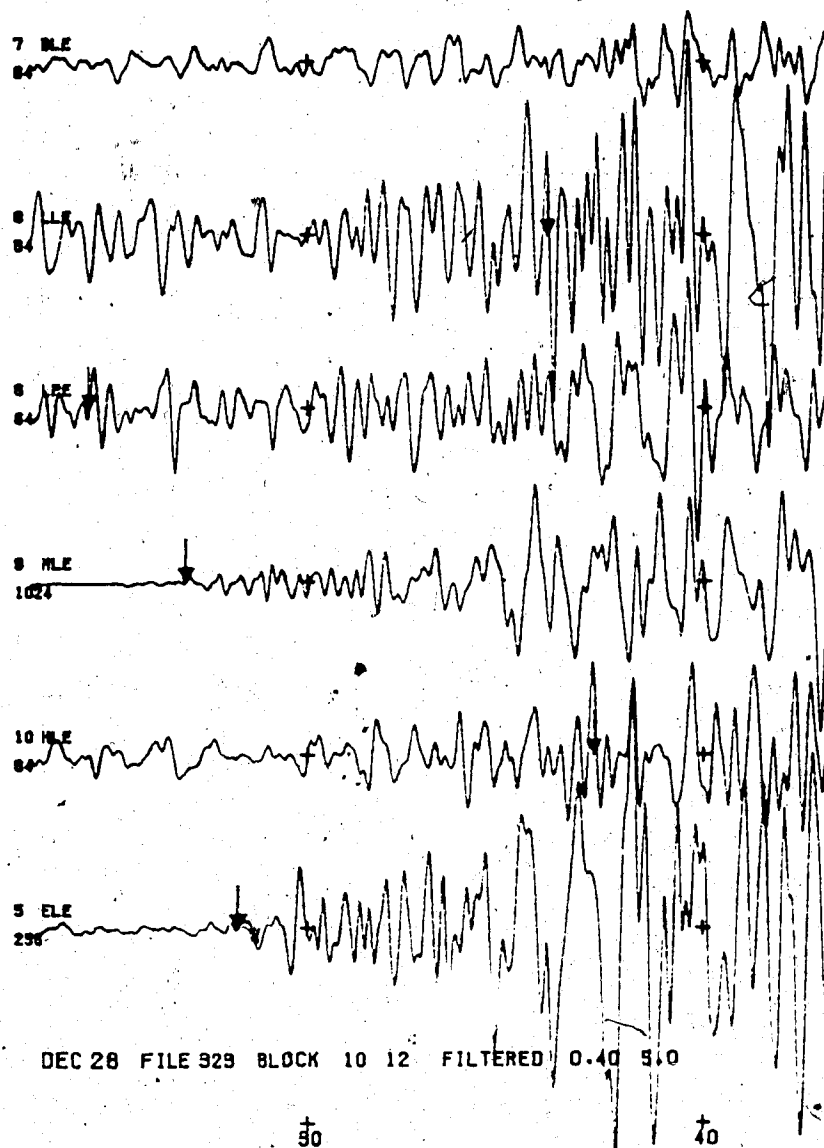


Figure 52.... Autopick results for an "A" type event that occurred on December 28, 1982. Noise contamination effected the stability of the routine. The results cannot be considered accurate.

1984 A44 AUTOPICK RESULTS  
 YEAR DAY HOUR MIN SEC MSEC  
 1984 24 0 59 55 1126

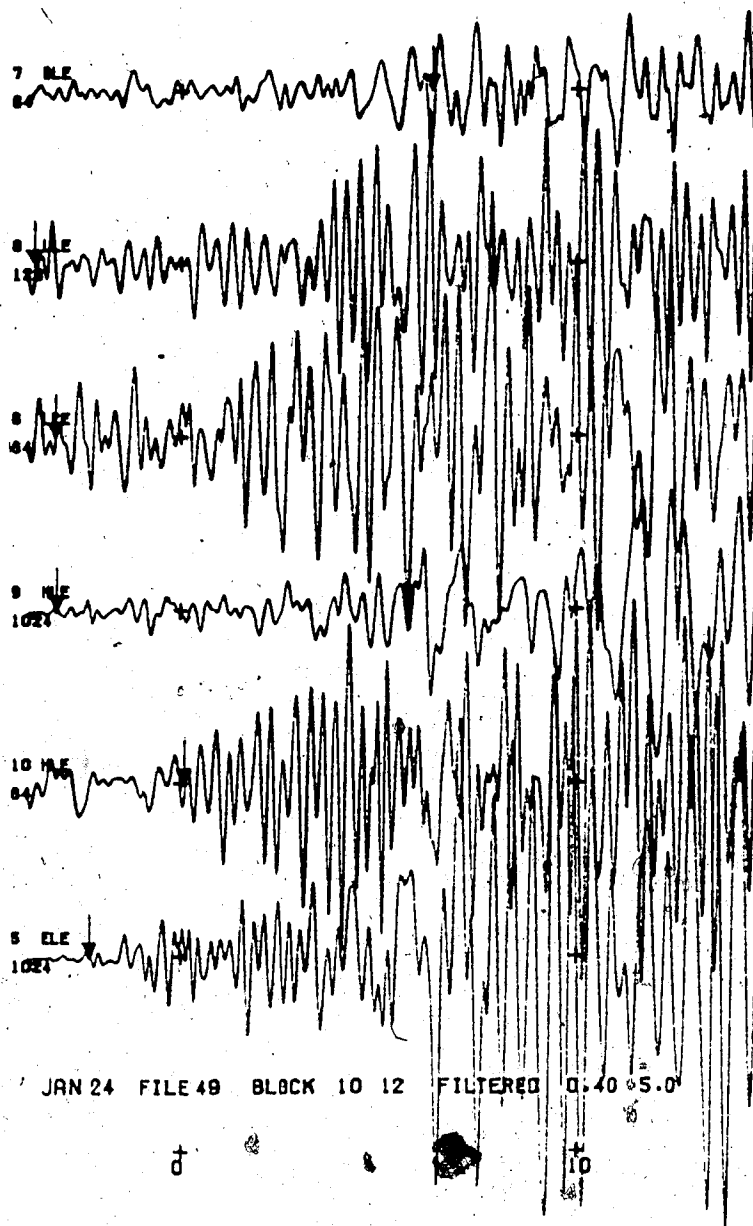


Figure 53.... Autopick results for an "A" type event that occurred on January 24, 1984. Not satisfactory results were obtained as can be seen by the arrows.

place.

Also, the present algorithm with some modifications could be used at the base station of the array so that detection of events is done locally. Then storage of events could be done to save tape space as well as the extra human processing time. —

## 4. INTERPRETATION AND DISCUSSION

### 4.1 INTRODUCTION

The major part of this interpretation is based on the characteristics and analysis of the so called "A" type events. The nature of these events initially became clear when a number of them ( approximately 100) occurred in December 1982. Looking at the histogram of daily occurrences, Figure 54, we can see that there are sporadic occurrences of the events throughout the study period. Even though the operation of the array was marginal during this period, a fair number of "A" type events were detected and a good percentage of them has been used for further analysis.

In terms of station location and wave energy distribution, during the early years of the study, stations MLE and ELE detected elastic waves the with largest amplitudes. The amplitude falls off rapidly with distance at stations BLE and HLE. In more recent years there seems to be a migration in the epicenters and in the amplitude-distance relationship so that the wave energy tends to increase towards the NW approaching station BLE.

This type of distribution of "A" type events, as well as the periodic presence of activity leads to an investigation with the assumption that the potential sources are either related to disturbances in the hydrological cycle or the heavy oil recovery projects.



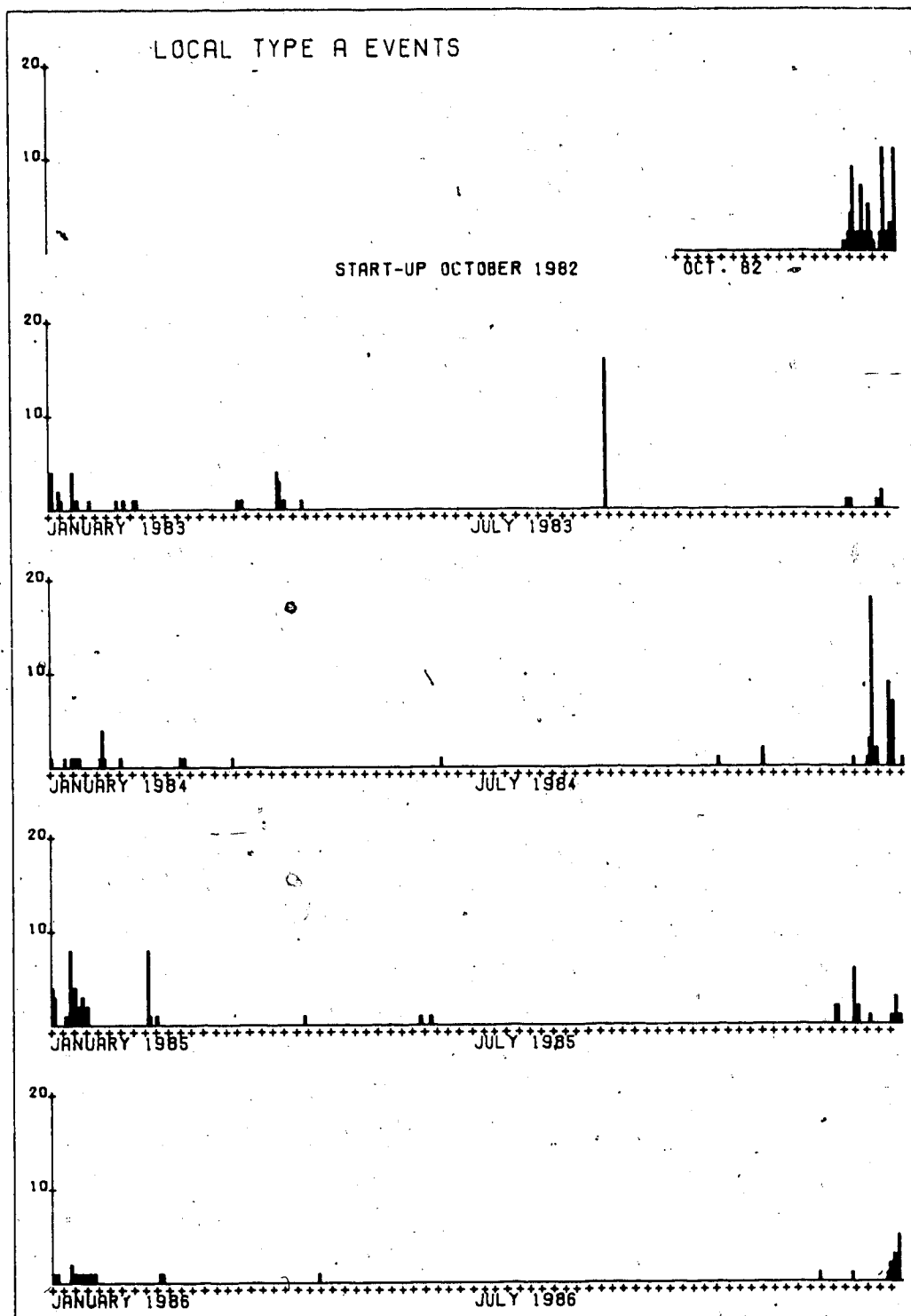


Figure 54.... Daily occurrence of "A" type events for the period of January 1982 to December 1986.

The compressional (P) wave is always very weak with a shear wave (S) not always clear and a very strong Rayleigh wave. This well developed surface wave is a strong indication of shallow source.

Using HYPO71, a location program mentioned in chapter 2, locations for some "A" type events were obtained. Figure 55 shows these locations, plotted on a township grid indicating the total area of study. Results of the location estimations are shown in Table 13. Some of the solutions were constrained to specific depths, related to the investigation for potential sources. There were three major depth categories that the events seem to be separated at: depths between 10-180m, 250-550m, and 600-1000m.

No major tectonic features are present in the area although the Athabasca axis, a prominent linear series of gravity lows passes 80km NW of Cold Lake. Since most of these events are located at depths less than 1 km, and well away from this axis, it is doubtful that there is any direct relationship between seismicity and gravity or magnetic lineaments.

Using the location of the events as an indicator and the strong Rayleigh waves present that constrains this study to shallow depths, three hypothesis were developed for investigation.

The first hypothesis relates the potential sources, due to local stresses at very shallow depths, with disturbances on the hydrogeology. The second hypothesis relates the



| EVENT | DATE   | ORIGIN | LAT N | LONG W   | DEPTH     | MAG  | NO   | RMS    |
|-------|--------|--------|-------|----------|-----------|------|------|--------|
| A92   | 821225 | 21 6   | 0.78  | 54-33.54 | 110-19.82 | 0.15 | 1.3  | 3 0.00 |
| A101  | 821226 | 1457   | 24.41 | 54-34.56 | 110-22.73 | 0.62 | 0.6  | 3 0.01 |
| A105  | 821226 | 1825   | 6.04  | 54-34.31 | 110-22.93 | 0.62 | 0.6  | 3 0.00 |
| A109  | 821228 | 550    | 32.34 | 54-34.30 | 110-19.99 | 0.47 | 0.8  | 3 0.00 |
| A110  | 821228 | 1111   | 27.22 | 54-34.34 | 110-20.91 | 0.15 | 1.2  | 5 0.90 |
| A115  | 821229 | 1712   | 9.96  | 54-35.10 | 110-22.64 | 0.62 | 0.6  | 3 0.01 |
| A116  | 821229 | 1822   | 34.74 | 54-33.48 | 110-24.43 | 0.62 | 1.0  | 3 0.01 |
| A4    | 830102 | 2156   | 12.42 | 54-31.63 | 110-21.93 | 0.01 | 1.2  | 5 0.15 |
| A8    | 830111 | 2133   | 27.61 | 54-33.16 | 110-24.49 | 0.01 | 1.1  | 4 1.38 |
| A12   | 830113 | 1528   | 2.69  | 54-35.58 | 110-23.24 | 0.30 | 1.3  | 6 0.32 |
| A16   | 830206 | 2149   | 31.18 | 54-35.21 | 110-18.63 | 0.01 | 1.4  | 6 0.32 |
| A17   | 830207 | 035    | 8.26  | 54-33.60 | 110-22.33 | 1.37 | 1.4  | 5 0.33 |
| A18   | 830322 | 2212   | 3.74  | 54-35.73 | 110-21.69 | 0.47 | 1.2  | 5 0.69 |
| A19   | 830323 | 055    | 19.55 | 54-35.00 | 110-23.28 | 0.50 | 1.3  | 6 1.20 |
| A1    | 840101 | 546    | 48.52 | 54-32.66 | 110-21.11 | 0.01 | 1.3  | 5 0.32 |
| A4    | 840111 | 21 6   | 53.76 | 54-33.36 | 110-19.89 | 0.02 | 1.2  | 5 0.33 |
| A7    | 840122 | 2035   | 56.71 | 54-32.99 | 110-18.32 | 0.02 | 1.5  | 6 0.31 |
| A12   | 840124 | 053    | 55.84 | 54-35.73 | 110-20.80 | 1.45 | 1.2  | 5 0.46 |
| A17   | 840616 | 336    | 15.68 | 54-38.34 | 110-33.14 | 0.24 | -0.8 | 4 0.19 |
| A19   | 841101 | 21 4   | 21.11 | 54-37.84 | 110-31.86 | 0.01 | -0.3 | 5 0.04 |
| A20   | 841101 | 23 6   | 22.43 | 54-37.85 | 110-32.13 | 0.47 | -0.5 | 4 0.02 |
| A1    | 850101 | 1054   | 6.92  | 54-36.53 | 110-26.64 | 0.01 | 0.0  | 4 0.59 |
| A4    | 850101 | 1926   | 16.04 | 54-37.67 | 110-27.08 | 0.15 | 1.4  | 3 0.64 |
| A5    | 850102 | 810    | 57.97 | 54-35.46 | 110-24.26 | 0.62 | 1.3  | 4 0.58 |
| A7    | 850102 | 1526   | 56.96 | 54-34.35 | 110-24.95 | 0.62 | 0.6  | 5 0.15 |
| A30   | 850116 | 233    | 15.27 | 54-37.75 | 110-26.52 | 0.47 | 0.9  | 5 0.39 |
| A43   | 850608 | 1711   | 33.90 | 54-35.63 | 110-30.58 | 0.01 | -0.8 | 5 0.17 |
| A44   | 850612 | 1132   | 37.88 | 54-36.45 | 110-29.61 | 0.08 | -1.2 | 5 0.00 |
| A45   | 851203 | 1932   | 2.04  | 54-35.90 | 110-23.54 | 0.72 | -0.5 | 4 0.09 |
| A2    | 860103 | 152    | 17.35 | 54-35.13 | 110-21.71 | 0.74 | 0.8  | 4 0.04 |
| A3    | 860109 | 0 2    | 39.34 | 54-34.91 | 110-29.09 | 0.15 | 1.3  | 4 0.04 |
| A7    | 860114 | 2138   | 14.28 | 54-33.44 | 110-24.38 | 0.01 | 0.9  | 4 0.66 |
| A9    | 860117 | 23 3   | 37.76 | 54-33.12 | 110-19.89 | 0.02 | 0.9  | 4 0.30 |
| A15   | 861210 | 637    | 36.10 | 54-32.90 | 110-25.91 | 0.62 | 0.9  | 3 0.42 |

Table 13.... Hypocenter determinations for "A" type events.

source with fluid injection and withdrawal. Some data on steam injection and production of oil in the area has been obtained from Esso Resources. The data have been cross-correlated with the activity. The overall period of injection, production, as well as the pressure variation with depth have been examined. The third hypothesis relates the events to the disposal of waste fluids by injecting into deeper wells at very high pressures which could by reducing the frictional resistance of the rocks trigger earthquakes. Each one of these hypothesis has been analyzed in detail here.

#### 4.2 INDUCED SEISMICITY AND HYDROGEOLOGY

There are not many significant case studies, Carvajal (1984), that relate induced earthquakes to disturbances in the hydrological cycle. Investigating this relationship at Cold Lake is a very difficult task because of the following reasons. First, the station distribution is very sparse and the reliability of the depth estimation of the source to accurately pinpoint the origin of disturbance is low. Second, these shallow events, at depths less than 150 m, could be due to change in effective stress from activity generated at greater depths and, if a zone of weakness is present near the surface, this could release some stress resulting to minor tremors.

It is known that the area has a number of buried valleys, representing old river beds cutting deeply into the

Upper Cretaceous sands and shales ( Gold, in prep.). These channels are present day aquifers which contain a major water reservoir in the area. As can be seen in Figure 56, most of the "A" type events are located at the confluence of these old river channels. This observation lead to an investigation related to disturbances of the hydrological cycle in the area. Looking at some observation well hydrograph data provided to us by Alberta Environment, it can be seen that no major change of water level has taken place in the area for a number of years (Figure 57). A one meter change during a pumping period occurs at the end of 1985. Note, however that there are also small changes at the begining of 1982, 1983, 1984. It is also unfortunate that the Bourque Lake well is so far from the seismic setting and the injection sites, as indicated in Figure 55 (WTR).

Correlating the water level change information with "A" type event occurences is obviously difficult, mainly because of the location of the well. Small reservoir level changes and consequent ground water disturbances have been correlated with minor induced seismicity in some cases ( Nurek, Monteynard, Bajina-Basta, Vajont, Benmore ), ( Simpson, 1976). These cases are mainly related to the increase in vertical stress due to the weight of the water mass and a decrease in effective stress caused by increase in pore pressure. In this study, where no extra water load is present, a different approach is to be used in examining the seismicity present.

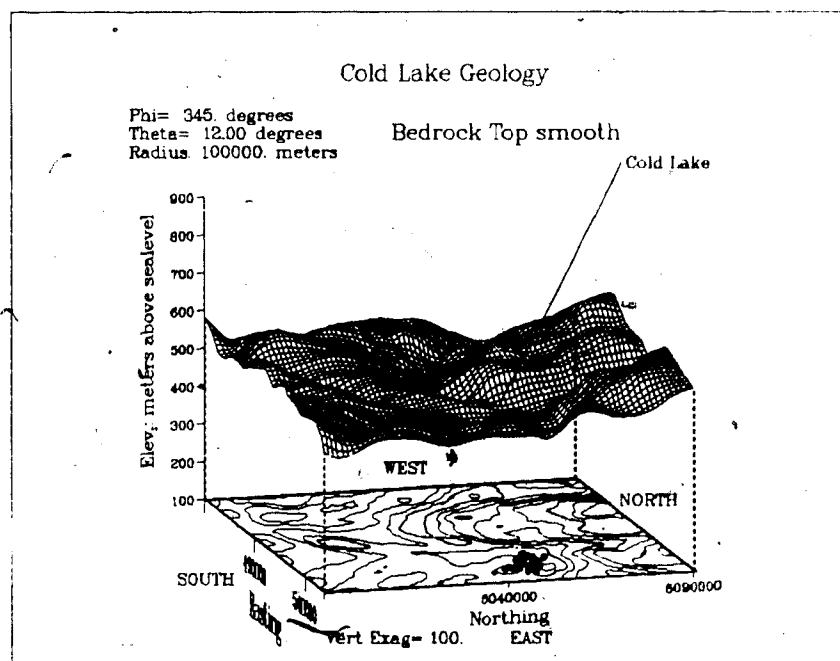
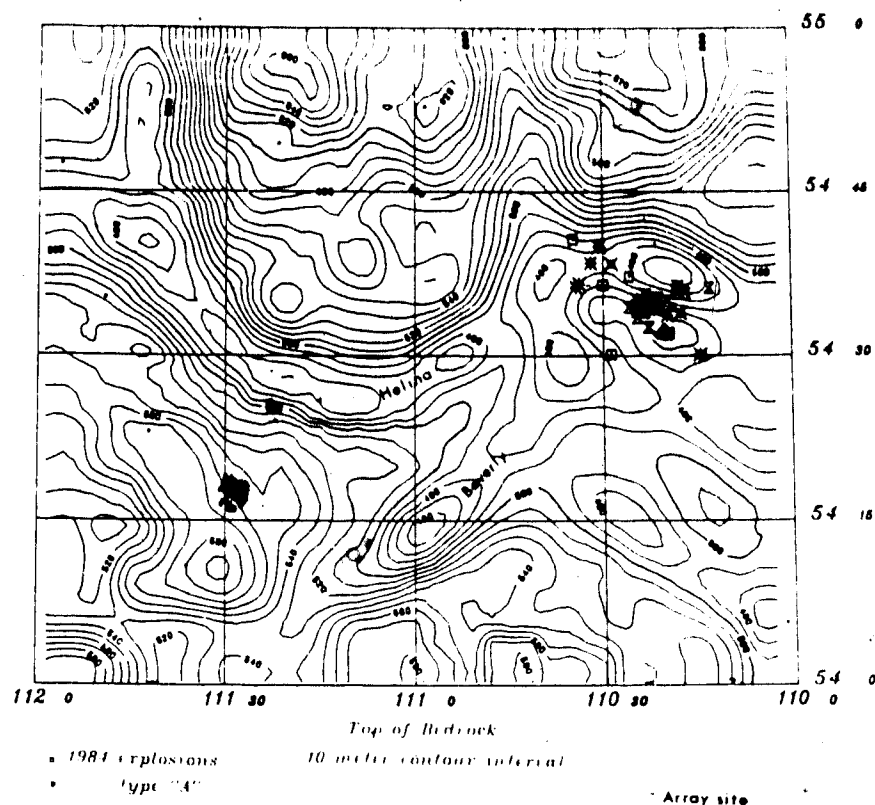


Figure 56.... Location of "A" type shallow events (above).  
Location with respect to bedrock topography (below).

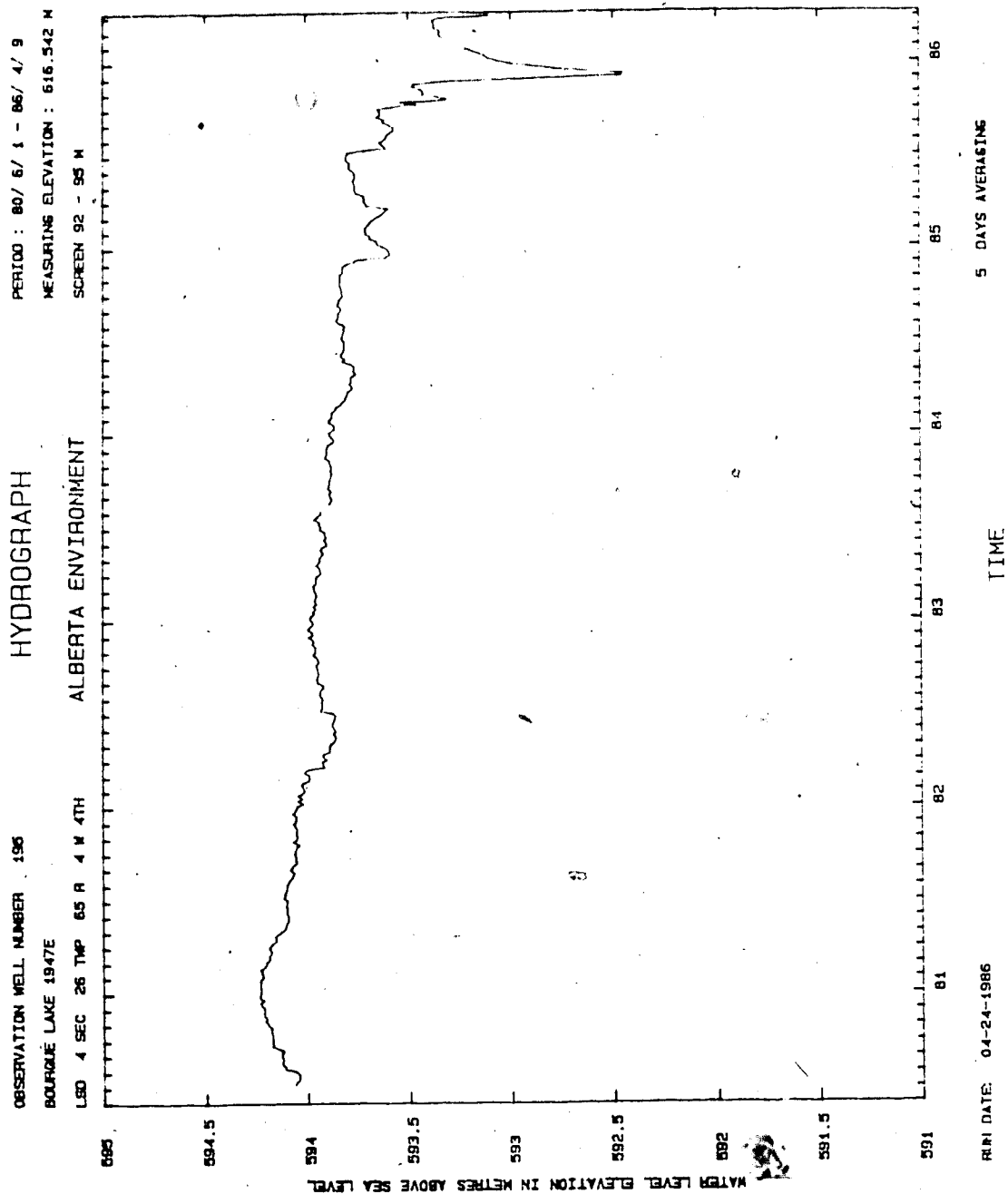


Figure 57.... Water level from well 1947E Burque Lake. The period is from 1980 to the end of 1986. Modified from Alberta Environment information.



A complex hypothesis could be given for events triggered in that level. Possible artificial disturbances created by both fluid injection and fluid extraction at deeper strata could create an effective pressure or even an uplift in the layers located directly above. A sudden release of this pressure (water withdrawal due to pumping or other hydrological disturbances) could generate a sequence of stress drop through the region or even a decrease in effective stress, especially at the shallow zones of weakness, resulting to an induced type of earthquake.

Another complex hypothesis could relate increase in pore pressure in the oil production layers causing formation expansion. The gravitational force due to the weight of the above layers resists this disturbance. If there is fluid withdrawal of a substantial volume, then the effective pressure of the overburden decreases, resulting in stress release in those zones of weakness.

The seismicity in this area is not related to any tectonic activity. The overall seismicity of Western Canada (Figure 58), indicates no significant epicenters in the area. Tremors were felt by the residents of the area after the initiation of the heavy oil recovery projects, but these may have been due to sonic overflights. It is logical, therefore, to hypothesize that the triggering mechanisms of these very shallow earthquakes could be related directly or indirectly to the heavy oil projects and to the zones of weakness present in the area.

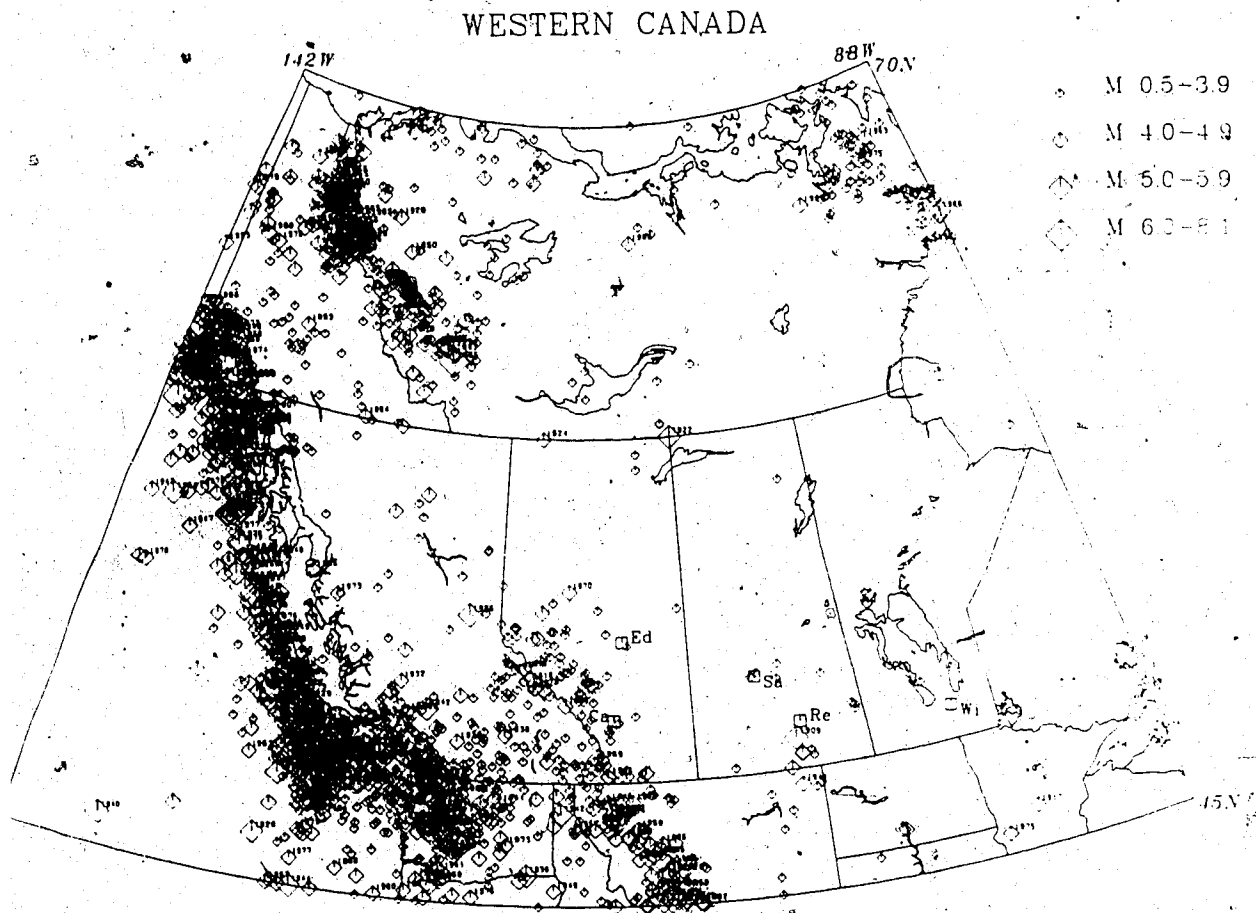


Figure 58.... Earthquake epicenters for the Western Canada region. This data was compiled by E.R. Kanasewich and C.H. McCloughan from GSC and USGS listings

Focal mechanism solutions for A110/2 and A3/6 , shown in Figure 59, for these shallow events, give directions of motions that follow a somewhat consistent pattern. One of the planes ( A3/6) dips  $70^{\circ}$  NE with a strike of  $25^{\circ}$  NW. This could be explained as slumping on the edge of the buried river channels. It should be noted that this solution was obtained using events with more clearly observed first motion data. Discordant first motions could be due to errors in first arrival picking.

The relation between hydrogeology and seismicity is difficult to document with available data. One objective is to determine if these are natural or artificial events. If the events are due to artificial triggering one would like to find the relation to the heavy oil recovery methods in the area. One would like to determine if there are zones of weakness which are slightly disturbed by water pumping or other surface activity.

#### 4.3 INDUCED SEISMICITY AND HEAVY OIL RECOVERY

There are numerous case studies published relating induced seismicity with fluid injection or fluid withdrawal. Healy et al. (1968), related earthquake triggering to fluid injection into deep wells. Similar cases were studied also by Tseng et al (1973), Ohtake (1974), Flecher and Sykes (1977), Pennington et al (1986) who studied the evolution of seismic asperities caused by depressurization of oil and gas fields. Mereu et al (1986), and Evans et al (1987) examined

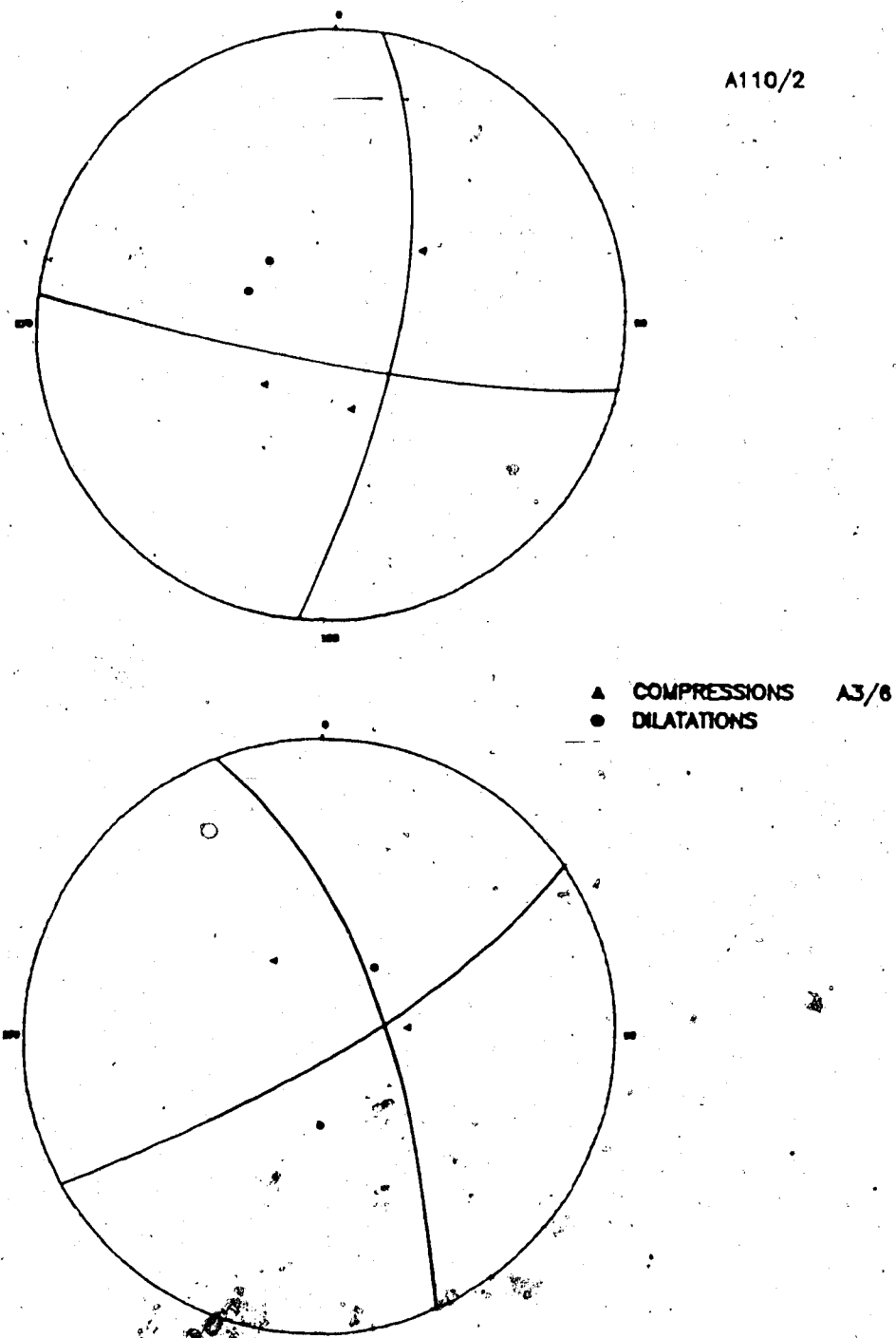


Figure 59.... Focal mechanism solutions for shallow events.  
A110/2 plane dips  $70^\circ$  SE with a strike of  $10^\circ$  NE and A3/6  
plane dips  $70^\circ$  NE with a strike of  $25^\circ$  NW.

local earth tremors in oil field areas. Also at the First International Symposium for induced seismicity in Banff, Canada 1975, cases of seismicity associated with fluid injection were presented.

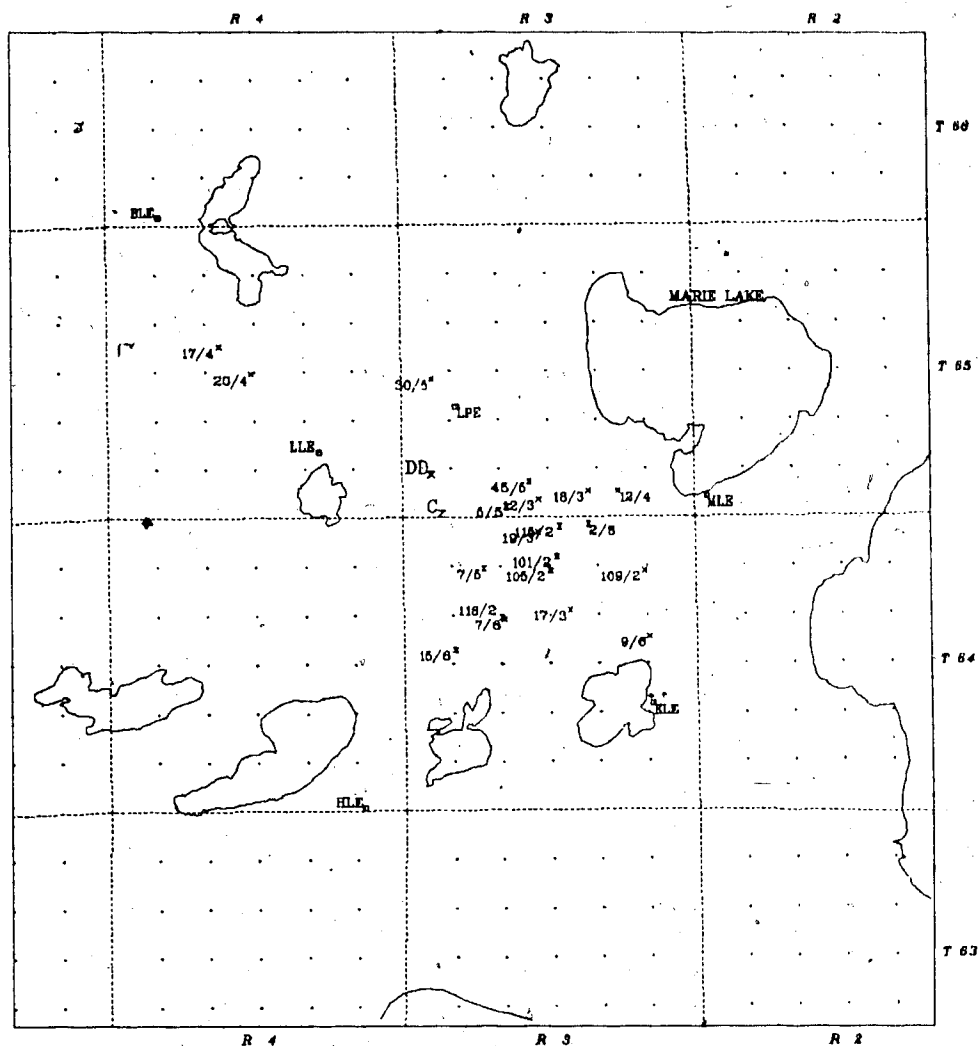
Basically, in some cases induced seismicity and fluid injection or withdrawal are without doubt well correlated phenomena. In the Cold Lake area a major heavy oil recovery project has been in operation since 1975 as described in Chapter 1. It is therefore logical to examine the implications of this activity in relation to local tremors observed by the array. There are several points that should be noted:

1. Was the regional tectonic stress state which is near to the breaking strength of the rocks before injection is initiated?
2. The reservoir formation should accept the fluids due to moderate porosity, but its permeability needs to be low enough so that pore-pressure buildup is possible.
3. The injection of fluids into the formation must be at such rates and pressures that the formation pore pressures are significantly increased over the whole area.

The depth of the oil recovery activity is known. The locations of a number of "A" type events are associated with that depth as shown in Figure 60. As can be seen in Figure 60, a migration of epicenters to the northwesterly direction is apparent. This is in the direction of expansion of the oil recovery projects.

Further analysis was made on the relation between steam injection volume and oil production volume vs "A" event occurrence. A first attempt to correlate events with steam injection volume or oil production volume during the total duration of observation was unsuccessful. The operation in the area is very complex. Some wells might produce, other wells might be on a "soak period" and others could be used for steam injection. Even a net volume ( steam - oil produced ) correlation does not give a positive result. This may be because the exact net volume was not obtained, due to the fact that waste water withdrawal volumes were not included because this waste fluid is injected back in the ground at another area. Exact wellhead pressures were not officially obtained.

Steam injection rate data throughout the duration of study is shown in Figure 61. The "A" event occurrence is shown in Figure 62. A cross correlation was carried out to estimate any possible relationship between the two. Examining Figure 63 which is the crosscorrelation function, we may have a small correlation between the two with about 2 to 4.5 month delay.



A EVENT(nn/y)

(DATE) /y=1980+y

nn=EVENT NUMBER

1982 to 1986

■ DEPTH 550-1000m

■ DEPTH 300-500m

● ARRAY CENTRE

● ARRAY - SURFACE STAT

● UTM INTERSECTIONS

Figure 60.... Location of deep "A" type events depths of 300m and 1000m. These locations relate to oil recovery formation depths.

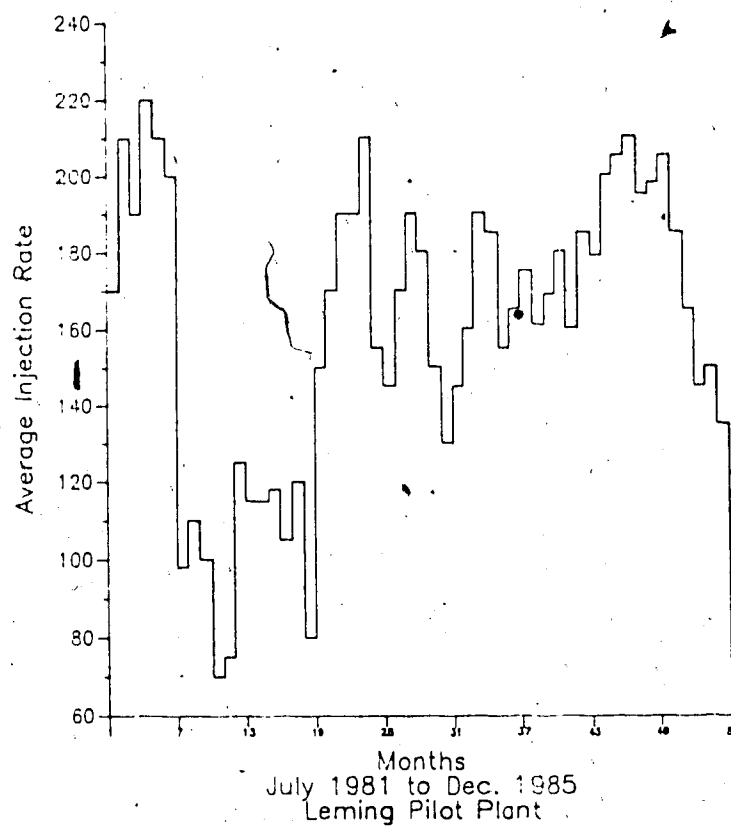


Figure 61.... Average steam injection rate for Leming Pilot Plant. The period covered is January 1982 to December 1986.



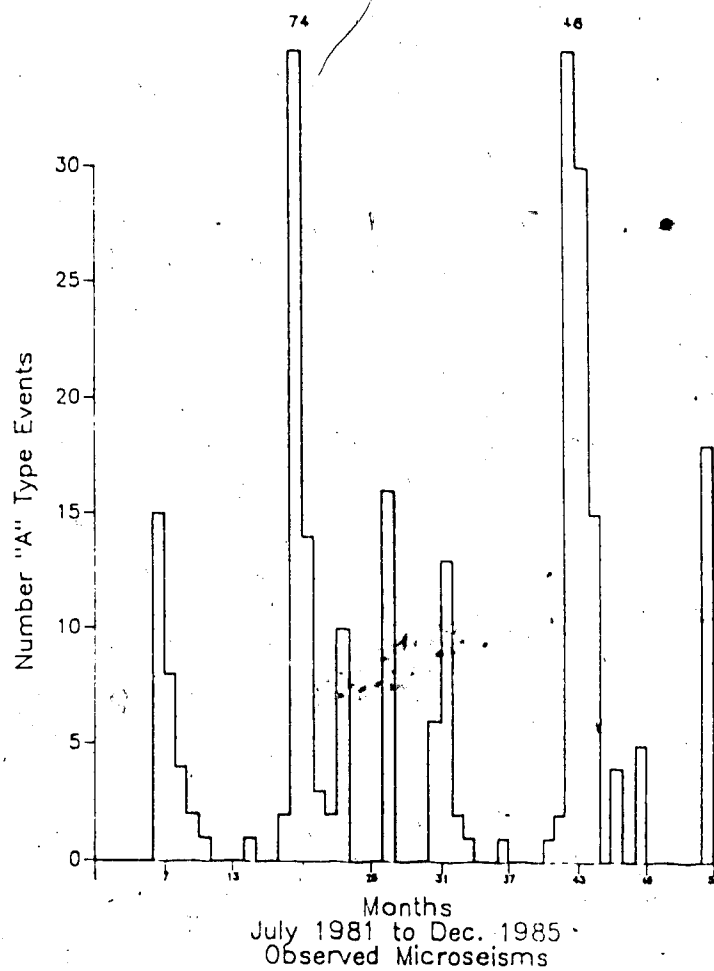


Figure 62.... Frequency of "A" type events during the total period of study. Each histogram indicates the number of events recorded per month.

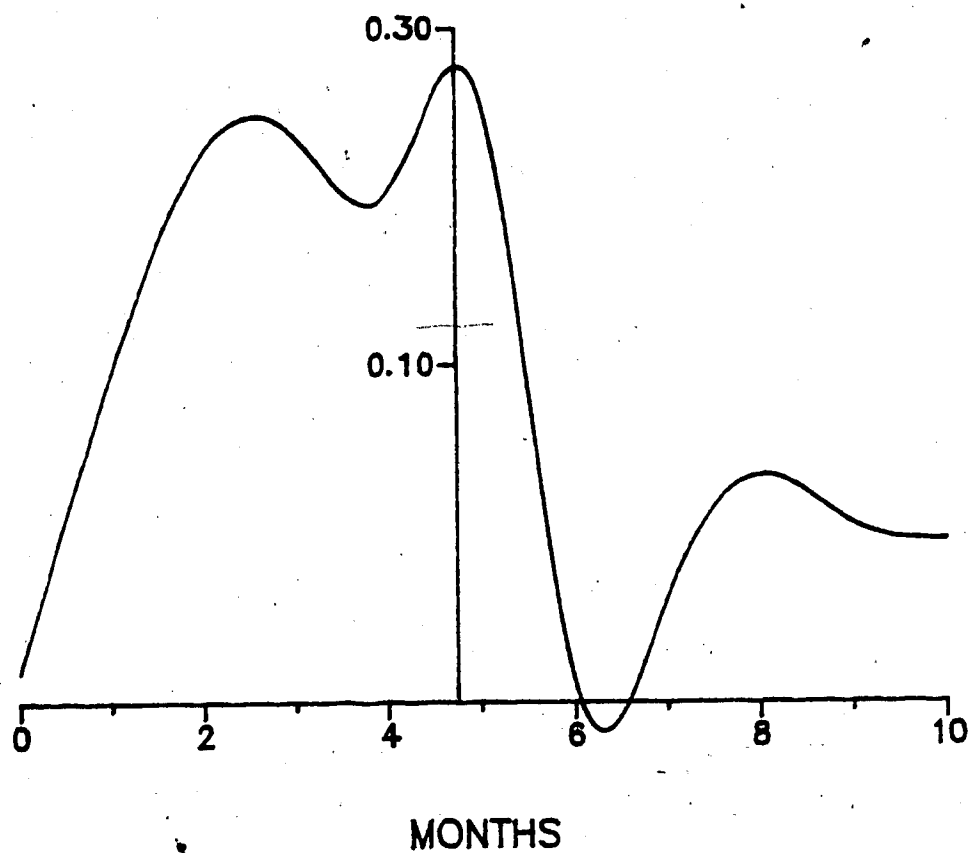


Figure 63.... Crosscorelation between average steam injection rate and "A" type event occurence per month. A 2 and 4.5 month lag shows the best correlation.

This weak correlation could indicate that as the steam injection rate increased ( or pore-pressure built up in the formation) then a burst of activity seemed to occur with some time delay in some cases. This delay could be explained as due to the period of time needed for steam injection to change the reservoir parameters.

Focal mechanism solutions, for these events have also been obtained. Figure 64, shows such a solution for events A30/5 and A9/6, indicating a dip of 60-70° SE and strikes of 35-65° NE. This is normal faulting and could be related to fracturing in the formation due to pore-pressure built up. Alternatively, the stress state of the rocks may be near the breaking strength then with a small disturbance by fluid injection or withdrawal results in a sudden stress release or dislocation in the rocks surrounding the reservoir. The fault plane analysis is consistent with a triggering mechanism at the oil recovery formation level.

The above hypothesis, relating microtremors to fluid injection, could be also examined by the analysis of the Coulomb-Mohr theory of shear failure. Many studies have been done on this technique especially in cases of induced seismicity, Gough (1987), Kisslinger (1976), Talwan (1976). Much of the analysis is based on stress failure related to pore pressure changes. In our case if we assume that the vertical "principal" stress is equal to the lithostatic pressure, and being the  $S_1$  component as suggested by the focal mechanism solution and stress directions, it's given

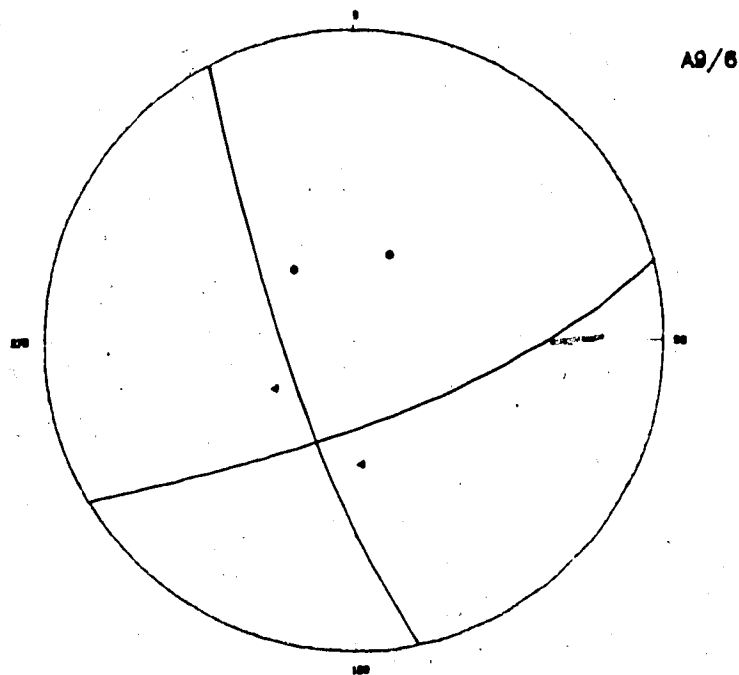
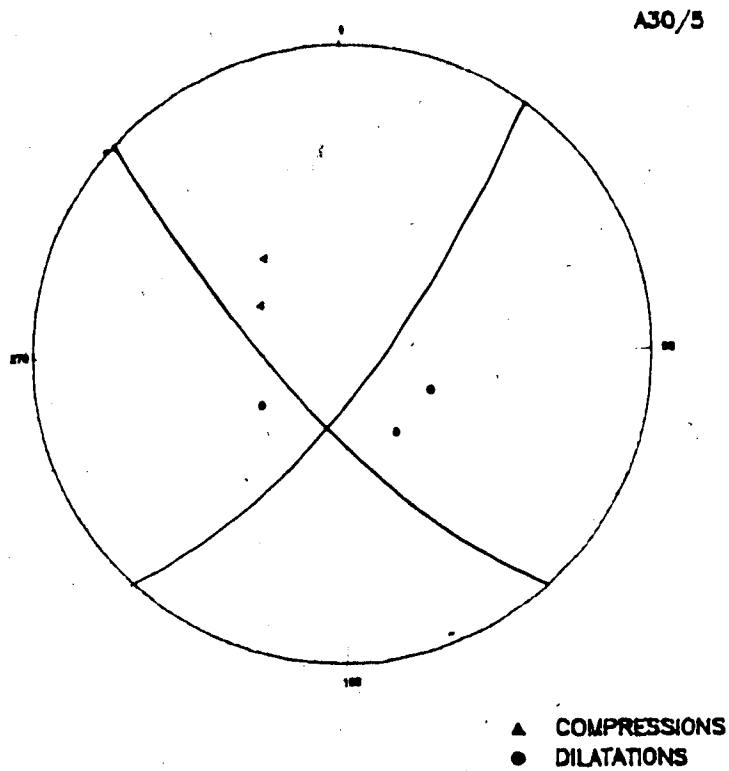


Figure 64.... Focal mechanism solution semi-deep events. A30/5 plane dips  $70^\circ$  SE with a strike of  $35^\circ$  NE and A9/6 plane dips  $64^\circ$  SE with a strike of  $54^\circ$  NE.

by:

$$S_1 = \int \rho g dz$$

If we consider this as the maximum compressive stress, due to the overburden, and  $S_3$ , the least compressive stress we can apply the failure criteria for the medium, in our case the Clearwater formation at depth  $z=470\text{m}$ , and average density  $\rho = 2 \text{ gr/cc}$ . Then  $S_1 = 94 \text{ bars}$  (9.4 MPa), assuming also that the least compressive stress is approximately  $S_3 = S_1/3 = 32 \text{ bars}$ , and taking the inherent shear strength of the sedimentary rock  $\tau_0$  between 100-150 bars (Ragan, 1968), and the coefficient of internal friction  $\tan\phi = 0.6$  ( $\phi = 30^\circ$ ) we can estimate the rock failure parameters.

If the medium is porous, which is the case with Clearwater formation, and contains fluid with pore pressure,  $p$ , then the principal stresses are reduced to the effective stresses  $\sigma_1 = S_1 - p$  and  $\sigma_3 = S_3 - p$ . Then the required pressure,  $p_d$ , to bring the rock to failure is given by (Kisslinger, 1976):

$$p_d = \{(2/\sqrt{3})\tau_0 + 2S_3 - S_1\}/2$$

which in our case is between 60 to 90 bars.

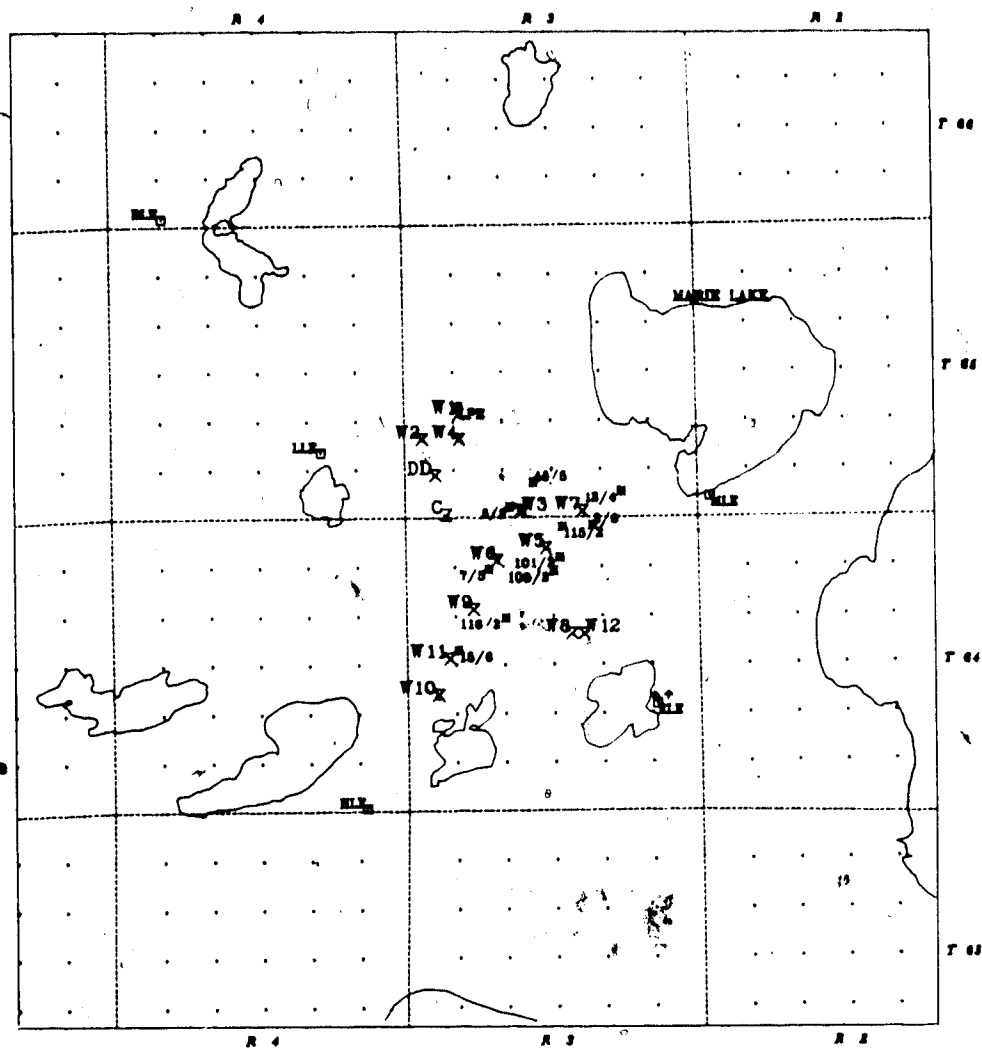
We know that the injection pressure in the area is of the order of 100 bars, it is logical to assume that the pore pressure is of that order and in some cases larger. This

change of pore pressure by fluid injection may be sufficient to create fault failure or fracturing as indicated by the low level of seismicity present, without creating any local hazards.

#### 4.4 INDUCED SEISMICITY AND WASTE WATER DISPOSAL

In most heavy oil recovery projects there is a vast volume of waste fluids produced at the wells, proportional to the steam volume injected. In Cold Lake some of the waste fluid, after approval by the Energy Resources Conservation Board, of the Province of Alberta, is injected back into the ground. The location of most of the waste water disposal wells is within the study area as shown in Figure 65 and the injection depth varies between 550-800m, at the top of the Cambrian.

Most of these wells are located at the SE corner of the seismic array, this implies that the location of "A" type due to waste water disposal can not be reliably determined. Only a small number of these events gave "good" hypocenter solutions at a depth of about 620m, located NW of the Ethel Lake area ( Figure 65 ). It is not expected that these locations need comply with the location of the waste water wells they do point to the complexity of an investigation on seismic activity in the area. Composite focal mechanism solution was obtained to study the directions of compression in the area. Figure 66, indicates reverse faulting with a right lateral component. The direction of maximum tensile



A EVENT(NN/Y)

(DATE) /Y=1980+Y

NN=EVENT NUMBER

1982 to 1986

■ DEPTH 550-1000m

✕ FLUID INJECTION WELLS

● ARRAY CENTRE

▲ ARRAY - SURFACE STAT

• UTM INTERSECTIONS

Figure 65.... Waste fluid disposal well locations and "A" type event epicenters at depths of 500 to 1000m.

▲ COMPRESSIONS  
● DILATIONS

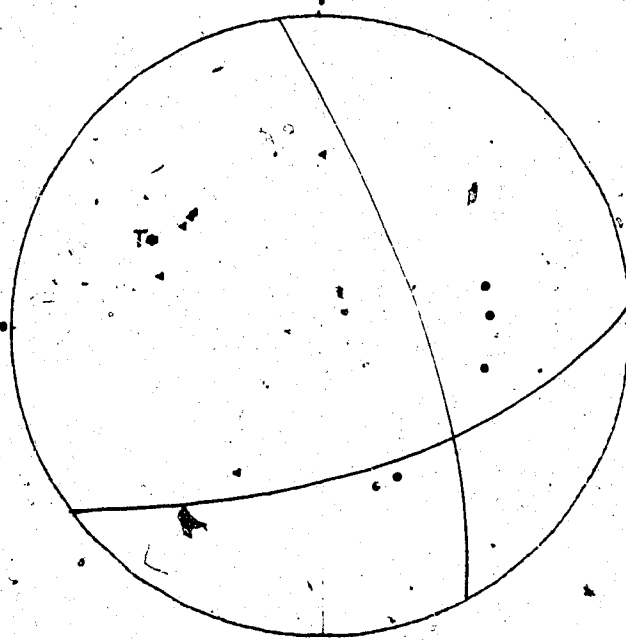


Figure 66.... Composite focal mechanism solution for deep events A5/5, A2/6, A45/5. The plane dips  $60^\circ$  NE with a strike of  $24^\circ$  NW.



stress, represented by T in Figure 66, could correspond to the release of stress due to formation fracturing.

Information with regards to waste water disposal, for our analysis, is based on an approval agreement between E.R.C.B. and Esso to inject at certain locations between 1978 to 1985. There are only 10 - 15 wells used for disposal purposes. Considering the amount of volume of steam injected and waste water produced in the wells during the period of operation, it seems that using only a small number of wells for waste disposal can only mean that injection rates at these wells must be at a maximum. The recommended maximum wellhead pressure by E.R.C.B. is about 16,000 kilopascals (160 bars), which is larger than the accepted pre-fracturing pressure in Cambrian formation level (12 MPa, 120 bars).

As mentioned in the previous discussions it is known that no natural tectonic activity exists in the area. So, there are two factors to consider as evidence of induced seismicity due to waste water disposal. First it is logical to consider that the amount of water produced (usually more than 60% of the injected steam volume) has to be disposed of. Two to three wells are used for disposal purposes per year and they must accept a great volume of waste fluids, possibly from all operating plants in the area, at that formation level. Second, in order to inject waste fluids into a formation at a speed relative to the production volumes of a large number of wells, it is logical to use very high injection pressures, which will cause a definite

fracture in the formation.

Due to limitations of the seismic array, exact epicentral locations are not possible. It is possible to assume on the basis of the two closest stations, MLE and ELE, which show larger wave energy concentration on the average throughout the year, that induced seismicity sources are located in that area. A reasonable hypothesis is that triggering of microearthquakes due to waste water disposal does occur.

#### 4.5 CONCLUSIONS

A minor level of induced seismicity has been found in the Cold Lake area based on the observation of approximately 300 local microtremors between November, 1981 and the end of December, 1986. The activity is periodic and may be related to increased drilling of new wells and initiation of new projects upon freezing of the ground. In the early period of recording 350 events were documented during a 7 month interval in 1979.

The Cold Lake area, lies 300 km. northeast of the Rocky Mountains, and its microseismicity is not related to any of the well defined seismically active areas in Western Canada. Regional stresses in the North American plate play a minor role in causing the instability. More likely the factors contributing to this seismicity are directly related to artificial disturbances in the area.

All of the "A" type microtremors are small, with magnitudes less than 1.5 and their epicenters fall into three categories.

A number of them occur at the confluence of the two buried river channels that have been incised into Upper Cretaceous bedrock and filled with glacial deposits. The generating mechanism of these events was analyzed under two hypotheses. One relating seismicity to water level changes, and it seems that such changes of annual water content or rate of flow could not have triggered such activity. The other hypothesis may be due to a complex relation between the shallow microseismicity and disturbances created by both fluid injection and fluid extraction at several depths.

Some of the microtremors are close to the steam injection zones and track the expansion of oil production plants in a northwesterly direction. These events occur at the injection-production depth, 450-500m. Casing failures when they occurred were not correlated with specific events. The only possible correlation obtained was that of steam injection rate versus "A" event occurrence. Also, focal mechanisms, indicating a fracture type dislocation, give stronger evidence for a triggering mechanism at that depth. It is fair to assume that artificial disturbances due to Heavy Oil recovery projects may be directly related to low level microseismicity.

Finally, another possible factor for the presence of microtremors in the area is the waste fluid disposal

operation that occurs near Ethel Lake. Due to the limited amount of information from the seismic array with respect to this area ( it is located at the edge of the array ) no accurate correlation was obtained. Some events were located in that area at depths associated with waste disposal well depths. It is suggested only, that due to higher injection pressures used ( above the formation fracture level ) possibility of fracturing exists, resulting to disturbances and in turn triggering of microearthquakes.

The Cold Lake seismic array has established its usefulness to inhabitants of the area by monitoring the potential hazards due to industrial activity as in Denver (Healy, et al 1968), and Canada Forces Base (CFB) activity present. Rapid and reliable information of the sources of sonic and elastic disturbances was provided to interested parties. Such seismic control and analysis proved valuable because the artificial disturbances, due to industrial activity or sonic overflights in the area apparently decreased since the array started operating normally. It is suggested that monitoring in the area should continue with an improved seismic array as long as the heavy oil operations last. It should be noted that the seismicity has a very low magnitude and none of the instrumentally recorded events were felt or created a hazard to the local community.

## Bibliography

- Aki, K., and Lee, W.H.K. (1976) Determination of three-dimensional velocity anomalies under a seismic array using first P arrival times from local earthquakes. *J. Geophys. Res.* 81, 4381-4399.
- Aki, K., Christofferson, A., and Husebye, E.S. (1976). Three-dimensional seismic structure of the lithosphere under Montana LISA. *Bull. Seism. Soc. Am.* 66, 501-524.
- Allen, R.V. (1978). Automatic earthquake recognition and timing from single traces. *Bull. Seism. Soc. Am.* 68, 1521-1532.
- Allen, R.V. (1982). Automatic phase pickers: their present use and future prospects. *Bull. Seism. Soc. Am.* 72, S225-S242.
- Anderson, K.R. (1977). Automatic analysis of microearthquake network data. *Geoexploration*. 16, 159-175.
- Anderson, K.R. (1982). Syntactic analysis of seismic waveforms using augmented transition network grammars. *Geoexploration*. 20, 161-182.
- Babcock, E.A. (1978). Measurement of subsurface fractures from dipmeter logs. *Am. Assoc. Pet. Geol. Bull.* 62, 1111-1126.
- Bakun, W.H., Houck, S.T., and Lee, W.H.K. (1978a). A direct comparison of "synthetic" and actual Wood-Anderson seismograms. *Bull. Seism. Soc. Am.* 68, 1199-1202.
- Bisztricsany, E. (1958) A new method for the determination of the magnitude of earthquakes. *Geofiz. Kozl.* 7, 69-96 (in Hungarian with English abstract).
- Boucher, G., and Fitch, T.J. (1969). Microearthquake seismicity of the Denali fault. *J. Geophys. Res.* 74, 6638-6648.
- Brune, J.N., and Allen, C.R. (1967). A microearthquake survey of the San Andreas fault system in southern California. *Bull. Seism. Soc. Am.* 57, 277-296.
- Burdick, L.J., and Powell, C. (1980). Apparent velocity measurements for the lower mantle from a wide aperture array. *J. Geophys. Res.* 85, 3845-3856.
- Carvajal, U. A. (1984). Seismic Stability near the

Middle America Trench. Ph.D. thesis. University of Alberta, Edmonton.

Combs, J., and Hadley, D. (1977). Microearthquake investigation of the Mesa geothermal anomaly, Imperial Valley, California. *Geophysics* 42, 17-33.

Comninakis, P., Drakopoulos, J., Moumoulidis, G., and Papazahos, B. (1968). Foreshock and aftershock sequences of the Cremasta earthquake and their relation to waterloading of the Cremasta artificial lake. *Ann. Geofis.* 21, 39-71.

Cook, N.G.W. (1976). Seismicity associated with mining. *Eng. Geol.* 10, 99-122.

Crampin, S., and Fyfe, C.J. (1974) Automatic analysis of tape-recordings from seismic networks. *Geophys. J. R. Astro. Soc.* 39, 155-168.

Crosson, R.S. (1972). Small earthquakes, structure, and tectonics of the Puget Sound region. *Bull. Seism. Soc. Am.* 62, 1133-1171.

Evans, D.G., and Steeples, D.W. (1987). Microearthquakes near the Sleepy Hollow oil field, Southwestern Nebraska. *Bull. Seism. Soc. Am.* 77, 132-140.

Farouq Ali, S.M. (1982) Elements of heavy oil recovery. *Dept. Petr. Eng., University of Alberta.*

Fletcher, J.B., and Sykes, L.R. (1977). Earthquakes related to hydraulic mining and natural seismic activity in western New York state. *J. Geophys. Res.* 82, 3767-3780.

Gaby, J.E., and Anderson, K.R. (1983). Using affinity to derive the morphological structure of seismic signals. *IEEE* 20-28.

Geiger, L. (1912). Probability method for the determination of earthquake epicenters from the arrival time only. *Bull. St. Louis Univ.* 8, 60-71.

Gold, C.M., Andriashek, L.D., and Fenton, M.M. (1983). Bedrock topography of the Sand River map area. *Alberta Research Council, Alberta Geological Survey, Edmonton.*

Gold, G.M. (in prep.). Surficial Geology in the Sand River (NTS73L) Map Area, *Alberta Environment, Edmonton, Alberta.*

Gough, D.I., and Gough, W.I. (1970a). Stress and deflection in the lithosphere near Lake Kariba. *Geophys. J. R. Astro. Soc.* 21, 65-78.

- Gough, D.I., and Gough, W.I. (1970b). Load-induced earthquakes at Lake Kariba. *Geophys. J. R. Astro. Soc.* 21, 79-101.
- Gough, D.I., and Gough, W.I. (1976). Time dependence and trigger mechanisms for the Kariba earthquakes. *Eng. Geol.* 10, 211-217.
- Gough, D.I., and Gough, W.I. (1987). Stress near the surface of the earth. *Ann. Rev. Earth Planet. Sci.* 15, 545-566
- Gupta, H.K., and Rastogi, B.K. (1976). "Dams and Earthquakes". Elsevier, Amsterdam.
- Hadley, D., and Kanamori, H. (1977). Seismic structure of the Transverse Ranges, California. *Geol. Soc. Am. Bull.* 88, 1469-1478.
- Hamilton, R.M. (1970). Time-term analysis of explosion data from the vicinity of the Borrego Mountain, California, earthquake of 9 April 1968. *Bull. Seism. Soc. Am.* 60, 367-381.
- Hamilton, R.M., and Healy, J.H. (1969). Aftershocks of the Benham nuclear explosion. *Bull. Seism. Soc. Am.* 59, 2271-2281.
- Healy, J.H., and Peake, L.G. (1975). Seismic velocity structure along a section of the San Andreas fault near Bear Valley, California. *Bull. Seism. Soc. Am.* 65, 1177-1197.
- Healy, J.H., Rubey, W.W., Griggs, D.T., and Raleigh, C.B. (1968). The Denver earthquakes. *Science*. 161, 1301-1310.
- Iyer, H.M. (1979). Deep structure under Yellowstone Park, USA: A continental hot spot. *Tectonophysics* 56, 165-197.
- Kanamori, H. (1967). Upper mantle structure from apparent velocities of P waves recorded at Wakayama Microearthquake Observatory. *Bull. Earthquake Res. Inst., Univ. Tokyo* 45, 657-678.
- Kanasewich E.R., Cold Lake Seismicity Project: Report No 1 (April 30, 1979)
- Kanasewich E.R., Cold Lake Seismicity Project: Report No 2 (Jan. 16, 1980)
- Kanasewich E.R., Cold Lake Seismicity Project: Report No 3 (Feb. 1983)
- Kanasewich E.R., Cold Lake Seismicity Project: Report No 4 (Jan. 1985)

- Kanasewich E.R., Cold Lake Seismicity Project: Report No 5 (Feb. 1986)
- Kanasewich, E.R. (1981). Time sequence analysis in Geophysics. Third edition. *The University of Alberta Press*.
- Kanasewich, E.R., Bingham, D., and Gold, C. (1984). Continuous monitoring of microtremors using a digital seismic array. *Advances in Geophysical Data Processing*. 1, 291-307.
- Kanasewich, E.R., Gold, C., Sneddon, D.T., Burke, M. and Kenway, D. (1982). The Cold Lake digital seismic monitoring array. *Fourth Canadian Symposium on Mining, Surveying, and Deformation Measurements, Banff, Alberta*.
- Kind, R. (1972). Residuals and velocities of P<sub>n</sub> waves recorded by the San Andreas seismograph network. *Bull. Seism. Soc. Am.* 62, 85-100.
- Kisslinger, C., (1976). A review of theories of mechanisms of induced seismicity. *Engineering Geology*, 10, 85-98
- Lee, W.H.K., and Lahr, J.C. (1975). HYP071 (Revised): A computer program for determining hypocenter, magnitude, and first motion pattern of local earthquakes. *USGS Open File Report*. 75-311, 1-116.
- Lee, W.H.K., and Stewart, S.W. (1981). Principles and Applications of Microearthquake Networks. *Advances in Geophysics, Academic Press*.
- Lee, W.H.K., Bennett, R.E., and Meagner, K.L. (1972). A method of estimating magnitude of local earthquakes from signal duration. *Geol. Surv. Open-File Rep.* 28.
- Majer, E.L., and McEvilly, T.V. (1979). Seismological investigations at the Geysers geothermal field. *Geophysics* 44, 246-269.
- McDougal, J.C. (1987) Open letter comments on S. Kapotas's thesis. *Esso Resources Canada Ltd.*
- Mereu, R.F., Brunet, J., Morrissey, K., Price, B., and Yapp, A. (1986). A study of the microearthquakes of the Gobles Oil field area of Southwestern Ontario. *Bull. Seism. Soc. Am.* 76, 1215-1223.
- Mitchell, B.J., and Hashim, B.M. (1977). Seismic velocity determinations in the New Madrid seismic zone. *Bull. Seism. Soc. Am.* 67, 413-424.
- Mizoue, M. (1971). Crustal structure from travel times of



reflected and refracted seismic waves recorded at Wakayama Microearthquake Observatory. *Bull. Earthquake Res. Inst., Univ. Tokyo* 49, 33-62.

Ohtake, M. (1974). Seismic activity induced by water injection at Matsushiro, Japan. *J. Phys. Earth* 22, 163-176.

Pennington, W.D., Davis, S.D., Carlson, S.M., DuPree, J., and Ewing, T.E. (1986). The evolution of seismic barriers and asperities caused by the depressurizing of fault planes in oil and gas fields of South Texas. *Bull. Seism. Soc. Am.* 76, 939-948.

Ragan, D.M., (1968) Structural Geology, Wiley & Sons, New York.

Richter, C.F. (1935). An instrumental earthquake magnitude scale. *Bull. Seism. Soc. Am.* 25, 1-32.

Ryall, A., and Savage, W.U. (1969). A comparison of seismological effects for the Nevada underground test Boxcar with natural earthquakes in the Nevada region. *J. Geophys. Res.* 74, 4281-4289.

Simpson, D.W. (1976). Seismicity changes associated with reservoir loading. *Eng. Geol.* 10, 123-150.

Solov'ev, S.L. (1965). Seismicity of Sakhalin. *Bull. Earthquake Res. Inst., Univ. Tokyo* 43, 95-102.

Stevenson, P.R. (1976) Microearthquakes at Flathead Lake Montana: A study using automatic earthquake processing. *Bull. Seism. Soc. Am.* 66, 61-80.

Stewart, S.W. (1977) Real-Time detection and location of local seismic events in Central California. *Bull. Seism. Soc. Am.* 67, 433-452.

Stewart, S.W., Lee, W.H.K., and Eaton, J.P. (1971). Location and real-time detection of microearthquakes along the San Andreas fault system in central California. *Bull. R. Soc. N.Z.* 9, 205-209.

Storm, N.A., and Dunbar, R.B. (1979). Bitumen resources of Alberta: Converting resources to reserves. Chapter 6 of "The Future of Heavy Oil Sands and Tar Sands". p 47-60.

TALWANI, P., (1976) Earthquakes associated with the Clark Hill reservoir, South Carolina. *Engineering Geology*, 10, 239-253

Teng, T.L., Real, C.R., and Henyey, T.L. (1973). Microearthquakes and water flooding in Los Angeles.

*Bull. Seism. Soc. Am.* 63, 859-875..

Thacher, W. (1973). A note on discrepancies between local Magnitude and microearthquake Magnitude scales. *Bull. Seism. Soc. Am.* 63, 315-319.

Tsumura, K. (1967). Determination of earthquake magnitude from total duration of oscillation. *Bull. Earthquake Res. Inst., Univ. Tokyo* 45, 7-18.

Ward, P.L. (1972). Microearthquakes: Prospecting tool and possible hazard in the development of geothermal resources. *Geothermics* 1, 3-12.

Wesson, R.L., Roller, J.C., and Lee, W.H.K. (1973b). Time-term analysis and geological interpretation of seismic travel time data from the Coast Ranges of central California. *Bull. Seism. Soc. Am.* 63, 1447-1471.